UNIVERSITY OF CALIFORINA,
IRVINE

Characterization of Volatile Organic Compounds from Oil and Natural Gas Emissions in North America

DISSERTATION

Submitted in partial satisfaction of the requirements for the degree of

DOCTOR OF PHILOSOPHY

in Chemistry

by

Josette Elizabeth Marrero

Dissertation Committee:
Professor Donald R. Blake, Chair
Professor Barbara J. Finlayson-Pitts
Professor Sergey Nizkorodov

2015

TABLE OF CONTENTS

LIST OF FIGURES

LIST OF TABLES

ACKNOWLEDGMENTS

I would like to give a big thanks to my advisor Dr. Donald Blake. For the past five years you have been my mentor, but more importantly, a friend. You believed in my abilities when I didn't and pushed me to become an independent thinker, better researcher, and a stronger person.

Thank you to Dr. F. Sherwood Rowland for being such an inspiration. It was a pleasure to know and work with you during my early years at UCI.

There are some other very important people in the Rowland-Blake group without whom this work would not have been possible. Simone Meinardi, you are the key piece in this crazy lab puzzle. Thank you for all of the help and advice you have provided throughout the years. And thank you for always putting a smile on my face. Barbara Barletta, thank you for being a great resource and someone to bounce ideas off of. Brent Love and Gloria Liu Weitz keep this lab group running. Thanks for the help with sample analysis, learning the instruments, and answering all of my questions. I would also like to thank Barbara Chisholm for helping to keep everything organized. You all will be missed.

To the other grad students in the group, thanks for all of your help and for making work such a fun place to be everyday. I need to give a special thanks to my office-mate and co-pilot, Dr. Greg Hartt. Without you and our conversations about everything, I would've lost my mind years ago.

Thank you to Dr. Sergey Nizkorodov, for providing me with academic guidance, support, and friendship. I've enjoyed being an honorary member of your group.

To my collaborator and friend Dr. Amy Townsend-Small, thank you for all of your help and in the field and keeping me focused during data analysis and writing.

A sincere thank you to all of the friends I have made since moving to California. There are way too many of you to list here, but thank you all for making my graduate school experience unforgettable. I will cherish all the memories we made.

A special shout out to Aurora Pribram-Jones. I'm so glad that I met you on visit day 6 years ago. I don't think that friend is the right word; you have become my sister. Thank you for keeping me sane, and helping me to navigate the ups and downs of this grad school rollercoaster. I wouldn't have survived without you (and David). I can't wait for us to take over the Bay!

To my friends back home: Bob, Pooja, CJ, Sean, Ashley, and Rich, thank you for being my biggest supporters and best friends.

Most importantly, I want to thank my family. Mom, thank you for being my biggest inspiration in life and for all of the support you have given me. Without your love and sacrifice I wouldn't have achieved any of this. To Jessica and Jazmin, thank you being such amazing sisters and always being there for me. Throughout the tough times, we've always been there for each other, and proven that laughter is the best medicine. And lastly, to Demetrius, thank you for being the coolest person I know. I love you guys.

This work was funded by the Tides Foundation and the Environmental Defense Fund.

CURRICULUM VITAE

Josette Elizabeth Marrero

Department of Chemistry
University of California, Irvine

Irvine, CA 92617
jmarrero@uci.edu

Education:

University of California, Irvine. Irvine, CA.
Ph.D in Chemistry
Expected Graduation 2015.

University of California, Irvine. Irvine, CA.
M.S. in Chemistry
Received June 2011.

The College of New Jersey. Ewing, NJ.
B.S. in Chemistry. Concentration in Forensics; Minor in Criminology and Justice Studies
Received May 2009.

Research Experience:

Graduate Research Assistant, University of California, Irvine (Fall 2009 - Present)
Department of Chemistry, Principle Investigator: Dr. Donald Blake
Research focuses on changes in atmospheric composition in areas of oil and gas extraction and processing, remote locations with pristine air, and convective storm systems. Samples are collected on the ground or on various mobile platforms, including vehicles, boats, or aircrafts. Experimental techniques include gas chromatography using flame ionization detection, electron capture detection and mass spectrometry.
Field campaign experience:
NASA Deep Convective Cloud and Chemistry (DC3) – 2012
NASA Deriving Information on Surface conditions from Column and Vertically Resolved Observations Relevant to Air Quality (DISCOVER-AQ) – 2013
NASA Studies of Emissions and Atmospheric Composition, Clouds, and Climate Coupling by Regional Surveys (SEAC4RS) – 2013
Barnett Shale Coordinated Campaign – 2013

Participant, NASA Student Airborne Research Program (Summer 2010)
National Suborbital Education and Research Center, Research Mentor: Raphael Kudela
Took part in a six week NASA/University of North Dakota internship. Research project was entitled "Detection of Methane Using Remote Sensing." Utilizing NASA's MODIS/ASTER (MASTER) airborne simulator, naturally occurring methane seeps in the Santa Barbara Channel were imaged.

Undergraduate Research Assistant, The College of New Jersey (January 2008 - May 2009)
Department of Chemistry, Principle Investigator: Dr. John Allison
Research focused on the analysis of pigments and dyes used in inkjet printer inks and printed documents, as well as gunshot residue and other inorganic compounds of forensic interest. Laser desorption mass spectrometry was the primary analytical technique used.

Publications:

Townsend-Small, A; **Marrero, JE**; Alvarez, R; Lyon, D; Harriss, RW; Meinardi, S; Blake, DR. "Integrating isotopic and alkane ratio tracers into a bottom-up inventory of methane emissions in an urban natural gas producing region: the Barnett Shale of Fort Worth, Texas." (*in review*)

Simpson, IJ; **Marrero, JE**; Batterman, S; Meinardi, S; Barletta, B; Blake, DR. "Air quality in the Industrial Heartland of Alberta, Canada and impacts on human health." *Atmos. Environ.* 81, 702-709, 2013.

Donnelly, S; **Marrero, JE**; Cornell, T; Fowler, K; Allison, J. "Analysis of pigmented inkjet printer inks and printed documents by Laser Desorption/Mass Spectrometry." *J Forensic Sci*, 55(1), 129-135, 2010.

Presentations:

Marrero, JE; Townsend-Small, A; Meinardi, S; Blake, DR. "Hydrocarbon Emissions and Characterization of Methane Sources in the Barnett Shale." American Geophysical Union Fall Meeting, December 2014. (poster)

Lebel, E; Marrero, JE; Bertram, T; Blake, DR. "Dimethyl Sulfide Emissions from Dairies and Agriculture as a Potential Contributor to Sulfate Aerosols in the California Central Valley." American Geophysical Union Fall Meeting, December 2014. (poster)

Guo, J; Marrero, JE; Blake, DR. "Chemical and Trajectory Analysis of an Air Mass Plume from Asia." American Geophysical Union Fall Meeting, December 2014. (poster)

Blake, NJ; Barletta, B; Simpson, IJ; Schroeder, J; Hughes, S; Marrero, JE; Meinardi, S; Blake, DR; Apel, E; Hornbrook, RS; Emmons, LK. "Spatial Distributions and Source Characterization of Trace Organic Gases during SEAC4RS and Comparison to DC3." American Geophysical Union Fall Meeting, December 2014. (poster)

Simpson, IJ; Marrero, JE; Blake, NJ; Barletta, B; Hartt, G; Meinardi, S; Schroder, J; Apel, EC; Hornbrook, RS; Blake, DR. "VOC signatures from North American oil and gas sources." American Geophysical Union Fall Meeting, December 2013.

Blake, NJ; Hartt, G; Barletta, B; Simpson, IJ; Schroeder, J; Hung, Y; Marrero, JE; Gartner, A; Hirsch, C; Meinardi, S; Blake, DR; Zhang, Y; Apel, EC; Hornbrook, RS; Campos, TL; Emmons, LK. "VOC Source and Inflow Characterization during the Deep Convective Cloud and Chemistry (DC3) experiment." American Geophysical Union Fall Meeting, December 2013. (poster)

Kirpes, R; Blake, DR; Marrero, JE. "Investigating high concentrations of three greenhouse gases in the Los Angeles Basin and San Bernardino Valley." American Geophysical Union Fall Meeting, December 2013. (poster)

Simpson, IJ; Marrero, JE; Meinardi, S; Barletta, B; Krough, E; Blake, DR. "Volatile Organic Compound observations near oil sands mining, upgrading and refining facilities in Alberta, Canada," American Geophysical Union Fall Meeting, December 2012.

Marrero, JE; Simpson, IJ; Meinardi, S; Blake, DR. "Characterization of Volatile Organic Compounds (VOCs) at Sites of Oil Sands Extraction and Upgrading in Northern Alberta," American Geophysical Union Fall Meeting, December 2011. (poster)

Simpson, IJ; Barletta, B; Meinardi, S; Marrero, JE; Rowland, FS; Akagi, SK; Yokelson, RJ; Blake, DR. "New insights into halocarbon emissions in boreal regions: Forest fires and Alberta oil sands," American Geophysical Union Fall Meeting, December 2011. (poster)

Marrero, JE; O'Neill, E; Cornell, T; Allison, JA. "Laser Desorption Mass Spectrometry of Inorganic Compounds of Forensic Interest," American Society of Mass Spectrometry 57th Annual Conference, June 2009. (poster)

Teaching Experience:

Teaching Assistant, University of California, Irvine
General Chemistry discussions (Winter 2012 & 2013); Advanced Analytical Chemistry laboratory (Winter 2011); Quantitative Analytical Chemistry laboratory (Fall 2009 & 2010); General Chemistry laboratory (Winter and Spring 2010)
Supervised undergraduate students; consulted and assisted other TAs and instructors; managed experimental setups, sample preparation, equipment and instrumentation; graded lab reports and laboratory exams.

Mentor, NASA Student Airborne Research Program
Whole Air Sampler group mentor (Summer 2013, 2014)
Instructed a group of 8 undergraduate students on airborne sample collection, and gas chromatographic data analysis; helped each student develop and present an individual research project during the 8 week program.

Scholarships and Awards:

NASA Langley Peer Award (April 2014)
Outstanding Contributions to Education by a Chemistry Teaching Assistant (May 2011)
The College of New Jersey, Chairman of the Board/Board of Trustees Scholar (Fall 2005-Spring 2009)
Dean's List (Fall 2005, Fall 2007, Spring 2008, Fall 2008, Spring 2009)

Affiliations:

American Geophysical Union, Member (2011-Present)
American Chemical Society, Member (2010-2012)
Iota Sigma, Pi, National Honor Society for Women in Chemistry, Member (2010 -Present)

ABSTRACT OF THE DISSERTATION

Characterization of Volatile Organic Compounds from Oil and Natural Gas Emissions in North America

By

Josette Elizabeth Marrero

Doctor of Philosophy in Chemistry

University of California, Irvine, 2015

Professor Donald R. Blake, Chair

Emissions of hydrocarbons associated with oil and natural gas infrastructure are of current significant interest to atmospheric scientists. Studies aim to address the local and regional air quality impacts of oil and gas operations throughout North America. In Fort McMurray, multiple facilities mine and upgrade crude bitumen. The "Industrial Heartland" in Fort Saskatchewan, Alberta is Canada's largest hydrocarbon processing center, home to over 40 chemical and petrochemical facilities. Ambient samples collected in both regions during the summer of 2010 revealed significant enhancements in over 40 VOCs. Many of these measured values were similar to or greater than some of the world's largest urban and industrial centers. The primary sources of these VOCs included propene fractionation, diluent separation, and bitumen processing facilities. Hydroxyl radical reactivity (R_{OH}) was calculated in each region as a measure of ozone formation potential. On average, background samples had a R_{OH} of 4.4 s^{-1}, while industrial plumes averaged 9.2 s^{-1}, with reactivity reaching up to 60 s^{-1} in the most concentrated plumes. Acetaldehyde, propene, and 1,3-butadiene had the largest contributions to the R_{OH} values.

The Barnett Shale of northern Texas is one of the most developed and active natural gas shale plays in the United States. Emissions from the many oil and gas system components in the region have not been fully characterized. Whole air samples were collected throughout the region in October 2013, targeting known methane sources. Hydrocarbon mixing ratios, correlation plots, and stable isotopes were used to discern emission signatures for thermogenic (oil and gas) versus biogenic sources of methane. Ratios of ethane and propane to methane were distinct for each source type, although highly variable, and used to characterize natural gas as either wet or dry. Integration of these ratios into a bottom-up methane emissions inventory for the region predicted a median ethane flux of 5500 kg C_2H_6 hr^{-1}, which was consistent with top-down estimates. Lastly, the impact of emissions on local photochemistry and a statistical source apportionment suggested that thermogenic sources are responsible for nearly 70% of hydroxyl reactivity, matching the 64-72% predicted by the CH_4 inventory. Overall, oil and natural gas activities were the dominant source of CH_4 in the Barnett Shale region.

In addition to their influence on air quality and climate, VOCs emitted from oil and natural gas operations are of concern because of their potential health risks. Compounds such as 1,3-butadiene and benzene are hazardous air pollutants and known cancer-causing agents. In the communities closest to the Industrial Heartland, a 13-year record revealed a higher rate of male hematopoietic cancers than other communities in Alberta. The industrial emissions cannot directly be linked to cancer rates, but the elevated VOC concentrations in the region warrant further monitoring and research. In the Barnett Shale, oil and wet natural gas emit increased amounts of potentially harmful gases, including benzene. Using two methods, benzene emission estimates were calculated for the region, and ranged from 48 ± 16 to 84 ± 26 kg C_6H_6 hr^{-1}.

Chapter 1.
Introduction

1.1 Trace Gases in the Atmosphere

The composition and chemistry of the atmosphere have been of interest to scientists for centuries. While the majority of the atmosphere is well understood (N_2 = 78%, O_2 = 21%), is it the trace gases present at only a fraction of a percent that can be of significant importance. These gases, often in mixing ratios of less than a part per million (ppm), play a part in the formation of tropospheric smog, depletion of stratospheric ozone, potential for climate change, and human health impacts. Therefore, to fully understand the role trace gases play in atmospheric processes, several factors must be considered, including measurement of these gases and their spatial and temporal distributions; characterization of their sources; and knowledge of their chemical reactivities.

Changes in composition of atmospheric trace gases occur on a global scale, as evidenced in the cases of global warming and Antarctic ozone depletion. Measurements have shown that concentrations of greenhouse gases (GHGs), such as carbon dioxide (CO_2), methane (CH_4), and nitrous oxide (N_2O), have increased drastically over the past several hundred years. GHGs absorb thermal radiation from the Earth's surface and reradiate it back down. This warming effect occurs naturally, but has become amplified with increased emissions of GHGs from human activities [Finlayson-Pitts and Pitts, 2000; Seinfeld and Pandis, 2006].

As a result, an international agreement known as the Kyoto Protocol was enacted in 1997 with the aim of reducing GHG emissions. The Kyoto Protocol was the implementation of the United Nations Framework Convention on Climate Change (UNFCCC), which seeks the "stabilization of greenhouse gas concentrations in the atmosphere at a level that would prevent dangerous anthropogenic interference with the climate system" [UNFCCC, 2014]. For most of

the 37 countries that ratified the protocol, this meant a reduction to 1990 baseline emissions levels by the first commitment period of 2008-2012 [Kyoto Protocol, 1998]. The protocol has been further expanded to 2020, with a follow-up document in development [UNFCCC, 2014].

Also heavily impacted by anthropogenic influences is the stratospheric ozone layer, which has experienced severe depletion due to synthetically produced chlorofluorocarbons (CFCs) and other halogen-containing compounds. Because of their long atmospheric lifetimes, CFCs are able to be transported to the upper atmosphere, where they are dissociated by UV radiation and start the catalytic destruction of ozone. The effects are most strongly observed in the polar regions, particularly in the Antarctic, which experiences an "ozone hole" every spring [Anderson et al., 1989]. The first major legislation to address the ozone issue was the Montreal Protocol on Substances that Deplete the Ozone Layer, signed in 1987. The document, which has been ratified by 197 parties, called for the total phase out of these ozone-depleting substances. Since its ratification, concentrations of these compounds are declining and near full recovery of the ozone layer is expected within this century [Douglass et al., 2013].

1.1.1 Atmospheric Hydrocarbons and Their Sources

Many of the volatile organic compounds (VOCs) emitted into the atmosphere are hydrocarbons, consisting of hydrogen and carbon atoms. Methane is the most predominant VOC in the atmosphere, with a present-day background concentration of approximately 1.8 ppm [Blasing, 2011; Simpson et al., 2012]. This is a factor of one thousand to one million times more than other hydrocarbons in the atmosphere. As a result, methane is often distinguished from other, non-methane hydrocarbons, or NMHCs. These carbon containing compounds fall into various classes, including alkanes, alkenes, alkynes, aromatics, terpenes, aldehydes, ketones, etc. Sources of NMHCs can be biological, geological, or anthropogenic in nature. For

instance, vegetation and oceans naturally emit isoprene and monoterpenes. Geologically, sediments and underwater seeps can be a source of light hydrocarbons. Human activities, such as fossil fuel burning, chemical manufacturing, agriculture, and biomass burning are a source of many VOCs. Furthermore, once present in the atmosphere, VOCs undergo chemical oxidation, leading to the formation of ozone, alkyl nitrates and a variety of other oxygenated species [Finlayson-Pitts and Pitts, 2000; Seinfeld and Pandis, 2006].

Currently of significant interest to atmospheric scientists, and the focus of this dissertation, are the emissions of hydrocarbons associated with oil and natural gas infrastructure. Recent studies have addressed the local and regional air quality impacts of oil and gas operations throughout North America. Katzenstein *et al* [2003] reported significant light hydrocarbon emissions associated with oil and natural gas industry in the Southwestern United States. Studies from Ryerson *et al* [2003] and Gilman *et al* [2009] show enhanced alkene emissions from petrochemical facilities and refineries in Houston. In Utah and Colorado, natural gas has been shown to be a source of methane and NMHCs [Petron et al., 2012; Karion et al., 2013]. Simpson *et al* [2010] reported high concentrations of VOCs over areas of oil sands mining in Alberta, Canada. These studies reveal that in addition to the increased GHG impact, regions of oil and natural gas operations also contribute to tropospheric ozone formation and potentially have human health implications. It is important to continue to improve our understanding of hydrocarbon emissions associated with oil and natural gas production, particularly as energy demand from these sources continues to rise.

a. Methane

The primary sink for hydrocarbons in the atmosphere is reaction with the hydroxyl (OH) radical. Methane is the least reactive, meaning it has the smallest rate constant for the reaction with OH compared to other alkanes, e.g., 6.2×10^{-15} cm^3 $molecule^{-1}$ s^{-1} for methane

versus 2.5×10^{-13} for ethane [Aktinson, 2003]. This contributes to methane's relatively high atmospheric concentration and long lifetime (9 years) when compared to other hydrocarbons. As a result, CH_4 does not play a large role in the formation of photochemical pollution, but it does contribute significantly to the total radiative forcing of atmospheric GHGs. It is responsible for approximately 0.5 Wm^{-2} of a total 2.77 Wm^{-2} for these long-lived species [Dlugokencky et al., 2011].

With global emissions rates ranging from 500-600 Tg yr^{-1}, methane is the most abundant atmospheric hydrocarbon. Over the past 1000 years, concentrations of CH_4 have increased by over 1000 ppbv from preindustrial levels of 700 ppb. The global methane budget is summarized in Table 1.1, and shows the annual emissions from natural and anthropogenic sources. Wetlands are the major natural source of methane, while the energy sector (coal and natural gas burning) and enteric fermentation (ruminants) are the dominant anthropogenic methane sources [Dlugokencky et al., 2011].

The continued accumulation of CH_4 from a pre-industrial total budget of roughly 215 Tg yr^{-1} has been witnessed since 1978 [Dlugokencky et al., 2011; Blake et al., 1982]. During the 10-year period from 1978-1987, the average CH_4 growth rate was 1.1% yr^{-1} [Blake and Rowland, 1988]. By the 1990s, the rate slowed to 0.3-0.6% yr^{-1}, and has since declined to less than 0.2% per year [Simpson et al., 2006]. The fluctuations in methane growth rate can be associated with changes in biomass burning or the use of natural gas. In fact, the slowed growth rate implies improvements in the infrastructure associated with oil and natural gas production [Simpson et al., 2012].

However, the natural gas industry is continually growing, particularly in the United States, where it is becoming more relied upon for electricity generation and transportation fuel. In the US, the anthropogenic CH_4 budget was estimated to be 33.4 ± 1.4 Tg yr^{-1}, or nearly 7% of

the global source, with the largest contributions from the oil and gas and cattle industries in the south-central region [Miller et al., 2013]. As a result, the CH_4 emissions associated with the various stages of extraction, production, and storage of natural gas have become debated [Howarth et al., 2011] and will continue to be of interest as the industry expands further.

Table 1.1. Global atmospheric methane emissions estimates (in Tg yr^{-1}). Adapted from Dlugokencky et al., [2011] and Seinfeld and Pandis, [2006] and references therein.

	Bousquet et al.	Lelieveld et al.	IPCC
years	1984-2003	1992	1997-2006
Anthropogenic sources			
Energy	97-113	110	74-106
Enteric Fermentation	76-104	115	76-92
Rice Agriculture	26-36	—[a]	31-112
Biomass Burning	42-58	40	14-88
Landfills/Sewage	44-66	40	35-69
Natural sources			
Wetlands	132-162	225[a]	100-231
Termites	19-27	20	20-29
Oceans	13-25	15	4-15
Sources Total	517-533	600	503-610
Sinks			
Reaction with OH	447-449	510	428-511
Stratospheric Loss	36-38	40	30-45
Soils	18-24	30	26-34
Sinks Total	501-511	580	492-581

[a]rice agriculture included in wetlands estimate

b. Anthropogenic Non-Methane Hydrocarbons

Non-methane organics, including hydrocarbons and oxygenated compounds, have short atmospheric lifetimes, on the order of hours to months. Consequently, these NMHCs have a small impact on climate forcing. Their importance in the atmosphere is therefore related to the photochemical reactions they undergo to produce ozone (in the presence of sunlight and nitrogen oxides) and organic aerosols [IPCC, 2001]. NMHC sources vary both geographically and in terms of their abundance, making the development of an accurate global inventory

challenging (few comprehensive estimates exist from the past twenty years). Emissions estimates range from 680-950 Tg yr^{-1} for both natural and anthropogenic sources [Muller, 1992].

Piccot *et al* [1992] estimated that global anthropogenic NMHC emissions were 109.5 Tg yr^{-1}. Recent model simulations put the global estimate closer to 130 Tg NMHC yr^{-1} [Lamarque et al., 2010]. The largest global source of non-methane VOCs is biomass burning, which is estimated to contribute nearly 60% to emissions [Lamarque et al., 2010]. This includes the use of fuelwood, savanna burning, and other deforestation practices [Piccot et al., 1992]. Due to its widespread biomass burning tropical Africa is a significant NMHC emitter, responsible for nearly 16 Tg, annually [Piccot et al., 1992]. The United States is an equally large emitter of NMHCs, also generating 15-16 Tg per year, with large contributions from fuel combustion and the transportation sector [Lamarque et al., 2010; US EPA, 2006]. Table 1.2 shows decadal trends in global anthropogenic NMHC emissions.

Light alkanes, those with 2-5 carbon atoms, contribute the most to the anthropogenic NMHC budget. These alkanes, often emitted from the oil and natural gas industry, have been estimated to make up 46.1 Tg yr^{-1} of the total VOC emissions [Pozzer et al., 2010].

Table 1.2. Estimates of global anthropogenic NMHC emissions [Lamarque et al., 2010].

Year	NMHC emissions (Tg yr^{-1})
1900	18.5
1910	21.0
1920	23.5
1930	27.4
1940	31.2
1950	43.4
1960	70.4
1970	101.2
1980	126.8
1990	137.5
2000	129.5

c. Biogenic Non-Methane Hydrocarbons

There are a wide variety of hydrocarbons emitted naturally from plants and agriculture, as a byproduct of processes like photosynthesis or photorespiration. The most highly emitted of these compounds is isoprene (C_5H_8), or 2-methyl-1,3-butadiene [Lamb et al., 1987; Guenther et al., 1995]. Other monoterpenes with characteristic C_5 units, such as α- and β-pinene, as well as ethene and oxygenated hydrocarbons, can all be emitted from vegetation [Kesselmeier and Staudt, 1999]. Globally, biogenic hydrocarbon emissions greatly exceed those from anthropogenic sources. However, there is high variability and uncertainty in global budgets. Estimates from the 1990s have the biogenic contribution to the total NMHC budget ranging from 500 [Mueller, 1992] to 1150 [Guenther et al., 1995] Tg yr^{-1}. A recent model simulation, which uses data from over a thirty-year period from 1980 to 2010, estimates a global biogenic NMHC emission of 760 Tg yr^{-1} [Sindelarova et al., 2014]. Table 1.3 compares emission estimates for the biogenic compounds most abundantly emitted. In each estimate isoprene is a major contributor, accounting anywhere from 44 to 69% of global emissions [Guenther et al., 1995; Sindelarova et al., 2014]. For most plant species, emissions of natural VOCs are dependent on temperature and sunlight, and in general, are highest on hot, summer days [Lamb et al., 1987]. As a result, the regions with the largest biogenic VOC emissions are in the tropics and the southeastern United States [Guenther et al., 1995; Lamb et al., 1987].

The lifetimes of isoprene and many monoterpenes are on the order of minutes to hours. The presence of carbon double bonds causes these compounds to be highly reactive in the atmosphere [Kesselmeier and Staudt, 1999]. Because they are naturally occurring, emissions of biogenic NMHCs cannot be reduced by environmental regulations. However, these compounds can be emitted in regions far from other anthropogenic sources. Without the presence of

nitrogen oxides (NO and NO_2) produced from fossil fuel combustion, biogenic hydrocarbons do not produce significant amounts of photochemical ozone [Finlayson-Pitts and Pitts, 2000].

In addition to vegetation, oceans are a large source of atmospheric NMHCs. In comparison to the air, ocean water has a much higher concentration of dissolved organic matter (DOM). The photochemical lability of this organic matter results in the emission of VOCs from the water column [Guenther et al., 1995]. Some of the gases emitted from ocean-atmosphere exchange include dimethyl sulfide (DMS), halogen containing compounds, nitrogen compounds (ammonia, amines, alkyl nitrates), isoprene and oxygenated VOCs. Through photochemical processing, these compounds can play a role in ozone depletion, aerosol formation, and associated climate effects [Carpenter et al., 2012].

Table 1.3. Estimated global emissions (Tg yr^{-1}) of biogenic VOCs. Adapted from Guenther et al., [1995] and Sindelarova et al., [2014].

Class of compound	Guenther et al.	Sindelarova et al.
Isoprene	503	523
Monoterpenes	127	84
Other reactive organics	520	153
Total VOC	1150	760

1.1.2 The Photochemistry of Ozone Formation and Its Regulation

a. Photochemical reactions

The chemistry of the troposphere and stratosphere both involve reactions that lead to the formation and destruction of ozone (O_3). The stratosphere contains nearly 90% of the O_3 in the atmosphere [Seinfeld and Pandis, 2006]. The steady state of ozone is maintained by reactions known as the Chapman cycle. In this cycle, ozone is formed from the photodissociation of O_2 and subsequent reaction of those oxygen atoms with another oxygen molecule (in the presence of a third body, M). Photolytic decomposition of O_2 occurs in the UV, at wavelengths less than 242 nm [Finlayson-Pitts and Pitts, 2000]:

$$O_2 + h\nu\ (\lambda < 242\ nm) \rightarrow 2O \quad (1.1)$$

$$O + O_2 + M \rightarrow O_3 \quad (1.2)$$

Generally, the greater the amount of sunlight available, the more O_3 is produced. Stratospheric ozone is also naturally destroyed by reaction with a ground state oxygen atom, or through dissociation by photons at wavelengths smaller than 336 nm. The result of the latter, is the production of and excited O atom [Finlayson-Pitts and Pitts, 2000]:

$$O + O_3 \rightarrow 2O_2 \quad (1.3)$$

$$O_3 + h\nu\ (\lambda < 336\ nm) \rightarrow O(^1D) + O_2 \quad (1.4)$$

The mechanisms by which tropospheric ozone (photochemical smog) is produced are more complex, and involve hydrocarbons and nitrogen oxides (NO_x). Haagen-Smit was first to suggest this recipe for ozone formation, which occurs by free-radical chain reactions [Haagen-Smit, 1952; Haagen-Smit et al., 1953]. This process is initiated by the reaction of hydroxyl radical (•OH) with a hydrocarbon. OH, which can be formed by the reaction of $O(^1D)$ (from reaction 1.4) and water vapor (H_2O), is found at concentrations of roughly 10^6 molecules cm^{-3}. Despite this small concentration, it is most prominent free radical oxidizing agent in the atmosphere [Levy, 1971; Seinfeld and Pandis, 2006]. In the presence of alkanes OH is able to abstract a hydrogen atom, forming an alkyl radical, as shown in reaction 1.5 [Atkinson, 1997]. The alkyl radical can then react with O_2, creating an alkylperoxy radical (RO_2•):

$$RH + OH \rightarrow R\bullet + H_2O \quad (1.5)$$

$$R\bullet + O_2 \rightarrow RO_2\bullet \quad (1.6)$$

In the next step, RO_2• is removed, resulting in the formation of an alkoxy radical (Reaction 1.7a). In polluted environments, like cities, this step involves NO_x (NO and NO_2). Urban areas are considered 'high NOx,' having concentrations ranging from 5 to 20 ppb (primarily in the form of NO). This is compared to less than 1 ppb in more rural areas [Seinfeld and Pandis,

2006]. In a second possible pathway, alkyl nitrates can be formed from the reaction with NO [Atkinson, 1997]:

$$RO_2\bullet + NO \rightarrow RO\bullet + NO_2 \quad (1.7a)$$

$$RO_2\bullet + NO \rightarrow RONO_2 \quad (1.7b)$$

The first pathway is the more likely outcome of this reaction, and forms NO_2. This conversion process is part of the NOx cycle. Formation of NO_2 is important, because it goes on to produce ozone [Atkinson, 1997],

$$NO_2 + h\nu \rightarrow NO + O(^3P) \quad (1.8)$$

$$O(^3P) + O_2 \rightarrow O_3 \quad (1.9)$$

while the remaining RO radical can decompose, isomerize, or react with O_2 to produce HO_2 and catalyze the HO_x cycle [Finlayson-Pitts and Pitts, 2000].

For tropospheric alkenes, instead of hydrogen abstraction, addition across the double bond dominates. Subsequent reactions with O_2 and NO also produce an alkoxy radical (RO) and NO_2, as described in reactions 1.6-1.9. However, the difference between the two reaction pathways is the speed at which they occur; alkenes have a much faster rate of reaction than alkanes. For instance, $k = 8.52 \times 10^{-12}$ cm^3 $molecule^{-1}$ s^{-1} for ethene compared to 2.5×10^{-13} cm^3 $molecule^{-1}$ s^{-1} for ethane [Atkinson, 1997]. Therefore, an alkene molecule has a greater contribution towards photochemical ozone formation than an alkane of similar carbon number [Atkinson, 1997].

In conditions of 'low NOx,' ozone formation can be dampened due to competing reactions with the alkylperoxy radical. In less polluted areas, the pathway for reaction with NO becomes less important and reactions with RO_2 and HO_2 dominate. Reaction with HO_2 primarily forms a hydroperoxide but can lead to other products for complex RO_2 radicals:

$$RO_2\bullet + HO_2 \rightarrow ROOH + O_2 \quad (1.10a)$$

$$\rightarrow \text{carbonyl} + H_2O + O_2 \quad (1.10b)$$

$$\rightarrow ROH + O_3 \quad (1.10c)$$

The self-reaction with another alkylperoxy radical ($R'O_2$) can also react by several pathways [Finlayson-Pitts and Pitts, 2000]:

$$RO_2\bullet + R'O_2\bullet \rightarrow 2RO\bullet + O_2 \quad (1.11a)$$

$$\rightarrow ROH + R'CHO + O_2 \quad (1.11b)$$

$$\rightarrow ROOR' + O_2 \quad (1.11c)$$

With the countless number of VOCs emitted into the troposphere, the photochemical reactions that can occur quickly become numerous and complex. However, in order for the formation of ozone to occur, the presence of both hydrocarbons and oxidants are required.

b. Air Quality Standards

Since its establishment in 1963, the Clean Air Act has served as the primary US federal law to regulate air pollution. Amendments to the original act, made in 1970 and 1990, authorize the Environmental Protection Agency (EPA) to develop and enforce National Ambient Air Quality Standards (NAAQS). These standards, which are classified as primary or secondary, work to protect public health and the environment from hazardous air pollutants [US EPA, 2013]. Primary standards aim to protect public health, especially populations considered sensitive to air quality, and secondary standards protect public welfare from decreased visibility, and damage to animals, vegetation and buildings [US EPA, 2011].

While numerous compounds are considered harmful pollutants, 6 stand out as "criteria" pollutants. These include carbon monoxide, lead, nitrogen dioxide, ozone, particulate matter ($PM_{2.5}$ and PM_{10}), and sulfur dioxide. Concentrations below the NAAQS for these pollutants are considered to not have any detrimental effects to the population or environment [US EPA, 2011]. However exceedances of the national standards are not uncommon, and failure to meet

the standards results in the declaration of an area as a non-attainment zone, subject to various penalties. For ozone the national 8-hour standard (primary and secondary) is 0.075 ppm [US EPA, 2011].

In Texas, a nonattainment designation was given to the Dallas-Fort Worth-Arlington (DFW) metropolitan area, which contains parts of the Barnett Shale [TCEQ 2014a]. Beginning in 2012, the nonattainment status for the region was downgraded from serious to moderate. Annual ozone data for DFW are provided in Table 1.4, beginning with the year 2000 [TCEQ, 2014b].

Table 1.4 Maximum annual ozone concentrations (in ppm) for the Dallas-Fort Worth region and the number of days during which the air quality standard was exceeded [TCEQ, 2014b].

	Dallas		Fort Worth-Arlington	
Year	Maximum (ppm)	Days > standard	Maximum (ppm)	Days > standard
2014	0.088	6	0.091	8
2013	0.090	26	0.100	21
2012	0.109	25	0.110	23
2011	0.102	34	0.103	29
2010	0.087	12	0.094	15
2005	0.108	64	0.117	54
2000	0.111	63	0.105	39

In Canada, the CAAQS (Canadian Ambient Air Quality Standards) were adopted in 2013 to regulate outdoor ozone and PM concentrations. Prior to the current standards, the Canadian Council of Ministers of the Environment (CCME) established the Canada-wide Standards (CWS) in 2000. This set the 8-hour ozone limit to 0.065 ppm [CCME, 2014]. While concentrations above this target were not common for the 3-year period of 2010-2012, 6 locations in Alberta consistently recorded average O_3 within 10% of the limit. These included the Edmonton census metropolitan area, which is home to several petrochemical and oil and gas facilities that process bitumen mined from oil sands of northern Alberta [CCME, 2014].

1.2 Oil and Natural Gas in North America

1.2.1 Formation and Composition

Crude petroleum and natural gas are formed from organic matter preserved in sedimentary rocks deep below the earth's surface, where temperature and pressure are high. The resultant oil and gas then migrate upward and outward, towards the surface, through faults and fractures in the rocks. These hydrocarbons accumulate in a reservoir and begin to naturally separate according to density, with natural gas settling at the top and oil below. It is common however, for the oil to be saturated in natural gas. A rock layer (caprock) forms a seal over the gas cap and allows for drilling into the reservoir [Hyne, 2001].

This geologically formed crude oil and natural gas are primarily composed of hydrocarbons with chains of varying length. Those with five or more carbon atoms exist naturally as liquids, and are responsible for the structure and properties of crude oil. The hydrocarbons that make up crude oil have carbon chains ranging from 5 to 60 atoms are typically cycloalkanes (49%), alkanes (30%), aromatics (15%) and asphaltics (6%) [Hyne, 2001]. Natural gas on the other hand, is composed of methane and C_2-C_5 alkanes (ethane, propane, butanes, pentanes). The percentages of each alkane in natural gas vary form field to field, with methane being the most common (anywhere from 70 to 98%) [Hyne, 2001].

1.2.2 Current Trends in the Oil and Natural Gas Industry

Of the total global oil reserves (1655 billion barrels), only about 30 percent is considered conventional [EIA, 2014b]. Conventional oil is of higher value and more desirable since it is less dense, lighter and requires simpler distillation. Heavy oils, on the other hand, generally contain a higher concentration of metals, require more intensive extraction and refining, and produce more waste. However, with decreasing conventional oil supply, increasing demand, and higher energy prices, more and more companies are investing in heavy

oil. As technologies improve and profits rise, exploitation of these vast, unconventional oil reserves is certain to be an important factor in the future of the oil industry [Alboudwarej et al., 2006]. For instance, half of the oil produced daily in Canada comes from heavy oil resources, making it the 5th largest crude oil producer in the world [CAPP, 2014a; CIA World Factbook, 2014].

Similarly, the development of energy from natural gas has continued to rise worldwide. The United States in particular has witnessed an expansion of its natural gas industry, quickly becoming one of the world's top gas producing countries. This stems from the desire for a resource that reduces dependency on foreign imports and is less environmentally damaging than other fossil fuels. In 2012, nearly 20% of the world's natural gas was produced by the US, edging out Russia as the top producing country [CIA World Factbook, 2014]. By the year 2040, natural gas is expected to surpass coal as the leading fuel for electricity generation in the US, accounting for 35% of the total [EIA, 2014a].

1.2.3 Industrial Processing and Infrastructure

The oil and gas industry requires a wide range of equipment and processing in order to move extracted product from wellhead to gas pump or household. Refining of the crude oil is a critical step in the generation of various end products including kerosene, diesel fuels, lubricating oils, liquefied petroleum gas, and of course, gasoline. The complete cycle of processing begins with the delivery of crude to a refinery and ends with the storage of refined products before shipment [EPA, 1995]. The first step in the refining process is the separation of crude into its constituent hydrocarbon by fractional distillation. During fractionation, the crude is heated to temperatures of up to 550 °C in a vacuum column, allowing heavy liquids to be collected at the bottom, while vapors to move up the column. Eventually the gases cool down and condense at different heights along the column into varying end products [EPA, 1995]. In

the next step, known as cracking, heat, pressure and catalysts are used to convert heavier hydrocarbons into lighter products. Further refining is achieved through treating processes, which are employed to remove undesired elements, such as nitrogen, sulfur, or oxygen [EPA, 1995].

Processing of natural gas often begins at the wellhead, where condensate is separated from the natural gas. Condensate is the term given to natural gas liquids, or the hydrocarbons bigger than methane that become liquid when brought up from underground to atmospheric temperature and pressure. To ensure passage of the natural gas through pipelines, sand and other large particles are removed here, and the gas is heated to prevent the formation of ice-like methane hydrates [EIA, 2006]. From gathering pipelines, the gas is transported to downstream facilities, for further processing and the removal of water, sulfur compounds, nitrogen and CO_2. During transit from each processing location, natural gas also passes through compressor stations, which are facilities that keep the gas pressurized in the pipeline [EIA, 2006]. From here, natural gas is delivered to city gates and finally, to customers.

Hydrocarbons are emitted into the atmosphere during each stage of the extraction, refining, transportation, and storage of crude oil and natural gas [Gilman et al., 2013]. Emissions from point sources like valves, flanges, pumps, compressors, and separators used to distribute oil and gas quickly accumulate when hundreds or thousands of wells are concentrated in one region [Gilman et al., 2013]. These emissions have an impact not only on air quality, but also human health. For instance, in addition to hydrocarbons, NO_x is also emitted from some of these components, which can lead to ozone formation. Furthermore, some of the VOCs emitted, like benzene or 1,3-butadiene, are known carcinogens [Petron et al., 2012; Simpson et al., 2013]. The quantification and characterization of these emissions has

become the focus of many recent studies, in order to fully understand the impacts of the oil and gas industry.

1.2.4. Oil and Natural Gas Production in Canada

a. Background

Next to Saudi Arabia and Venezuela, Canada has the third highest volume of proven oil reserves, with estimates of 173.1 billion barrels (1 bbl = 159 L) of recoverable oil [CIA World Fact Book, 2014]. Of these reserves, only 4.9 billion barrels are considered conventional crude oil. The remaining portion is in the form of bitumen, an exceedingly viscous mixture of quartz sand, water and clay covered in heavy oil. Bitumen, which makes up 30% of worldwide heavy oil resources, does not flow like conventional oil and cannot be pumped through pipelines or diluted without first being heated [Alboudwarej et al., 2006]. Development of the Canadian oil sands began in 1930, when a former farmer and businessman mined and produced the first barrels of bitumen. While development has continued since then, rapid expansion of the oil sands industry has only been seen in the last two decades [GACCS, 2009]. As of 2013, roughly 1.93 million barrels of oil are produced each day from the oil sands, and by 2022 this number is expected to reach over 3.8 million barrels [CAPP, 2014a; Government of Alberta, 2014]. In addition to oil however, Canada is also the 5th largest global producer of natural gas, with 14.1 billion cubic feet (bcf) generated daily [CAPP, 2014a].

As seen in Figure 1.1, Canadian oil sands deposits cover an area of approximately 140,000 square kilometers and are primarily located in three regions in Alberta: Athabasca, Peace River and Cold Lake [Government of Alberta, 2014]. The oil sands are collected either by surface mining or *in situ* drilling, depending on how deep the reserves are located. Surface mining, for instance, only occurs in the Athabasca region (north of Fort McMurray), where many deposits are less than 75 meters from the surface. This accounts for 20% of total oil

sands recovery. During surface mining, layers of forest and overburden are removed to uncover and collect the oil sands. To extract the bitumen, hot water and diluents are mixed with the oil sands, forming a slurry which is then sent to a separation vessel [GACCS, 2009]. Diluents used include naphtha (a volatile, flammable mixture of hydrocarbons) or other mixtures of pentanes and hexanes [Siddique et al., 2006]. Once the bitumen is collected, it is centrifuged to remove excess sand and water, and is then ready for upgrading.

Figure 1.1. Map of Alberta, Canada, highlighting the locations of oil sands deposits and surface mineable areas [Government of Alberta, 2014].

Note: 1 km² = 1 square kilometre = 0.39 square miles

Of the current 114 active oil sands extraction projects, only 6 utilize surface mining [Government of Alberta, 2014]. The remaining projects recover bitumen by *in situ* technology, such as Toe to Heal Air Injection (THAI), Vapor Extraction (VAPEX), Cyclic Steam Stimulation, and most commonly, Steam Assisted Gravity Drainage (SAGD). In this process, two horizontal wells stacked on one another are drilled. Steam is injected into the top well, heating the bitumen and causing it to drain into the lower well. Once this separation occurs, the bitumen is pumped to the surface and prepared for upgrading [GACCS, 2009]. While in situ extraction involves minimal land disturbance and does not require tailings ponds, the methods used to generate heat and steam are energy intensive. Natural gas is used extensively for these processes, nearly 2 billion cubic feet per day [NEB, 2006].

b. Environmental Impacts

While the oil sands industry provides major economic benefits for Canada, as well as the United States, the environmental impacts are also substantial. The ongoing oil sands development raises concerns with regard to land disturbance, water use and air quality. Of the available surface mineable area, 767 km^2 has been disturbed by mining as of 2012. However, only about 77 km^2 are under active reclamation, a process that takes up to two decades to complete [Government of Alberta, 2014]. In terms of water use, approximately 3.5 barrels of fresh water are required for each barrel of bitumen produced. Water left over from the separation of bitumen from the oil sands is stored in tailings ponds, which currently take up an area of 170 km^2 [CAPP, 2014b]. Because of concerns regarding possible seepage of tailings into groundwater, water quality monitoring is employed regularly.

However, the air quality impacts associated with this industry deserve significant attention, particularly because of the energy intensive nature of extraction, transport and upgrading of the oil sands. Some of the surface mining companies in Fort McMurray have

upgraders located on site, while other transport diluted bitumen to Fort Saskatchewan for processing. This region, known as Industrial Heartland of Alberta, is also home to over 40 chemical and petrochemical facilities [AIHA, 2012]. Each of these facilities emits GHGs and other VOCs. To date, the oil sands industry is estimated to be responsible for about 8.7% of GHG emissions in Canada [CAPP, 2014a]. While air quality in Alberta is monitored by organizations like the Wood Buffalo Environmental Association (WBEA), representing community members, environmental groups, government and industry, characterization of emitted trace gases is still not fully understood and has been lacking in peer-reviewed literature [Timoney and Lee, 2009; Simpson et al., 2013]. The limited number of independent studies in this region led to the work presented in this dissertation.

1.2.5 Oil and Natural Gas Production in Northern Texas

a. Background

The total volume of natural gas produced in the United States in 2013 was 25.7 trillion cubic feet (tcf). This includes major contributions from shales in Louisiana (Haynesville Shale), Pennsylvania (Marcellus and Utica Shales), Oklahoma (Woodford Shale), and Wyoming. However, the top gas producing state in the US is Texas, which produced 7.5 tcf of natural gas in 2013, primarily from the Eagle Ford and Barnett Shales [EIA, 2014b]. Located in northern Texas, the Barnett Shale (Figure 1.2) extends over 5000 square miles and throughout 18 counties [TCEQ, 2014c]. The organic-rich Barnett Shale was discovered in late 1800s, but was not considered economically viable until the 1980s. Over the past 20 years the Barnett Shale has experienced particularly significant development. For instance, the number of wells increased from 150 in 1993 to nearly 17,500 in 2013. As a result, the shale region has grown to produce over 5 billion cubic feet of natural gas each day [Railroad Commission of Texas, 2014]. In total, the Barnett Shale produces 6% of natural gas in the United States, making it one of the

Figure 1.2. Map of the Barnett Shale and the gas and oil producing wells in each county. Active natural gas wells are highlighted in red, while oil wells are in blue [TCEQ, 2014c].

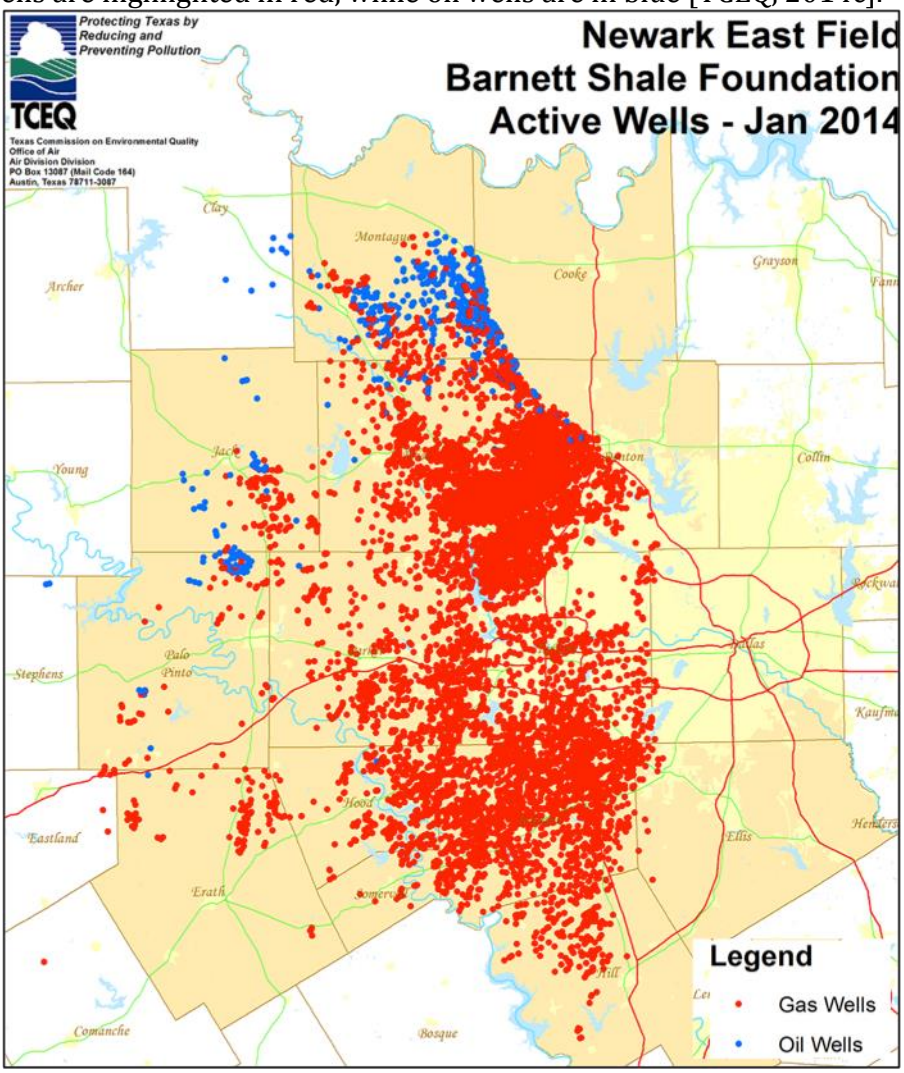

most productive in the country [Energy from Shale, 2014]. In addition to natural gas however, the shale also produces oil, generating an average of 6,700 barrels per day in 2013 (Figure 1.3).

Shale plays are evaluated for their oil or gas content on the basis of their thermal maturity. The most commonly used indicator of thermal maturity is vitrinite reflectance (R_o). Values for R_o between 0.6 and 1.0 are indicative of oil, whereas values greater than 1.0 indicate gas. More specifically, values greater than 1.4 are considered dry gas, or almost entirely methane [Mukhopadhyay and Dow, 1994]. The Barnett Shale has a large variability in its R_o

values, which range from 0.5 to 1.9 (Figure 1.4). A large percentage of the gas production in the Barnett region occurs in the core dry gas area, which includes portions of Wise, Denton, Johnson and Tarrant counties. North and west of the core area, the extraction and sustained production of natural gas from wetter and oil-like reservoirs has been achieved through technological advances [Hayden and Pursell, 2005].

Figure 1.3. Average daily production in the Barnett Shale of a) natural gas in million cubic feet (MMcf) and b) oil in barrels from 2000 to 2014. (Railroad Commission of Texas, 2014).

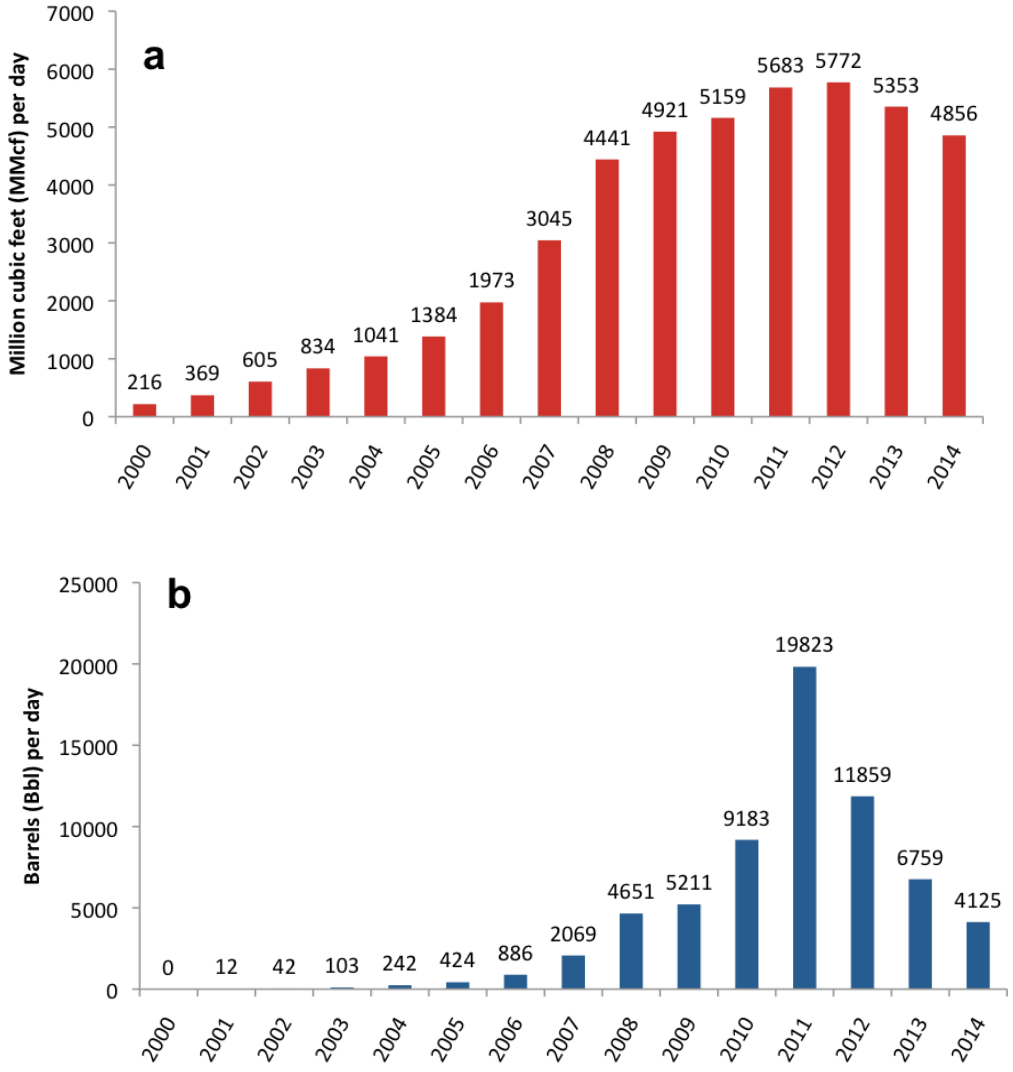

Figure 1.4. Map showing where natural gas and oil are likely located in the Barnett Shale reservoir, based on vitrinite reflectance. The higher the values indicate drier gas (Railroad Commission of Texas, 2014).

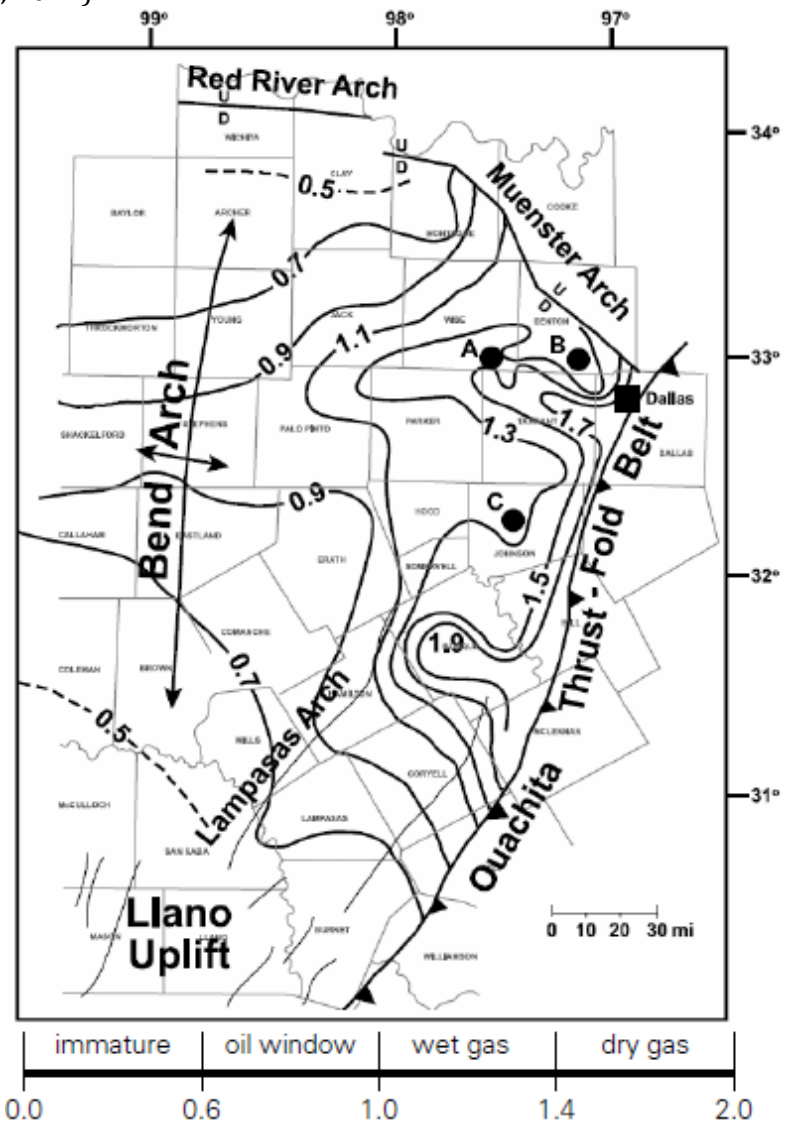

The two processes primarily used for natural gas extraction are horizontal drilling and hydraulic fracturing, or fracking. The horizontal drilling process begins similarly to that of a vertical well until the kickoff point, just above the target rock, is reached. From this point, the drilling curves outward and continues, horizontally. This orientation allows for a larger area of the reservoir to be reached than by conventional, vertical wells, and ensures that contact with neighboring aquifers is avoided [Hayden and Pursell, 2005]. Once a well has been drilled and

cemented in place, the fracking process can begin. Fracking takes place in two stages, injection and flowback. During injection, a mixture of water, sand, and chemical additives are pumped into the well at high pressure, creating fractures in the wellbore into which gas can flow. In the flowback stage, some of the fracking fluid resurfaces and the well begins to produce oil and/or gas [Helms, 2008].

b. Air Quality Impacts

While the use of natural gas continues to rise, and is expected to for years to come, the atmospheric impacts of this industry are still not fully understood. The primary component of natural gas is CH_4, which has global warming potential 34 to 86 times greater than CO_2 over a 100 and 20-year time scale, respectively [IPCC, 2001]. Yet, natural gas is hailed by some as an effective CO_2 mitigation strategy, because it has a carbon footprint half as large as power plants that burn coal, and does not contain sulfur or mercury [Pacala and Socolow, 2004]. Others argue however, that significant amounts of CH_4 are released to the atmosphere during the flowback stage of hydraulic fracturing [Howarth et al., 2011]. In addition, CH_4 emissions can also stem from the venting or flaring of excess oil and gas. However, the fugitive emissions resulting from leaks in the natural gas production and distribution infrastructure have recently received much attention [Alvarez et al., 2012; Allen et al., 2013; Jackson et al., 2014]. Their environmental impact is still unclear and can potentially give shale gas a larger GHG impact than coal.

Compressors, engines, pipelines, and storage tanks associated with oil and natural gas wells also emit C_2-C_{10} NMHCs and NO_x. In the work presented in this dissertation, emissions of VOCs in the Barnett Shale were studied in an effort to better characterize CH_4 sources and understand the contribution of the oil and natural gas industry on local air quality.

References

Alberta's Industrial Heartland Association. *Industry and Organization Profiles*; 2012; www.industrialheartland.com/images/stories/industry/aiha_industry_information_july_2012.pdf.

Alboudwarej, H.; Felix, J.; Taylor, S.; Bardy, R.; Bremmer, C.; Brough, B.; Skeates, C.; Baker, A.; Palmer, D.; Pattison, K.; Beshry, M.; Krawchuk, P.; Brown, G.; Calvo, R.; Triana, J.A.C.; Hathcock, R.; Koerner, K.; Hughes, T.; Kundu, D.; de Cardenas, J.L.; West, C. Highlighting Heavy Oil. *Oilfield Rev*. **2006**, 34–53.

Allen, D.T.; Torres, V.M.; Thomas, J.; Sullivan, D.W.; Harrison, M.; Hendler, A.; Herndon, S.C.; Kolb, C.E.; Fraser, M.P.; Hill, A.D.; Lamb, B.K.; Miskimins, J.; Sawyer, R.F.; Seinfeld, J.H. Measurements of methane emissions at natural gas production sites in the United States. *Proc. Natl. Acad. Sci*., **2013**, 100(44), 17768-17773.

Alvarez, R.A.; Pacala, S.W.; Winebrake, J.J.; Chameides, W.L.; Hamburg, S.P. Greater focus needed on methane leakage from natural gas infrastructure. *Proc. Natl. Acad. Sci*., **2012**, 109(17), 6435-6440.

Anderson, J.G.; Brune, W.H.; Lloyd, S.A.; Toohey, D.W.; Sander, S.P.; Starr, W.L.; Loewenstein, M.; Podolske, J.R. Kinetics of ozone destruction by ClO and BrO withing the Antarctic vortex: An analysis based on in situ ER-2 data. *J. Geophys. Res.* **1989**, *94*, 11480-11520.

Atkinson, R. Gas-phase tropospheric chemistry of volatile organic compound: 1. Alkanes and alkenes. *J.Phys. Chem. Ref. Data*. **1997**, *26*, 215-290.

Atkinson, R. Kinetics of the gas-phase reactions of OH radicals with alkanes and cycloalkanes. *Atmos. Chem. Phys.* **2003**, *3*, 2233-2307.

Blasing, T.J. Recent Greenhouse Gas Concentrations. Technical Report. US Carbon Dioxide Information Analysis Center, Oak Ridge, TN, 2011.

Blake, D.R.; Mayer, E.W.; Tyler, S.C.; Makide, Y.; Montague, C.; Rowland, F.S. Global increase in atmospheric methane concentrations between 1978 and 1980. *Geophys. Res. Lett.* **1982**, *9*, 477-480.

Blake, D.R.; Rowland, F.S. Continuing worldwide increase in tropospheric methane, 1978 to 1987. *Science*. **1998**, *239*, 1129-1131.

Canadian Association of Petroleum Producers. Basic Statistics.; 2014a; http://www.capp.ca/library/statistics/basic/Pages/default.aspx, accessed November 5th, 2014.

Canadian Association of Petroleum Producers. *The Facts on: Oil Sands*.; 2014b; http://www.capp.ca/getdoc.aspx?DocId=242473&DT=NTV, accessed November 5th, 2014.

Canadian Council of Ministers of the Environment. *Canada-Wide Standards for Particulate Matter and Ozone: 2012 Final Report*; Winnipeg, Manitoba, 2014;

http://www.ccme.ca/files/Resources/air/pm_ozone/PN_1526_2012_CWS_for_PM_and_Ozone_Final_Report.pdf, accessed November 2nd, 2014.

Carpenter, L.J.; Archer, S.D.; Beale, R. Ocean-atmosphere trace gas exchange. *Chem. Soc. Rev*. **2012**, *41*, 6473-6506.

Central Intelligence Agency: *The World Factbook. Country comparison: Natural gas production*; Washington, DC, 2014; https://www.cia.gov/library/publications/the-world-factbook/rankorder/2249rank.html, accessed May 15th, 2014.

Dlugokencky, E.J.; Nisbet, E.G.; Fisher, R.; Lowry, D. Global atmospheric methane: budget, changes and dangers. *Phil. Trans. R. Soc. A.* **2011**, *369*, 2058-2072, doi:10.1098/rsta.2010.0341.

Douglass, A.; Kramarova, N.; Strahan, S. New results from inside the Ozone Hole; Greenbelt, MD, 2013; http://www.nasa.gov/content/goddard/new-results-from-inside-the-ozone-hole, accessed September 13th, 2014.

Energy from Shale: *Shale Gas Economics: Extracting from domestic oil reserves,* 2014; http://www.energyfromshale.org/hydraulic-fracturing/shale-gas, accessed November 5th, 2014.

Finlayson-Pitts, B.J.; Pitts, J.N. *Chemistry of the Upper and Lower Atmosphere*; Academic Press: San Diego, 2000.

Gilman, J.B.; *et al.* Measurements of volatile organic compounds during the 2006 TexAQS/GoMACCS campaign: Industrial influences, regional characteristics, and diurnal dependencies of the OH reactivity. *J. Geophys. Res.* **2009**, *114*, D00F06, doi:10.1029/2008JD011525.

Gilman, J.B.; Lerner, B.M.; Kuster, W.C.; de Gouw, J.A. Source signature of volatile organic compounds from oil and natural gas operations in Northeastern Colorado. *Environ. Sci. Technol*., **2013**, 47, 1297−1305.

Government of Alberta. *Alberta's Oil Sands*, 2014; http://oilsands.alberta.ca, accessed November 5th, 2014.

Government of Alberta Culture and Community Services. *Oil Sands Discovery Centre: Facts About Alberta's Oil Sands and its Industry*; Fort McMurray, Alberta, 2009; http://history.alberta.ca/oilsands/docs/facts_sheets09.pdf.

Guenther, A.; Hewitt, N.; Erickson, D.; Fall, R.; Geron, C.; Graedel, T.; Harley, P.; Klinger, L.; Lerdau, M.; McKay, W.A.; Pierce, T.; Scholes, B.; Steinbrecher, R.; Tallamraju, R.; Taylor, J.; Zimmerman, P. A global model of natural volatile organic compound emissions. *J. Geophys. Res*. **1995**, *100*, 8873-8892.

Haagen-Smit, A. J. Chemistry and physiology of Los Angeles smog. *Ind. Eng. Chem.* **1952**, *44*, 1342-1346.

Haagen-Smit, A. J.; Bradley, C. E.; Fox, M. M. Ozone formation in photochemical oxidation of organic substances. *Ind. Ene. Chem.* **1953,** *45*, 2086-2089.

Hayden, J.; Pursell, D. Pickering Energy Partners, Inc., *The Barnett Shale: visitors guide to the hottest shale play in the US*; 2005; http://www.tphco.com/Websites/tudorpickering/Images/Reports%20Archives/TheBarnettShaleReport.pdf, accessed November 5th, 2014.

Helms, L.: Horizontal Drilling, *DMR Newsletter*, **2008**, 35(1), 1-3.

Howarth, R.W.; Santoro, R.; Ingraffea, A. Methane and the greenhouse-gas footprint of natural gas from shale formations. *Clim. Change*, **2011**, DOI 10.1007/s10584-011-0061-5.

Hyne, N.J., *Nontechnical Guide to Petroleum Geology, Exploration, Drilling and Production*, 2nd ed.; PennWell: Tulsa, 2001; pp 1-5.

Intergovernmental Panel on Climate Change (IPCC). *Climate Change 2001: The Scientific Basis. Contribution of the Working Group I to the Third Assessment Report*. Cambridge Univ. Press: Cambridge, 2001.

Jackson, R.B.; Down, A.; Phillips, N.G.; Ackley, R.C.; Cook, C.W.; Plata, D.L.; Zhao, K. Natural gas pipeline leaks across Washington, D.C. *Environ. Sci. Technol.*, **2014**, 48, 2051−2058.

Karion, A.; *et al*. Methane emissions estimate from airborne measurements over a western United States natural gas field. *Geophys. Res. Lett.* **2013**, *40*, 1-5, doi:10.1002/grl.50811.

Katzenstein, A.S.; Doezema, L.A.; Simpson, I.J.; Blake, D.R.; Rowland, F.S. Extensive regional atmospheric hydrocarbon pollution in the southwestern United States. *P. Natl. Acad. Sci.* **2003b**, *100*, 11975-11979.

Keddelmeier, J.; Staudt, M. Biogenic volatile organic compounds (VOC): An overview on emission, physiology and ecology. *J. Atmos. Chem*. **1999**, *33*, 23-88.

Kyoto Protocol to the United Nations Framework Convention on Climate Change. http://unfccc.int/essential_background/kyoto_protocol/items/1678.php, accessed September 13th, 2014.

Lamarque, J.F.; Bond, T.C.; Eyring, V.; Grainer, C.; Heil, A.; et al. Historical (1850-200) gridded anthropogenic and biomass burning emissions of reactive gases and aerosols: methodology and application. *Atmos. Chem. Phys*. **2010**, 10, 7017-7039.

Lamb, B.; Guenther, A.; Gay, D.; Westberg, H. A national inventory of biogenic hydrocarbon emissions. *Atmos. Environ*. **1987**, *21*, 1695-1705.

Levy, H. Normal atmosphere: Large radical and formaldehyde concentrations predicted. *Science*, **1971**, *173*, 141-143.

Miller, S.M.; Wofsy, S.C.; Michalak, A.M.; Kort, E.A.; Andrews, A.E.; et al. Anthropogenic emissions of methane in the United States. *P. Natl. Acad. Sci.* **2013**, 110 (50), 20018-20022.

Mueller, J.-F. Geographic distribution and seasonal variation of surface emissions and deposition velocities of atmospheric trace gases. *J. Geophys. Res*. **1992**, *97*, 3787-3804.

Mukhopadhyay, P.K.; Dow, W.G. Vitrinite reflectance as a maturity parameter: applications and limitations. American Chemical Society Symposium Series, 570, 1994.

National Energy Board. *Canada's Oil Sands. Opportunities and Challenges to 2015: An Update. An Energy Market Assessment*; Calgary, Alberta, 2006.

Pacala, S.; Socolow, R. Stabilization wedges: Solving the climate problem for the next 50 years with current technologies, *Science,* **2004**, 305, 968-972.

Petron, G.; *et al*. Hydrocarbon emissions characterization in the Colorado Front Range: A pilot study. *J. Geophys. Res.* **2012**, *117*, D04304, doi:10.1029/2011JD016360.

Piccot, S.D.; Watson, J.J.; Jones, J.W. A global inventory of volatile organic compound emissions from anthropogenic sources. *J. Geophys. Res*. **1992**, *97*, 9897-9912.

Pozzer, A.; Pollmann, J.; Taraborrelli, D.; Jöckel, P.; Helmig, D.; Tans, P.; Hueber, J.; Lelieveld, J. Observed and simulated global distribution and budget of atmospheric C_2-C_5 alkanes. *Atmos. Chem. Phys.* **2010**, *10*, 4403-4422.

Railroad Commission of Texas. Barnett Shale information; Austin, TX; 2014. http://www.rrc.state.tx.us/oil-gas/major-oil-gas-formations/barnett-shale-information/, accessed November 5th, 2014.

Ryerson, T.B.; *et al*. Effect of petrochemical industrial emissions of reactive alkenes and NOx on tropospheric ozone formation in Houston, Texas. *J. Geophys. Res.* **2003**, *108*, D84249, doi:10.1029/2002JD003070.

Seinfeld, J.H.; Pandis, S.N. *Atmospheric Chemistry and Physics: From Air Pollution to Climate Change, 2nd ed.*; John Wiley & Sons, Inc.: Hoboken, 2006.

Siddique, T.; Fedorak, P.M.; Foght, J.M. Biodegradation of Short-chain n-Alkanes in Oil Sands Tailings Under Methanogenic Conditions. *Environ. Sci. Technol*. **2006**, 40, 5459-5464.

Simpson, I.J.; Rowland, F.S.; Meinardi, S.; Blake, D.R. Influence of biomass burning during recent fluctuations in the slow growth of global tropospheric methane. *Geophys. Res. Lett.*, **2006**, *33*, L22808, doi:10.1029/2006GL0237330.

Simpson, I.J.; Andersen, M.P.S.; Meinardi, S.; Bruhwiler, L.; Blake, N.J.; Helmig, D.; Rowland, F.S.; Blake, D.R. Long-term decline of global atmospheric ethane concentrations and implications for methane. *Nature* **2012**, *488*, 490-494.

Simpson, I.J.; Blake, N.J.; Barletta, B.; Diskin, G.S.; Fuelberg, H.E.; Gorham, K.; Huey, L.G.; Meinardi, S.; Rowland, F.S.; Vay, S.A.; Weinheimer, A.J.; Yang, M.; Blake, D.R. Characterization of trace gases measured over Alberta oil sands mining operations: 76 speciated C_2-C_{10} volatile organic compounds (VOCs), CO_2, CH_4, CO, NO, NO_2, NO_y, O_3 and SO_2. *Atmos. Chem. Phys. Discuss.* **2010**, *10*, 18507–18560.

Simpson, I.J.; Marrero, J.E.; Batterman, S.; Meinardi, S.; Barletta, B.; Blake, D.R. Air quality in the Industrial Heartland of Alberta, Canada and potential impacts on human health. *Atmos. Environ*. **2013**, 81, 702-709.

Sindelarova, K.; Grainer, C.; Bouarar, I.; Guenther, A.; Tilmes, S.; et al. Global data set of biogenic VOC emissions calculated by the MEGAN model over the last 30 years. *Atmos. Chem. Phys*. **2014**, 14, 9317-9341.

Texas Commission on Environmental Quality. *Dallas-Fort Worth: Current Attainment Status*; Austin, TX, 2014a; https://www.tceq.texas.gov/airquality/sip/dfw/dfw-status, accessed November 2nd, 2014.

Texas Commission on Environmental Quality. *High Ozone in Your Metro Area*; Austin, TX, 2014b; http://www.tceq.state.tx.us/cgi-bin/compliance/monops/ozone_summary.pl, accessed November 2nd, 2014.

Texas Commission on Environmental Quality. Austin, TX, 2014c; https://www.tceq.texas.gov/airquality/barnettshale/bshale-maps, accessed November 5th, 2014.

Timoney, K.P.; Lee, P. Does the Alberta Tar Sands Industry Pollute? The Scientific Evidence. *Open Conserv. Biol. J*. **2009**, 3, 65-81.

U.S. Energy Information Administration. *Natural Gas Processing: The Crucial Link Between Natural Gas Production and Its Transportation to Market*; Washington, DC, 2006; http://www.eia.gov/pub/oil_gas/natural_gas/feature_articles/2006/ngprocess/ngprocess.pdf

U.S. Energy Information Administration: *Annual Energy Outlook 2014 with projections to 2040*; Washington, DC, 2014a; http://www.eia.gov/forecasts/aeo, accessed May 15th, 2014.

U.S. Energy Information Administration: *Natural gas gross withdrawals and production*; Washington, DC, 2014b; http://www.eia.gov/dnav/ng/ng_prod_sum_a_EPG0_VGM_mmcf_a.htm, accessed November 5th, 2014.

U.S. Environmental Protection Agency. *AP-42 Fifth Edition: Compilation of Air Pollutant Emissions Factors. Volume 1: Stationary Point and Area Sources*; Research Triangle Park, NC, 1995; http://www.epa.gov/ttn/chief/ap42/index.html.

U.S. Environmental Protection Agency. *Air Trends Reports and Data*. Air emissions summary through 2005. http://www.epa.gov/airtrends/2006/emissions_summary_2005.html, accessed April 15th, 2015.

U.S. Environmental Protection Agency. *Air and Radiation: National Ambient Air Quality Standards (NAAQS)*; Washington, DC, 2011; http://www.epa.gov/air/criteria.html, accessed November 2nd, 2014.

U.S. Environmental Protection Agency. *Clean Air Act – Title 1: Air Pollution Prevention and Control*; Washington, DC, 2013; http://www.epa.gov/oar/caa/title1.html, accessed November 2nd, 2014.

United Nations Framework Convention on Climate Change. *Full Text of the Convention, Article 2: Objectives;* http://unfccc.int/essential_background/convention/background/items/1353.php, accessed September 13th, 2014.

Chapter 2.
Experimental Methods

2.1 Preparation of Canisters

Whole air samples are collected in electropolished, 2 L stainless steel canisters, outfitted with a Nupro/Swagelok SS-4BG bellows-sealed valve. Prior to sampling, the canisters are evacuated to a pressure of 10^{-2} Torr and allowed to sit for two weeks. After this period, the canister is checked to ensure that the vacuum was held, and there were no leaks. Canisters are then pressurized with ultra high purity helium to approximately 300 Torr, in order to flush out remaining molecules that coat the interior surface of the canister. Lastly, each canister is once again evacuated to 10^{-2} Torr.

Because of repeated use of the whole air canisters for fieldwork, accumulation of particulate matter and heavy hydrocarbons on the metal surface can occur. The result is a reduction in the consistency of the canisters, due to reactions between molecules remaining on the surface of the canister and those in the air samples. This is of particular concern if samples are collected in highly polluted air. In order to minimize this contamination that may occur and to increase their reliability, the canisters are reconditioned every two years.

The reconditioning process begins with 'pumping and flushing' the canisters with clean air. During this step, the canisters are pressurized to 30 psi in Aldrich Park on the UC Irvine campus, where the air is generally removed from pollution sources. Flushing happens when the pressure is released and the canisters are returned to atmospheric pressure. Once this step has been carried out up to 10 times, the canisters are then baked at a temperature of 150 °C for 24 hours [Sive 1998]. The high temperature ensures passivation of the canister surface, or the formation of an oxide layer that prevents unwanted chemical reactivity. Next, the canisters are pressurized with air collected from the White Mountain Research Station. Air from this site is

considered clean due to its 10, 000 foot elevation and distance from sources of pollution. Pressure is held in the canisters for several days and then released to ensure thorough cleaning. As stated, canisters are ready for sampling when they are evacuated to a pressure of 10^{-2} Torr. However, an additional step is required for airborne sampling. Approximately 20 Torr of water vapor is added to the canisters after they have been evacuated. This is done to offset the low water vapor levels encountered at altitudes above 20 thousand feet [Baker 2008].

2.2 Laboratory Analysis

Whole air samples collected are returned to the Rowland-Blake laboratory for measurement of up to 150 volatile organic compounds (VOCs). The instrumental setup allows for trace gas analysis with high precision and accuracy. Three separate gas chromatographic (GC) systems are used for the measurement of carbon monoxide (CO), carbon dioxide (CO_2), methane (CH_4), and C_2-C_{10} VOCs, including non-methane hydrocarbons, halocarbons, alkyl nitrates, oxygenates, and sulfur containing compounds. Each system in described below in further detail.

2.2.1 Carbon Monoxide and Carbon Dioxide Analysis

While detection of CO and CO_2 is carried out on two different detectors on two HP 5890 GCs, they are there joined onto one manifold. A schematic of the manifold is shown in Figure 2.1. The manifold consists of two loops, one each for CO and CO_2, into which a sample aliquot of 500 Torr is loaded. Four switching valves are used to direct flow during analysis. The vacuum on the line is verified with a thermocouple, and a Wallace-Teirnan 1500 Torr pressure gauge is used to load the sample amount onto the loop.

Figure 2.1 Schematic of the manifold used for CO and CO_2 analysis.

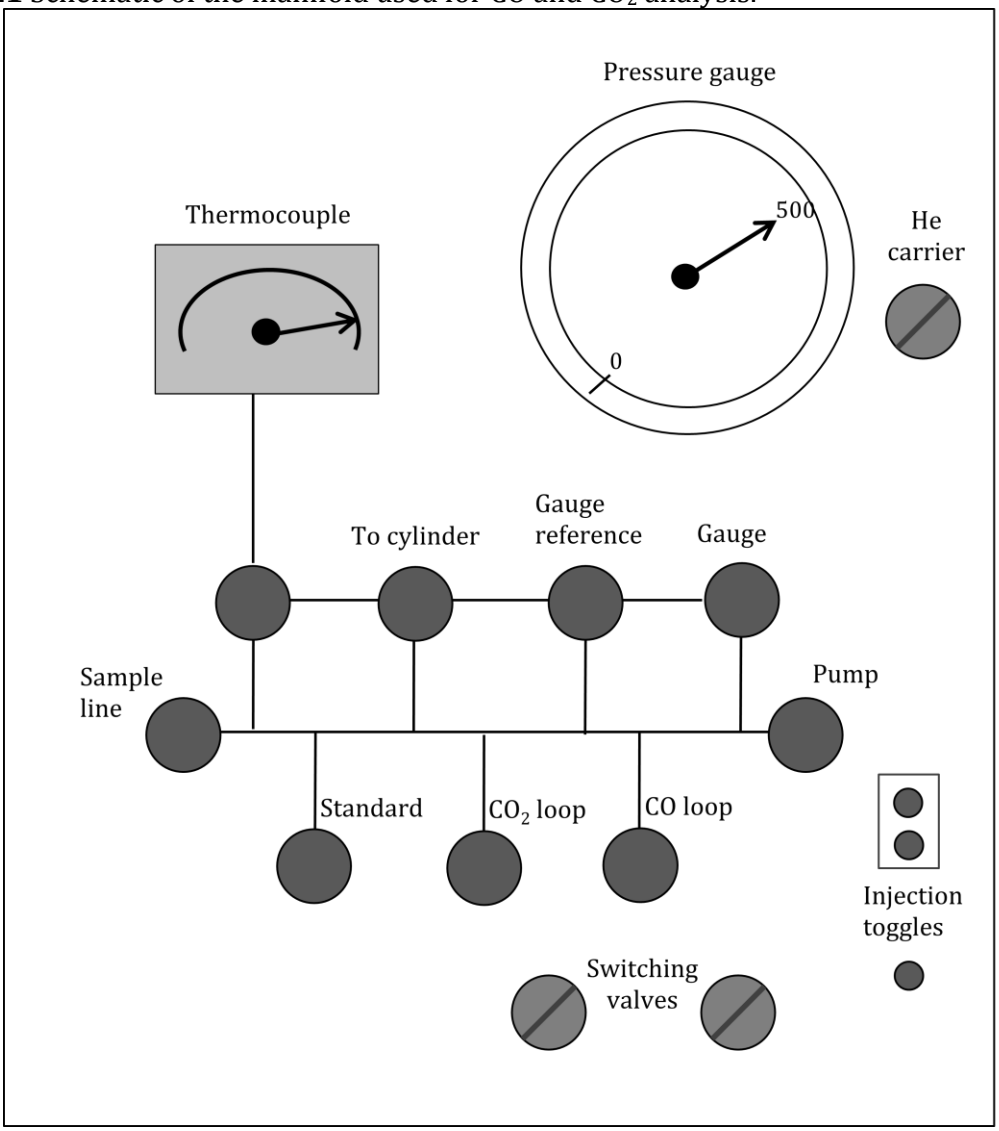

a. Carbon Monoxide

The CO sample column is a ¼" outside diameter (OD), 3 m long stainless steel loop packed with 5A mesh molecular sieve. Three of 4 switching valves on the manifold are used for CO analysis. An 8-port switching valve connected to the vacuum line is set to the 'load' position while the sample is loaded into the evacuated loop. During this time, the He carrier is vented to the room and not into the column. An automated 4-port switching valve is set to 'bypass' mode,

allowing He to flow onto a nickel plate catalyst [Barletta, 2006]. The Ni catalyst is used to convert CO to CH_4, in order to accurately measure the relatively low atmospheric CO levels with an FID detector. The reduction of CO is shown by the following reaction:

$$CO + 3H_2 \rightarrow CH_4 + H_2O \quad (2.1)$$

He is flowed over the catalyst to minimize the amount of oxygen it comes in contact with. Oxygen present in the whole air samples can oxidize the Ni surface and reduce its reactivity. The catalyst temperature is held between 360°C and 385°C, where reduction efficiency is 100% [Thompson and Wood, 1981].

When the sample is injected into the column, the 8-port switching valve goes into the 'inject' position, allowing He to carry the sample into the column for separation. The automated valve remains in the bypass position. During the 7.6-minute analysis time for CO, the GC oven temperature is increased from 60 to 110°C. After 3.5 minutes, the automated switching valve goes into 'load,' and flows sample over the catalyst, allowing for conversion to CH_4 and subsequent detection by the FID.

Once the CO peak is recorded, the automated valve goes back into bypass and the 8-port switching valve is returned to the load position. A second manual 8-port switching valve is simultaneously moved into a 'backflush' position. This reverses the He flow in the column, forcing any remaining CO_2 out of the column so it cannot interfere with the CO peak [Barletta, 2006]. During this back flush, the oven temperature is raised to 150°C before cooling back down to the starting temperature. Figures 2.2 and 2.3 show the positions of the switching valves throughout the sample run time.

The CH_4 signal is output to a computer with Dionex Chromeleon software. Integration of each chromatographic peak is manually inspected. After every eight samples a standard of 192 ppbv CO is run for mixing ratio quantification.

Figure 2.2. Positions of the 3 switching valves during sample injection. On the left is the 8-port switching valve in the inject position; the second 8-port switching valve before backflush is shown in the middle; and the automatic switching valve is shown on the right in load [Barletta, 2006].

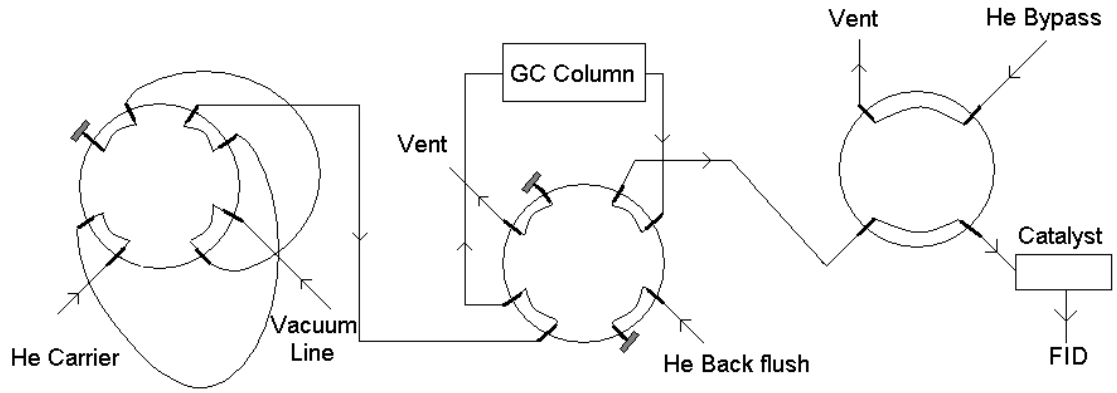

Figure 2.3. Positions of the 3 switching valves at the end of sample analysis. The 8-port switching valve in the load position is shown on the left; the second 8-port switching valve during backflush is shown in the middle; and the automated switching valve in bypass is shown on the right [Barletta, 2006].

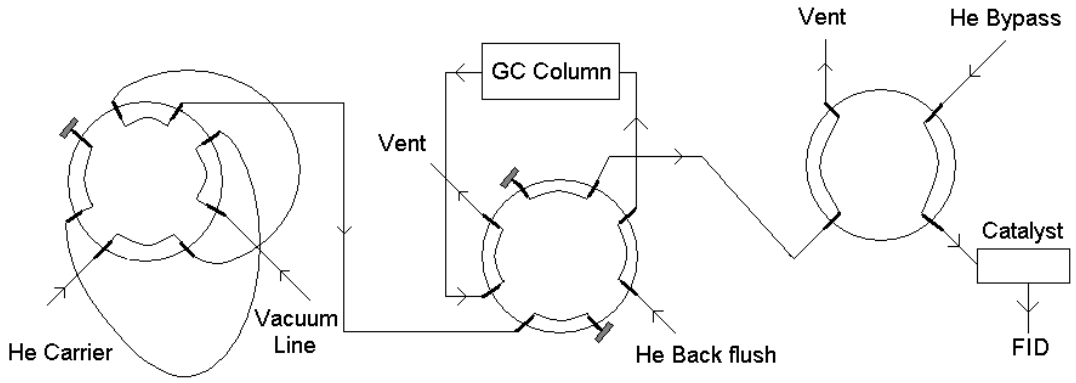

b. Carbon Dioxide

Carbon dioxide analysis is achieved using a similar GC, equipped with a thermal conductivity detector (TCD). Samples are loaded on the loop and injected into the 2 m × 1/8 inch 80/100 Carbosphere packed stainless steel column. He carrier gas is used and flows at a rate of 50 mL/min. During the run, temperature in the GC oven increases from 150°C to 220°C.

The TCD works by measuring the amount of thermal conductivity in the sample relative to the carrier gas. The resultant signal is output to a computer with Chromeleon software, where the peak baselines are inspected. To calculate CO_2 mixing ratios, a working standard of 364 ppmv is analyzed every eight sample runs.

2.2.2 Methane Analysis

Methane detection is achieved after injection of the sample into an HP 5890 GC. The column is 1/8" wide, 0.9 m long stainless steel and packed with 80/100 mesh molecular sieve Spherocarb. A sample aliquot of 400 Torr is loaded onto the evacuated manifold system. The N_2 carrier flows at a rate of 30 mL/min, carrying the sample from the loop to the column at a constant 85°C. After 1.1 minutes methane is detected from the FID and signal is observed on the Spectra-Physics Chromjet Integrator. Working standards of 1.771 ppmv CH_4 are analyzed every eight injections in order to calculate a system response factor. Sample peak heights are compared to the working standard in order to determine the mixing ratio of methane in the sample. A complete description of the system used for methane analysis can be found elsewhere [Blake 1984].

2.2.3 Non-Methane Hydrocarbon (NMHC) Analysis

Since 1983, the analytical system for the measurement and quantification of NMHCs has evolved and improved [Chen 1996]. The current system setup has not been significantly modified since 1998, as described in detail elsewhere [Sive 1998]. It is comprised of a vacuum line with a modified six-port switching valve, a liquid nitrogen delivery system, a splitter box to separate the sample stream, three GCs, and six detectors. A schematic of the NMHC analysis system is shown in Figure 2.4. The various trace gases measured along with the limits of detection, precision and accuracy, are listed in Table 2.1.

Before separation of the whole air samples by the columns contained within the three HP 6890 GCs, samples are first cryogenically preconcentrated. Depending on the "dirtiness" of the sample, different amounts of sample are injected into the system. This prevents samples of high concentrations from overloading the GC, which causes peaks to go off scale on the chromatogram and leads to an inaccurate measurement of sample concentration. For ambient ground samples, sample aliquots of 1265 cm^3 (500 Torr) are trapped in a quarter inch diameter, stainless steel loop immersed in liquid nitrogen. For clean, airborne samples ~2300 cm^3 of sample are used, while for source samples as little as 2.5 cm^3 aliquots are injected. Before trapping on the chilled loop, the sample is passed through a Brooks instrument mass flow controller, which limits the flow to 500 mL/min. The loop is filled with 3mm glass beads, providing increased surface area on which the VOCs can condense. Because of their volatilities N_2, O_2, and Ar remain in the gas phase and are pumped away through the vacuum line. The concentrated samples are then re-volatilized by immersion of the loop in hot water (80°C). The sample is then injected to a splitter box for reproducible delivery to each of the GC columns. Splitting is not equal amongst the columns, but rather is dependent on the column diameter and stationary phase. Detection is achieved with FIDs, electron capture detectors (ECDs), and a quadrupole mass spectrometer (MS).

The first GC houses two columns as well as two detectors, an ECD and a MS. One column is a DB-5 (30 m, I.D. 0.25 mm) connected in series to a Restek 1701 column (5 m, I.D. 0.25 mm). From here, the sample is output to an ECD, which is sensitive to halocarbons and alkyl nitrates. GC #1 also contains a DB-5ms column (60 m, I.D. 0.25 mm) coupled to a HP 5973 quadrupole MS. It is used for oxygenate detection, as well as in selected ion monitoring mode for unambiguous compound detection.

Figure 2.4. Schematic of the analytical system used for NMHC analysis.

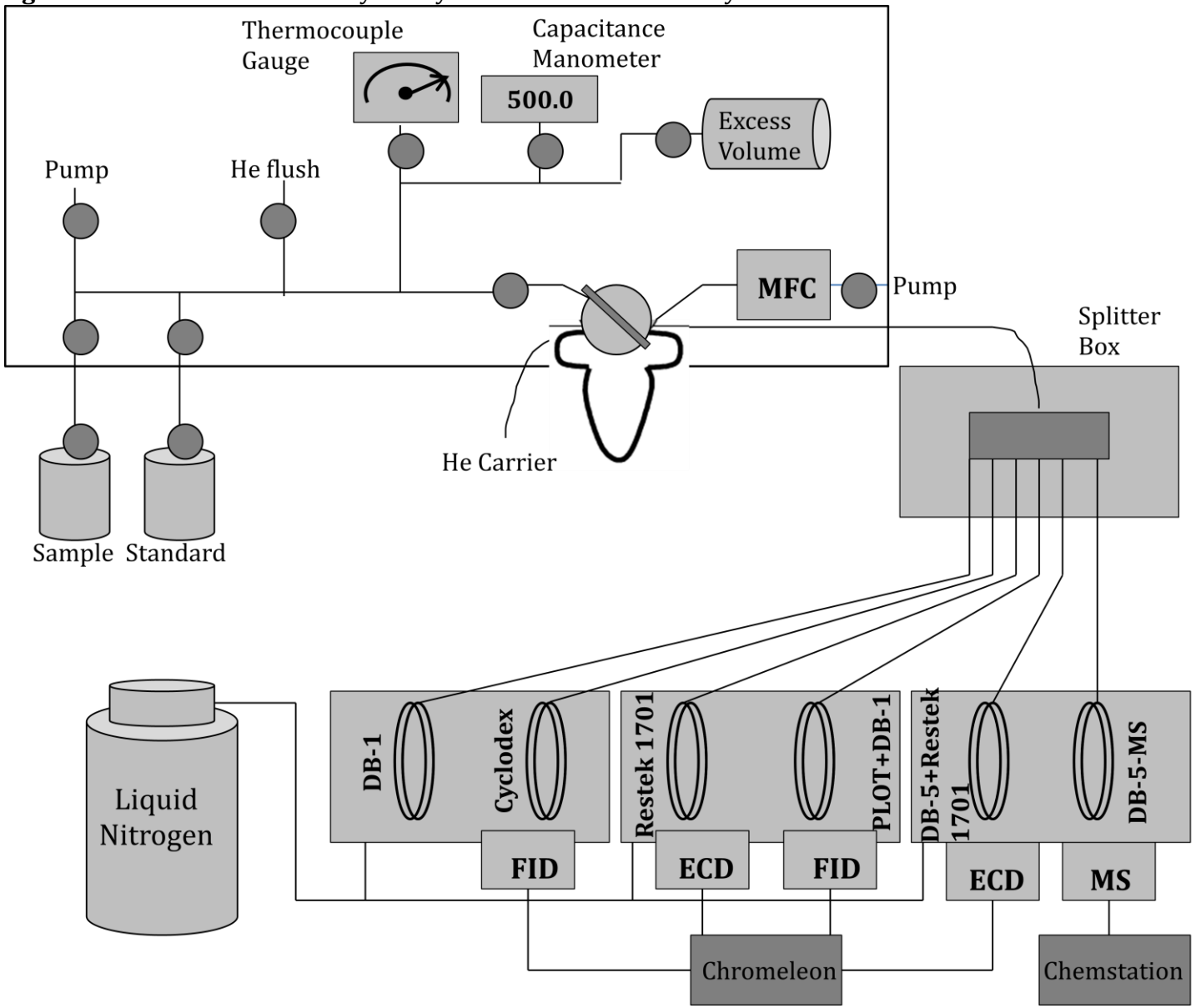

Table 2.1. Gases analyzed by the NMHC system, including alkanes, alkenes, aromatics, oxygenates, halocarbons, and alkyl nitrates. Also listed are limits of detection for each gas, percent precision of 1σ of error, which decreases as LOD is reached, and percent accuracy. [Colman et al., 2001; Simpson et al., 2010]

Compound	LOD (pptv)	Precision (%)	Accuracy (%)	Compound	LOD (pptv)	Precision (%)	Accuracy (%)
Ethane	3	3	5	CFC-11	10	1	3
Propane	3	3	5	CFC-12	10	1	3
i-, n-Butane	3	3	5	CFC-113	5	1	3
i-, n-Pentane	3	3	5	CFC-114	1	1	5
n-Hexane	3	3	5	Methyl Chloroform	0.1	1	5
n-Heptane	3	3	5	Carbon Tetrachloride	1	1	5
n-Octane	3	3	5	Halon-1211	0.1	1	5
2,3-Dimethylbutane	3	3	5	Halon-1301	0.1	10	5
Ethene	3	3	5	HFC-134a	1	3	5
Propene	3	3	5	HCFC-22	2	5	5
1-Butene	3	3	5	HCFC-141b	0.5	3	5
cis-, trans-2-Butene	3	3	5	HCFC-142b	0.5	3	5
1,3-Butadiene	3	3	5	Methyl Bromide	0.5	5	10
Ethyne	3	3	5	Methyl Chloride	50	5	10
Benzene	3	3	5	Methyl Iodide	0.005	5	20
Toulene	3	3	5	Dibromomethane	0.01	5	20
Ethylbenzene	3	3	5	Dichloromethane	1	5	10
m-p-,o-Xylene	3	3	5	Chloroform	0.1	5	10
i-, n-Propylbenzene	3	3	5	Trichloroethene	0.01	5	10
2-, 3-, 4-Ethyltoluene	3	3	5	Tetrachloroethene	0.01	5	10
1,2,3-Trimethylbenzene	3	3	5	1,2-Dichloroethane	0.1	5	10
1,2,4-Trimethylbenzene	3	3	5	Bromodichloromethane	0.01	10	50
1,3,5-Trimethylbenzene	3	3	5	Dibromochloromethane	0.01	5	50
Isoprene	3	3	5	Bromoform	0.01	10	20
α-, β-Pinene	3	3	5	Methyl Nitrate	0.01	2	5
Acetaldehyde	20	30	20	Ethyl Nitrate	0.02	2	5
Ethanol	20	30	20	i-, n-Propyl Nitrate	0.02	2	5
Methanol	50	30	20	2-Butyl Nitrate	0.02	2	5
Acetone	100	30	20	2-,3-Pentyl Nitrate	0.02	2	5

The second GC uses a DB-1 column (60 m, I.D. 0.32 mm) connected to an FID for measurement of C_3-C_{10} hydrocarbons. For detection of heavier hydrocarbons, a Cyclodex column (30 m, I.D. 0.25 mm) is output to an FID.

The third GC houses a Restek 1701 column (60 m, I.D. 0.25 mm) coupled to an ECD, for additional halocarbon and alkyl nitrate analysis. Furthermore, GC #3 also contains a GS-Alumina porous layer open tubular (PLOT) column (30 m, I.D. 0.53 mm) connected to a DB-1 column (5 m, I.D. 0.53 mm) with another FID detector. This allows for separation of C_2-C_5 hydrocarbons. Analytical system parameters for each column/detector are in Table 2.2.

Table 2.2. GC parameters, temperature information and percent flow received by each detector in the NMHC system.

label	Detector	Column type	Temp range (°C)	Run time	% Flow
A	MSD	DB-5ms	-60 – 200	18.5 min	10.1
B	FID	DB-1	-60 – 200	18.5 min	12.2
C	ECD	DB-5/Restek 1701	-60 – 220	17.5 min	11.4
D	ECD	Restek 1701	-20 – 200	17.5 min	9.4
E	FID	PLOT/DB-1	-20 – 200	17.5 min	47.5
F	FID	Cyclodex	-60 – 200	18.5 min	9.4

Detector signals for the ECDs and FIDs are output to Chromeleon software and stored on a computer, while the MSD signal is saved to a computer with HP Chemstation software. The software is programmed to draw baselines under each peak of interest in order to integrate the area under the curve. However, due to inconsistencies in separation, baseline shifting, and coelution, each peak is visually inspected and manually modified to ensure accurate peak integration. Many of the VOCs identified are measured by more than one column-detector combination. This allows for completion of quality control and assurance and the achievement of higher precision and lower limits of detection.

2.3 Calibration and Quantification with Standard VOC Mixtures

Quantitative analysis for a large array of hydrocarbons is achieved with the analytical set up used in the laboratory. To maintain accurate results, calibration procedures are frequently carried out. This includes working standards, which are analyzed every eight samples, and absolute standards that are analyzed daily.

Working standards are prepared in 34 L pontoons by adding reference mixtures of NMHCs to clean air from White Mountain Research Station, which contains background levels of hydrocarbons and halocarbons. The most commonly used reference standard contains a mixture of 1 ppmv NMHCs and a mixture of 10 ppbv alkyl nitrates. Oxygenates can be added from another reference standard. These mixtures are added to the pontoon and then pressurized to 350 psi with White Mountain air, which adds halocarbons but does not add significant amounts of hydrocarbons [Sive 1998]. This desired dilution amount can vary, but generally, standards with 200 pptv hydrocarbons and 10 pptv alkyl nitrates are prepared. Once the standard is made, it is analyzed on the NMHC system and calibrated against a known working standard to ensure the right VOC mixing ratios were achieved.

The primary purpose of the working standards is to determine the detector response factor (RF) for each compound analyzed. The RF is essentially a ratio of the peak area of the compound to its known (absolute) mixing ratio in the standard. The mixing ratio of a compound in the sample is then calculated by the following equation:

$$[C] = \text{Area}_C / \text{RF}_C \tag{2.2}$$

This calculation takes into account the proportionality of the peak area to the amount of analyte present, as well as the linearity of the detector response factors.

2.4 Sample Collection

Ground level ambient whole air samples are collected downwind of the sample target, in the direction of the wind. Wind speeds of at least 1 m/s are preferred for sampling. During sample collection, the valve is opened slightly, allowing ambient air to enter the canister until atmospheric pressure is reached within the canister. A typical canister fill time is between 30 to 60 seconds. To avoid contamination from the body of the sampler, the cans are held in front and above the sampler. In the event of rainfall while sampling, the canister is held at a downward angle so that water does not enter the canister. For each sample collected, several parameters are recorded including the date, canister open time, latitude, longitude, wind speed, and wind direction.

2.5 Alberta Sampling

In 2008, two studies carried out by Rowland-Blake members focused on the industrial regions in Alberta, Canada. The first, on April 10, was a ground based grid study carried out within a 12 x 12 km box in the Industrial Heartland, a large area northeast of the cities of Edmonton and Fort Saskatchewan which is home to over 40 chemical and petrochemical facilities [industrialheartland.com]. During this study, VOC emission hot spots were found downwind of facilities, such as the Shell-Scotford facility, where some aromatic compounds were elevated hundreds of times over local background levels [Simpson et al., 2013]. As part of the NASA ARCTAS airborne campaign in July 2008, seventeen whole air samples were collected over surface mining areas in northeastern Alberta. Measurements again revealed enhancements in concentrations of 53 VOCs over the region [Simpson et al., 2010]. As a result, ground samples were collected in Alberta in 2010, and again in 2012, with the aim of obtaining a more complete assessment of the air quality and impacts of hydrocarbon emissions on a local

and regional level. The main focus was on areas of upgrading refining in Fort Saskatchewan and on areas of surface mining, tailings and upgrading just north of Fort McMurray.

Throughout August 12 and 13, 2010, 70 air samples were collected downwind of the industrial and upgrading sites, including the Provident-Williams (PW), Dow Chemical, and Shell-Scotford facilities. Strong hydrocarbon or sulfurous odors were often associated with each facility and were used as indicators to collect a sample. Because sample collection was limited to two days, the data are considered to be a "snapshot" of emissions associated with industrial activities in the Heartland, and not necessarily representative of long term trends. Background air samples were collected concurrently at a local farm and in a residential neighborhood in Fort Saskatchewan (n = 20). Sample locations are highlighted on a Google Earth image [Google Inc., 2011] shown in Figure 2.5.

From July 5-12, 2012, the Fort Saskatchewan industrial sites were revisited in order to provide a comparison for the 2010 data. An additional 70 air samples were collected downwind of the PW, Dow, and Shell-Scotford facilities. Twenty canisters were also filled at the background farm location.

In Fort McMurray from August 23 – 27, 89 samples were collected downwind of the Syncrude Mildred Lake, Suncor Energy, and the Nexen Long Lake SAGD facilities. This includes areas near extraction, upgraders, tailings ponds and naturally exposed oil sands. Fifteen samples were also collected in local background areas. Furthermore, 29 samples, both background and during an odor episode, were collected in the community of Fort McKay, which lies about 25 km north of the Suncor and Syncrude facilities. The location of each facility is shown in Figure 2.6.

Figure 2.5. Locations of samples collected in Fort Saskatchewan on August 12-13, 2010.

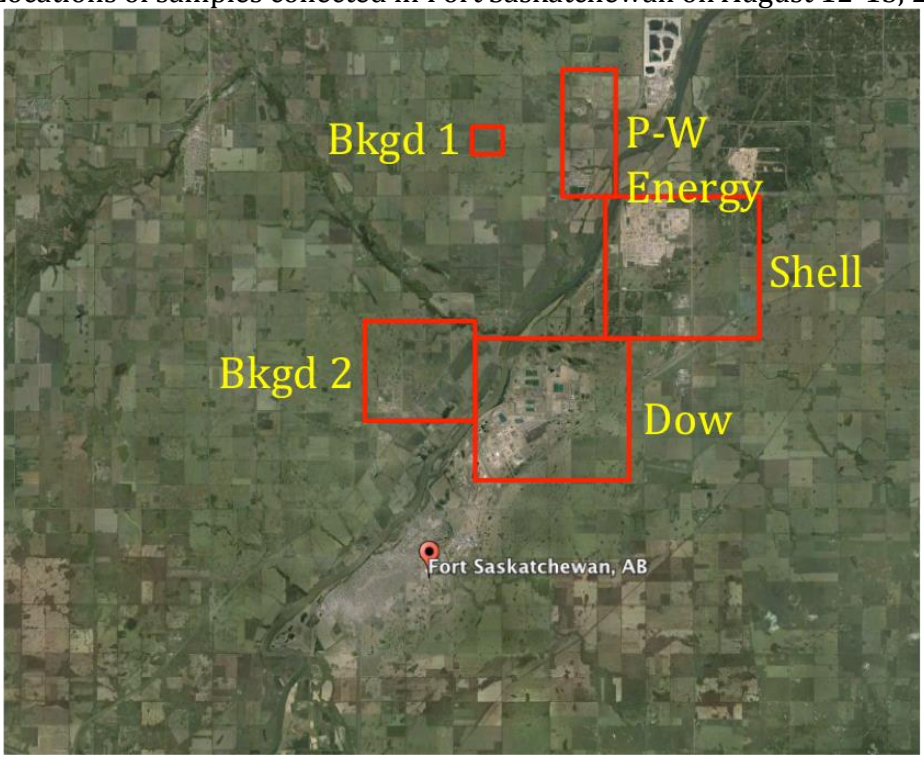

Figure 2.6. Sample sites in Fort McMurray and Fort McKay from August 23-27, 2010.

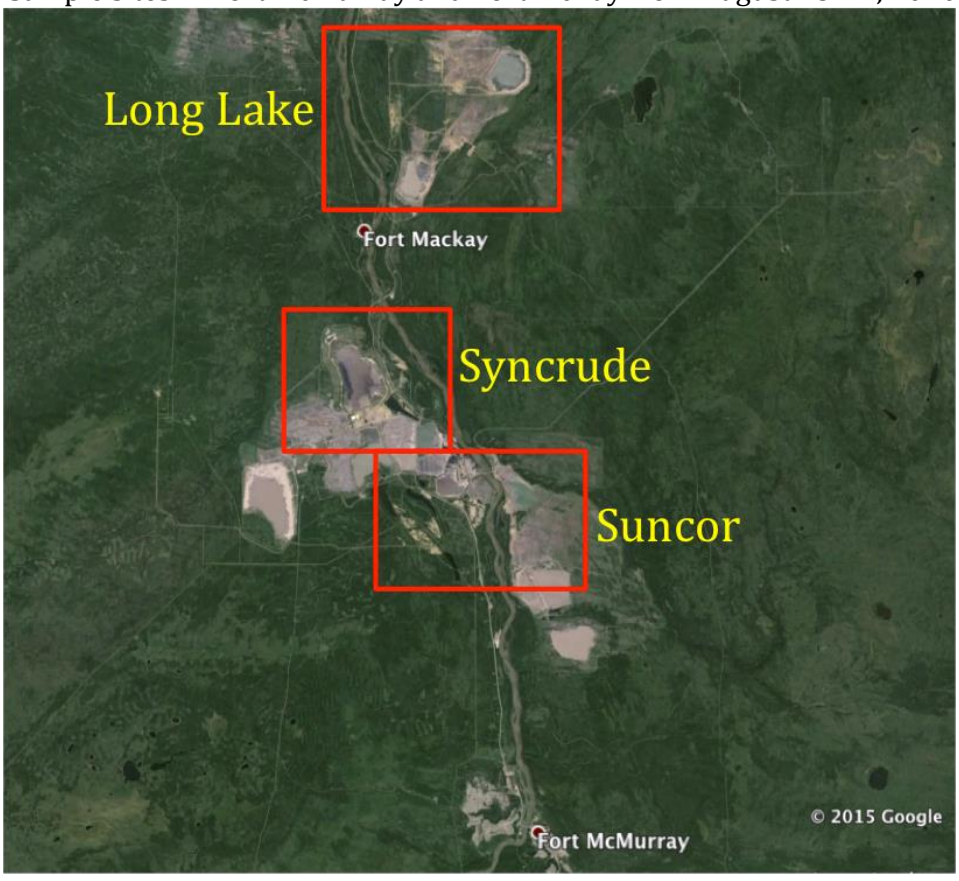

2.6 Barnett Shale Sampling

Oil and natural gas activities in the Barnett Shale are responsible for a variety of atmospheric emissions, including equipment associated with drilling and fracking, processing at facilities, and the transmission of natural gas through pipelines and city gates [Howarth et al., 2011]. From October 16-29, 2013, 120 ground-based whole air samples were collected at each of these sources. To best characterize methane sources in the region, biogenic sources, such as landfills and cattle feedlots were also targeted.

During this campaign a PICARRO trace gas analyzer was installed in vehicle, providing real time information on the ambient methane concentration. An increase of 50 parts per billion (ppbv) of methane over background concentration was used as a threshold for sampling. Oil and gas related sample locations included natural gas well pads (some of which housed separators, condensate tanks or compressors in addition to the well heads); conventional oil wells; compressor stations (both direct samples at leaky components and/or downwind of the station); distribution pipelines and city gates; gathering and processing facilities; and storage facilities. Biogenic methane sources sampled included landfills; cattle feedlots; and a freshwater wetland. Lastly, samples representative of well mixed air in the Barnett shale, both up and downwind, were collected. A drive around of the perimeter of the region was conducted on October 24th. Samples were collected every 15 miles, away from any visible point sources. (NW corner of the perimeter defined as: 33.58989°N, -97.80405°W; SE corner: 32.18464°N, -95.95449°W). Sample locations are presented in Figure 2.7, with red markers indicating the samples taken at the various methane sources, and blue indicating the 'local background' locations.

For the most accurate VOC analysis, air samples were generally collected 'downwind' of point sources, at a distance of 100 meters or less. This ensures trace gas concentrations, but not

significant dilution with background air, so plumes are still captured. Three samples were not included in analysis because they were collected in proximity to more than one CH_4 source, and therefore had mixed contribution from these sources.

Figure 2.7. Sample collection sites in the Barnett Shale from October 16-29, 2013.

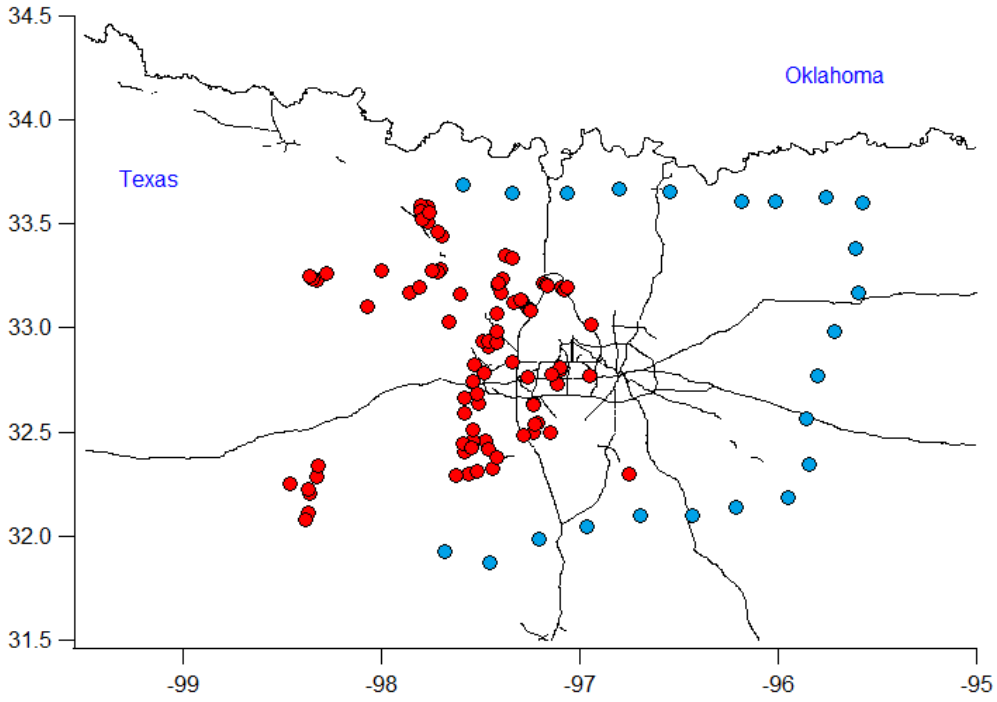

2.8 References

AIHA (Alberta's Industrial Heartland Association). Industry and Organization Profiles, 2012. Available from: www.industrialheartland.com/images/stories/industry/aiha_industry_information_july_2012.pdf.

Baker, A.K. Ground-Based and Aircraft Measurments of Volatile Organic Compounds in the United States and Mexico City Urban Atmospheres. PhD. Thesis, University of California, Irvine, 2008.

Barletta, B. Nonmethane Hydrocarbon and Halocarbon Distributions in Urban Atmospheres of China. PhD. Thesis, University of California, Irvine, 2002.

Blake, D.R. Increasing Concentrations of Atmospheric Methane: 1979-1893. PhD. Thesis, University of California, Irvine, 1984.

Chen, T.Y. 3D PEM-West A NMHC Distribution and Oceanic CH_3I Emissions. PhD. Thesis, University of California, Irvine, 1996.

Colman, J.J.; Swanson, A.L.; Meinardi, S.; Sive, B.C.; Blake, D.R.; Rowland, F.S. Description of the Analysis of a Wide Range of Volatile Organic Compounds in Whole Air Samples Collected during PEM-Tropics A and B. *Anal. Chem.* **2001**, *73*, 3723-3731.

Simpson, I.J.; Blake, N.J.; Barletta, B.; Diskin, G.S.; Fuelberg, H.E.; Gorham, K.; Huey, L.G.; Merinardi, S.; Rowland, F.S.; Vay, S.A.; Weinheimer, A.J.; Yang, M.; Blake, D.R. Characterization of trace gases measured over Alberta oil sands mining operation: 76 speciated C_2-C_{10} volatile organic compounds (VOCs), CO_2, CH_4, CO, NO, NO_2, NOy, O_3 and SO_2. *Atmos. Chem. Phys.* **2010**, *10*, 11913-11954.

Simpson, I.J.; Marrero, J.E.; Batterman, S.; Meinardi, S.; Barletta, B.; Blake, D.R. Air Quality in the Industrial Heartland of Alberta, Canada and Potential Impacts on Human Health. *Atmos. Environ*. **2013**, 81, 702-709.

Sive, B.C. Atmospheric Nonmethane Hydrocarbons: Analytical Methods and Estimated Hydroxyl Radical Concentrations. PhD. Thesis, University of California, Irvine, 1998.

Thompson, B. and Wood, R. The Methanizer in the Model 3700 & Vista Series Gas Chromatograph, *Varian Instruments at Work*, 1981.

Chapter 3.
Volatile Organic Compounds at Sites of Oil Sands Extraction and Upgrading in Northern Alberta

* portions of this chapter are adapted from Simpson, IJ; Marrero, JE; Batterman, S; Meinardi, S; Barletta, B; Blake, DR. "Air quality in the Industrial Heartland of Alberta, Canada and impacts on human health." *Atmos. Environ.* **2013**, 81, 702-709.

3.1 Overview

While the extraction and processing of the vast reserves of oil sands, or bitumen, has seen large development in the recent past, there have been minimal independent measurements or characterization of VOC emissions associated with this industry. Presented in this chapter are the results of a ground-based study conducted in the summer of 2010 in two locations in Alberta, Canada. Near the urban service area of Fort McMurray, which lies within the Athabasca oil deposit, whole air samples were collected downwind of oil sands surface mining areas, tailings ponds, and bitumen upgraders. In addition, samples were collected near various facilities in the Industrial Heartland of Alberta, which lies between the cities of Edmonton and Fort Saskatchewan. Samples were taken downwind of a chemical plant, an energy facility, and an oil sands refinery and upgrading facility. Data from the nearly 300 samples revealed enhancements in the concentration of 43 VOCs, including C_2-C_8 alkanes, C_2-C_4 alkenes and C_6-C_9 aromatic compounds. In industrial plumes, these compounds were elevated from 1.1 up to 90 times above local background levels. The VOCs were used to determine emissions signatures associated with industrial and petrochemical processing, and to assess the impact of these emissions on local photochemistry. Lastly, additional samples collected in Fort Saskatchewan during the winter of 2011 and summer of 2012 were analyzed for seasonal and yearly comparisons.

3.2 Results

3.2.1 Fort McMurray

From August 23 to 27, 2010, whole air samples (n=89) were collected in Fort McMurray (57°N, 111°W) downwind of the Syncrude Mildred Lake, Suncor Energy, and the Nexen Long Lake SAGD facilities. Syncrude and Suncor Energy are two of the major surface mining companies in the region. Air samples were collected near extraction sites; tailings waste ponds; and near their upgraders located on site. Fifteen samples were collected in local background areas, not directly downwind of any of the oil sands facilities. Furthermore, 29 samples were collected in the community of Fort McKay, which lies about 25 km north of the Suncor and Syncrude facilities. These samples were of local background air, including some during an odor episode. Sample sites are mapped in Figure 3.1. Enhancements over background mixing ratios were observed for 40 compounds, including alkanes, alkenes, and aromatics. Observed mixing ratios for background samples and industrial plumes (extraction at Suncor, Syncrude, and Long Lake, and upgrader plumes) are summarized in Table 3.1. Also shown are the average enhancements over background for the industrial sites.

Each of the alkanes measured in the Fort McMurray samples were elevated above background levels downwind of the oil sands extraction and processing facilities. Apart from methane (a long-lived VOC) the most abundant alkanes, based on average values, were ethane (ranging from 1480 ± 590 to 3360 ± 2610 pptv in plumes), propane (from 910 ± 450 to 1430 ± 990 pptv), and n-heptane (from 740 ± 1050 to 2430 ± 3320 pptv). Ethane had the highest maximum value of all the alkanes at 10770 pptv (compared to an average background of 1960 pptv). Industrial point sources had a definite influence on VOC mixing ratios, evident in the large standard deviations for many of the compounds listed in Table 3.1.

Figure 3.1. Sampling sites in the oil sands surface mining and upgrading region between Fort McMurray and Fort McKay, Alberta (57°N, 111°W).

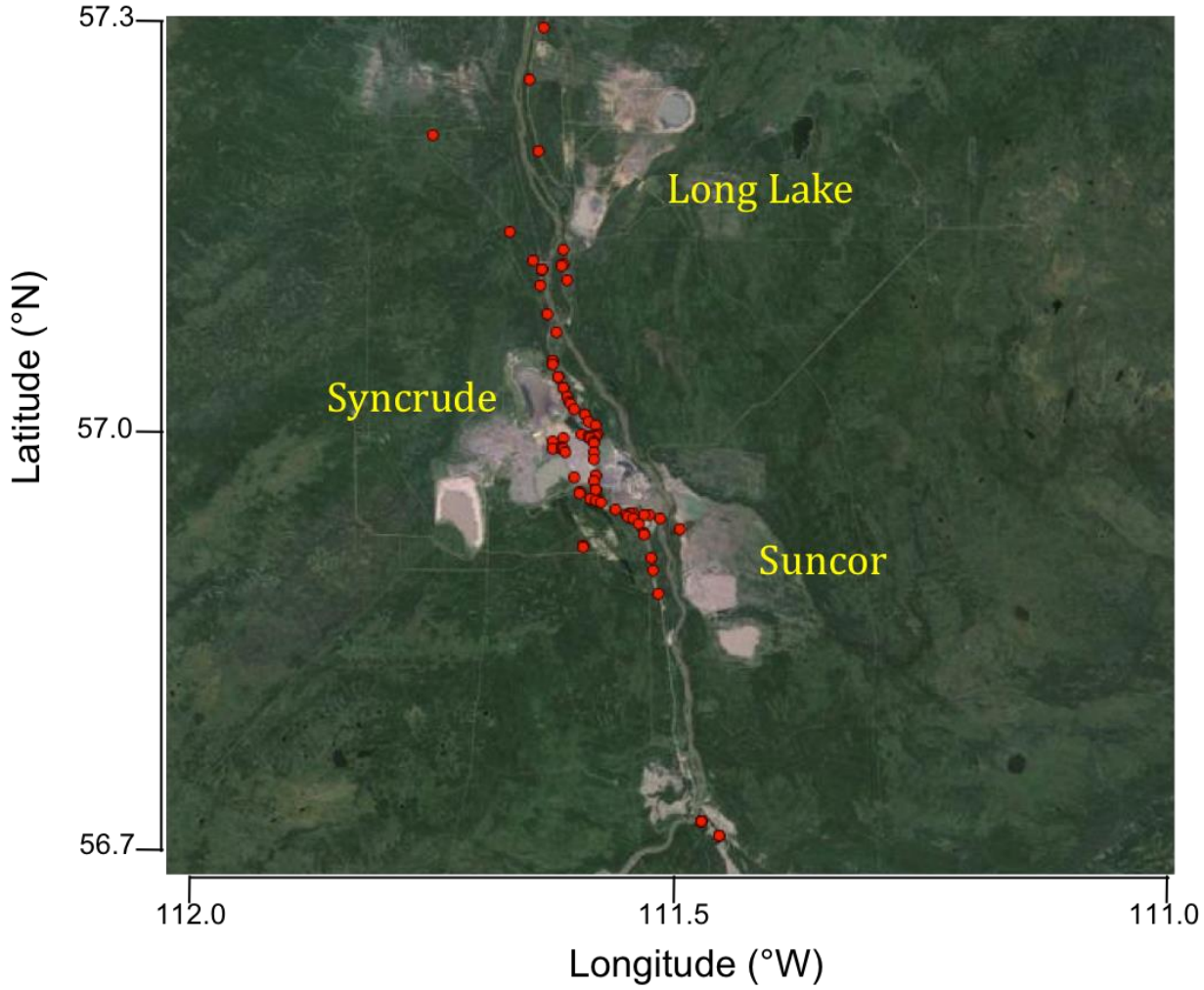

Table 3.1. Statistics for 37 VOCs measured in samples collected near Fort McMurray, Alberta that showed enhancements in industrial plumes compared to background mixing ratios (August 23-27, 2010). Standard deviation (± 1σ) is shown in parentheses. Samples below the limit of detection (3 pptv for hydrocarbons) are denoted as <LOD.

	Min	**Max**	**Bkgd**	**Suncor**	**Syncrude**	**Upgraders**	**Long Lake**	**Avg. Enh.**
			n = 17	n = 33	n = 12	n = 15	n=6	
CO (ppbv)	100	1015	130 (30)	200 (150)	180 (60)	140 (10)	140 (20)	1.3
Methane (ppmv)	1.82	3.53	1.97 (0.10)	2.15 (0.26)	2.19 (0.33)	2.09 (0.40)	1.975 (0.09)	1.1
Alkanes (pptv)								
Ethane	890	10770	1960 (750)	3180 (2510)	3360 (2610)	1480 (590)	2350 (660)	1.4
Propane	260	4680	910 (450)	1430 (990)	1350 (1170)	710 (490)	1330 (500)	1.3
i-Butane	33	4950	260 (160)	1040 (1270)	430 (390)	190 (260)	860 (900)	2.1
n-Butane	100	4740	630 (660)	920 (870)	1370 (1620)	610 (1160)	1340 (1280)	1.5
i-Pentane	42	7810	440 (490)	2050 (2440)	560 (470)	640 (1370)	850 (840)	2.5
n-Pentane	39	6290	360 (620)	940 (1350)	610 (680)	320 (510)	690 (680)	1.7
n-Hexane	10	2370	130 (180)	450 (510)	690 (770)	300 (540)	260 (260)	3.7
n-Heptane	6	10580	120 (150)	740 (1050)	2430 (3220)	800 (2020)	120 (120)	11.2
n-Octane	<LOD	7690	73 (110)	490 (730)	1820 (2570)	690 (1980)	83 (57)	13.7
2,3-Dimethylbutane	<LOD	2180	58 (110)	460 (620)	88 (84)	100 (160)	59 (53)	3.7
2-Methylpentane	21	2390	190 (380)	520 (650)	300 (270)	270 (470)	300 (290)	1.9
3-Methylpentane	7	3250	110 (220)	640 (860)	180 (140)	180 (310)	160 (155)	3.0
Alkenes (pptv)								
Ethene	96	4080	270 (140)	680 (800)	810 (800)	280 (100)	230 (60)	2.2
Propene	18	3760	73 (43)	290 (400)	510 (1000)	79 (62)	51 (25)	4.0
cis-2-Butene	<LOD	300	11 (14)	35 (53)	68 (90)	15 (30)	10 (3)	3.7
trans-2-Butene	<LOD	440	11 (14)	50 (80)	100 (140)	19 (37)	10 (4)	5.3
1,3-Butadiene	<LOD	6320	50 (100)	100 (200)	88 (240)	44 (120)	51 (20)	1.5
Ethyne	84	27000	220 (120)	1240 (4700)	660 (820)	180 (130)	180 (40)	3.2

Table 3.1. (continued) Statistics for 37 VOCs measured in samples collected near Fort McMurray, Alberta that showed enhancements in industrial plumes compared to background mixing ratios (August 23-27, 2010). Standard deviation (± 1σ) is shown in parentheses. Samples below the limit of detection (3 pptv for hydrocarbons) are denoted as <LOD.

	Min	Max	Bkgd	Suncor	Syncrude	Upgraders	Long Lake	Avg. Enh.
Aromatics (pptv)								
Benzene	49	1290	110 (50)	190 (150)	250 (120)	240 (310)	240 (180)	2.1
Toluene	26	8970	170 (130)	610 (670)	1890 (1930)	950 (2280)	200 (170)	6.7
Ethylbenzene	5	1650	33 (23)	120 (140)	380 (420)	160 (420)	37 (35)	6.7
m-Xylene	3	9190	160 (150)	530 (740)	1960 (2600)	690 (1630)	100 (90)	6.4
p-Xylene	<LOD	2560	64 (60)	260 (370)	590 (730)	290 (570)	50 (40)	5.9
o-Xylene	<LOD	2650	38 (36)	150 (210)	580 (800)	180 (400)	26 (25)	8.1
n-Propylbenzene	<LOD	470	5 (3)	23 (29)	89 (140)	23 (58)	10 (8)	8.2
2-Ethyltoluene	<LOD	950	9 (7)	45 (58)	170 (280)	42 (87)	8 (6)	9.9
4-Ethyltoluene	<LOD	880	12 (9)	33 (45)	150 (260)	30 (69)	15 (13)	6.1
1,2,3-TMB	<LOD	1320	10 (7)	65 (83)	240 (400)	26 (40)	8 (7)	10.9
1,2,4-TMB	<LOD	2100	20 (14)	92 (120)	370 (620)	48 (90)	7 (4)	8.4
1,3,5-TMB	<LOD	670	7 (5)	40 (49)	110 (190)	18 (34)	8 (5)	8.5
Oxygenates (pptv)								
Acetone	160	1840	540 (370)	510 (180)	580 (380)	470 (100)	640 (90)	1.1
MAC	3	510	58 (88)	100 (120)	52 (39)	95 (52)	140 (130)	1.4
MVK	61	1600	310 (360)	360 (130)	250 (170)	440 (180)	440 (60)	1.1
Acetaldehyde	130	11490	1790 (1260)	2400 (1760)	3250 (3790)	1510 (1800)	2530 (1450)	1.3
Sulfurous (pptv)								
DMS	2	81	11 (10)	13(7)	14 (3)	51 (21)	16 (5)	2.4

Figure 3.2. Average C_2-C_8 alkane mixing ratios observed in background and industrial samples collected in Fort McMurray between August 23 and 27, 2010.

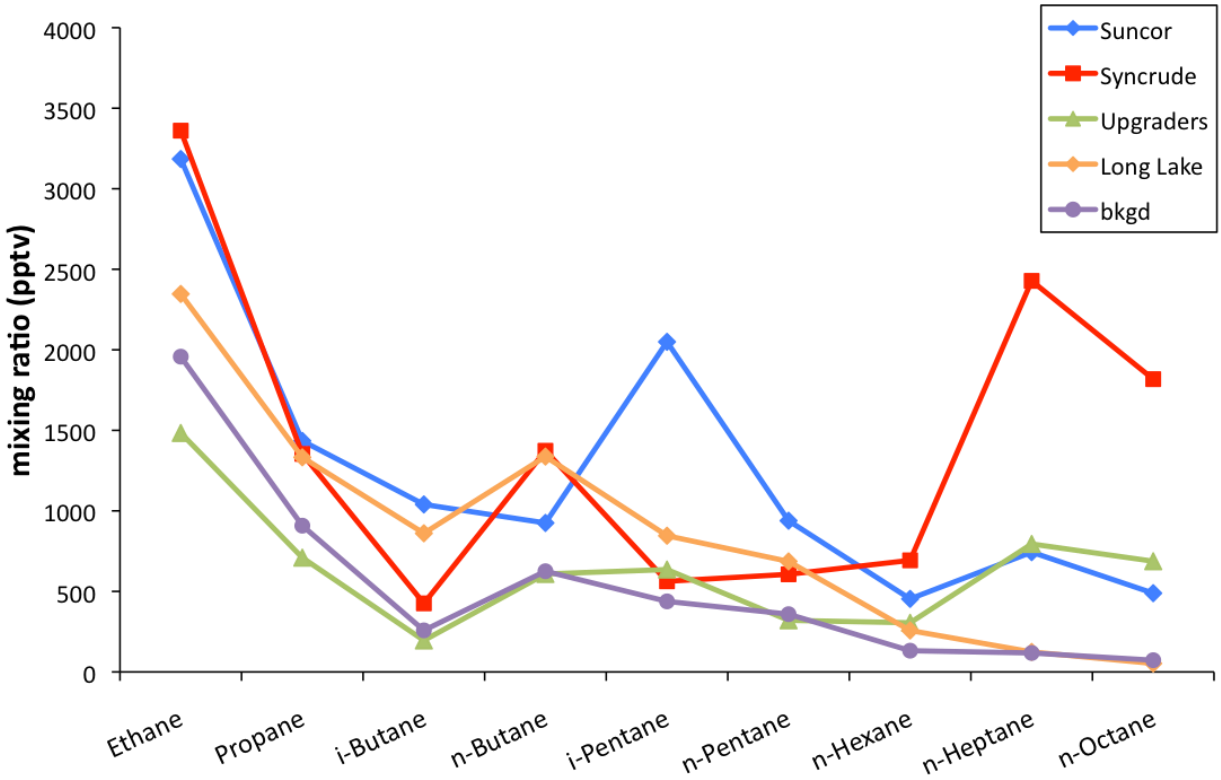

As illustrated in Figure 3.2, alkanes were emitted in abundance from the Suncor and Syncrude facilities. The high mixing ratios of methane (CH_4) and ethane (C_2H_6) at these facilities (Table 3.1) are indicative of emissions from natural gas, which is produced at these sites in addition to crude oil, and is also used as an energy source or extraction and upgrading processes [www.energy.alberta.ca]. The compounds with the highest average enhancements were n-heptane and n-octane, which were 11 and 14 times greater than average background levels. This is despite the general trend of decreasing alkane concentrations with increasing carbon number. The emission of longer chained alkanes from oil sands may not be unexpected however, due to the composition of oil sands crude, which is generally enriched in heavy hydrocarbons [Alboudwarej et al., 2006; Hyne, 2001]. Samples collected downwind of the Syncrude surface mining operations and upgraders had the highest average n-heptane mixing

ratios. This is likely due to the upgrading process, which tends to use pentane or heptane to dilute the bitumen, lower its viscosity and produce a higher quality crude oil [Gray, 2008]. Further, C_3-C_5 solvents are typically used at the Long Lake SAGD facility to precipitate out asphaltenes from the bitumen, explaining their higher observed mixing ratios when compared to other sample locations [Gray, 2008].

In general, average alkane concentrations were significantly lower than those observed in Houston and Galveston Bay (a large metropolitan and petrochemical manufacturing center). Values were more comparable to samples collected in oil fields in Kern County, California. For example, an average ethane value of 3360 ± 2610 pptv was observed in the Alberta samples, compared to 8353 pptv in Houston/Gavelston Bay (HGB) and 4200 ± 3300 pptv California oil fields during the same season [Gilman et al., 2009; Hartt, 2013].

As Table 3.1 shows, the alkenes measured in Fort McMurray were elevated up to 5 times above background. Ethene mixing ratios in the oil sands region ranged from 270 ± 140 pptv in background samples to 810 ± 800 pptv in the most concentrated plumes. These values are significantly larger than California oil fields, where local background levels did not exceed 50 pptv and average summertime mixing ratios near oil wells were less than 100 pptv [Hartt, 2013]. Samples collected in Alberta fell within the range of ethene mixing ratios observed in a study of 28 urban centers throughout the United States US (260-2430 pptv), despite the primarily forested and rural setting of Fort McMurray [Baker et al., 2008].

Within this sample region, C_6 to C_9 aromatics were roughly 2 to 11 times higher than average background concentrations, even though background concentrations were generally quite high. In comparison, background measurements in Fort Saskatchewan (Section 3.2.2) were 90 ± 34, 85 ± 142 and 22 ± 25 pptv for benzene, toluene, and m-xylene, respectively, compared to 110 ± 50, 170± 130, and 160 ± 150 pptv in Fort McMurray. A similar trend was

observed for nearly every aromatic compound in the Fort McMurray industrial plumes, where the highest mixing ratios were downwind of the Syncrude facility. Again, this is likely due to the high asphaltene content of crude bitumen, before it is upgraded [Gray, 2008]. There was also generally good correlation between aromatics and C_6-C_8 alkanes, further suggesting emissions of aromatics from extraction or dilution of bitumen.

Oxygenated and sulfur containing compounds also appeared to be enhanced over background concentrations, although not to the same extent as many of the other hydrocarbons in this study (Table 3.1). Acetaldehyde and acetone were the two most abundant oxygenated VOCs (OVOCs) measured. The largest source of atmospheric acetaldehyde is the photochemical oxidation of hydrocarbons, as described in Chapter 1.1.2 [Finlayson-Pitts and Pitts, 2000; Millet at al., 2010]. Alkyl nitrates are another class of compounds generated from photochemistry, but were not elevated in the air samples. This suggests an additional source of acetaldehyde, as photochemistry alone cannot explain observed mixing ratios. Furthermore, the two sulfur compounds measured, dimethyl sulfide (DMS) and dimethyl disulfide (DMDS), were enhanced over background. Reduced sulfur compounds are used for the cracking of hydrocarbons during bitumen upgrading [Wang et al., 2007]. Samples collected in the Fort McKay community on a day with a permeating smell, referred to as an odor episode, had the highest concentrations of DMDS as well as methyl vinyl ketone (MVK). While these compounds are typically characterized by a pungent odor, their odor threshold is above the concentrations observed. On this particular day however, winds were from the south of Fort McKay, or from the direction of the Suncor and Syncrude facilities, implying that the odor had an industrial source. Average values for OVOCs and the sulfur compounds are illustrated in Figure 3.3.

Figure 3.3. Average mixing ratios for oxygen and sulfur-containing compounds observed in background and industrial samples collected in Fort McMurray and Fort McKay in August 2010.

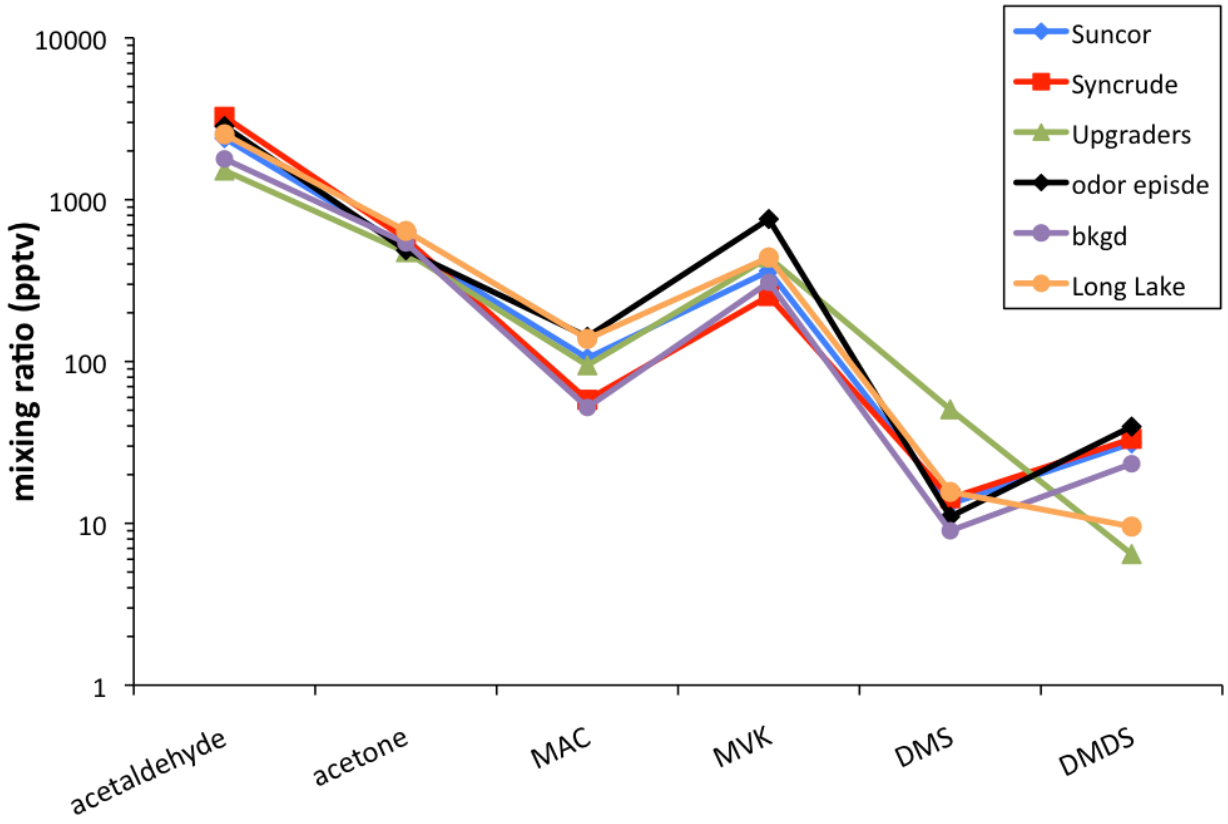

Correlations between hydrocarbons typically associated with ONG activities or combustion were used to assess the influence of such activities on local air masses. Two tracers of oil and natural gas are CH_4 and C_2H_6. Despite high mixing ratios, however, there was poor correlation between these light alkanes ($R^2 < 0.4$). This suggests either limited use of natural gas as diluents at each of these sites, or low leakage rates of produced natural gas. A stronger ONG signature is illustrated in a plot of propane against ethane, shown in Figure 3.4a. Slopes for each of the industrial locations ranged from 0.35 to 0.72 propane/ethane with moderate correlation ($R^2 > 0.6$), similar to ratios observed in California oil wells [Hartt, 2013]. In the instance of incomplete combustion, this ratio is much smaller, ranging from 0.06 – 0.27 mol propane/mol ethane [Fraser et al., 1998; Lough et al., 2005]. Urban regions, with a higher volume of vehicular combustion sources, would also be expected to have a higher ratio of

Figure 3.4. Correlation plot of a) propane/ethane, b) ethene/ethane, and c) benzene/ethyne for samples collected downwind of industrial facilities in Fort McMurray.

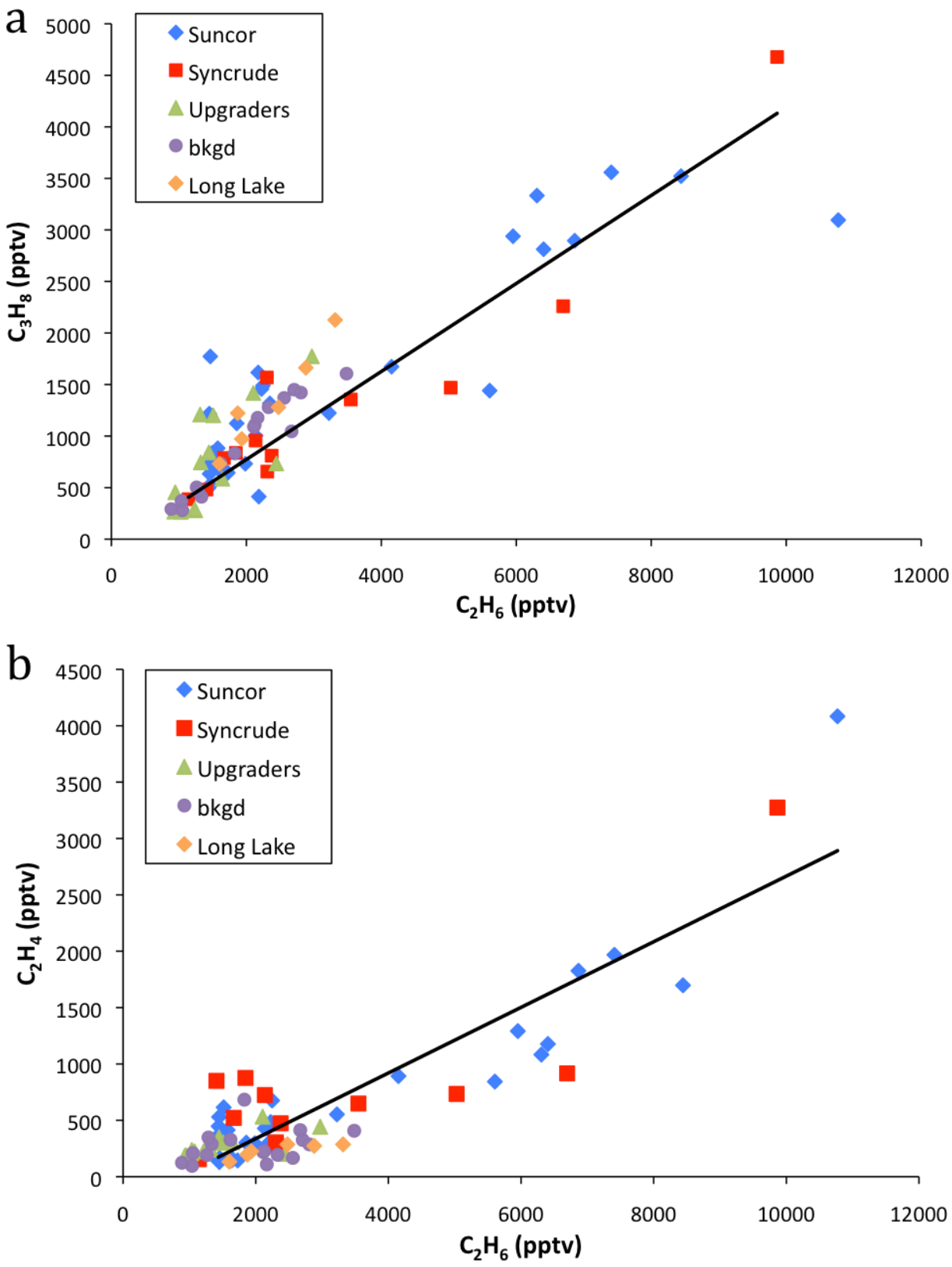

Figure 3.4. Correlation plot of a) propane/ethane, b) ethene/ethane, and c) benzene/ethyne for samples collected downwind of industrial facilities in Fort McMurray.

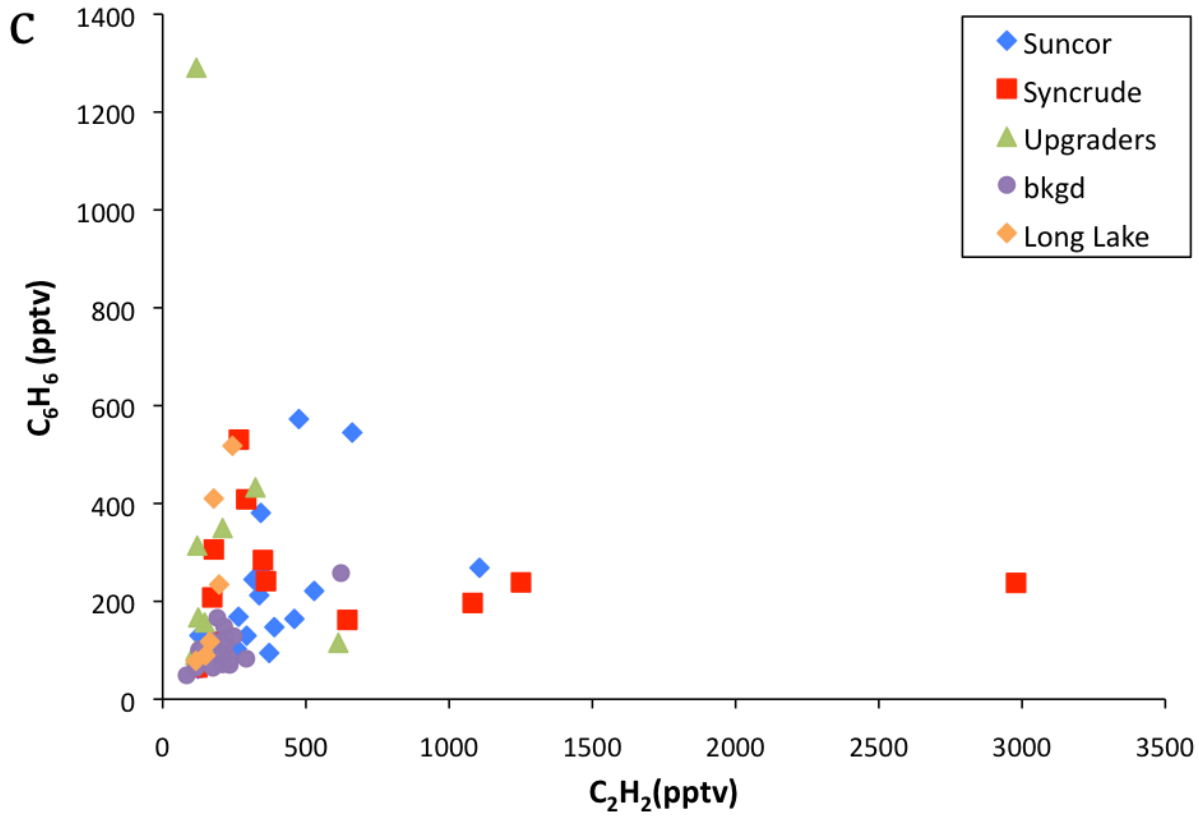

ethene to ethane. Samples collected in Fort McMurray however, exhibited ratios ranging from 0.1 to 0.3 pptv/pptv, implying the importance of emissions from ONG infrastructure. The influence of industrial sources is also seen in a correlation plot of benzene to ethyne (Figure 3.4c). These two gases can be used as urban anthropogenic tracers because they have low rates of reactivity and are emitted in abundance in vehicle exhaust. In such an environment, they would be expected to have strong correlation [Fortin et al., 2005]. However, in Fort McMurray benzene and ethyne have poor correlation ($R^2 < 0.5$) downwind of most of the extraction and processing sites, suggesting an additional benzene source [Gilman et al., 2009]. While samples collected near the Long Lake facility exhibited a stronger correlation, the benzene to ethyne ratio was also significantly higher (3.6 ± 1.1), suggesting that this additional benzene stems from a source that is petrochemical in nature.

Using tracer analysis, emissions signatures associated with oil and natural gas can be discerned from the Fort McMurray samples. However, the extent to which the distance of sample locations to large point sources (nearby or further away) affected the observed trends is unclear. Industrial plumes were generally fresh, meaning little air mass aging, as evidenced in the high ethyne to CO ratios [Xiao et al., 2007]. Despite this possible influence, it appears that emissions from oil are the dominant source of the elevated VOC concentrations in the region. More specifically, it is the extraction and processing of oil sands that lead to the observed VOC enhancements. By comparison, samples collected at naturally exposed bitumen along the Athabasca River were not elevated above background mixing ratios for most of the VOCs measured. Exceptions include 1,3-butadiene, toluene, ethylbenzene, the xylenes, methacrolein (MAC), MVK, and DMS, which were nearly double background levels. Emissions of alkenes like 1,3-butadiene and aromatic compounds, which are also elevated in industrial plumes, may be of concern in the region, as prolonged exposure to these compounds has also been associated

with negative health effects [Infante and White, 1983; Ware et al., 1993; Filley et al., 2004]. This will be further addressed in Chapter 5.

3.2.2 Fort Saskatchewan

Between August 12 and 13, 2010 air samples were collected concurrently upwind and downwind of several facilities in the Industrial Heartland of Fort Saskatchewan, as shown in Figure 3.5. Twenty upwind samples, representing background air, were collected at a local farm and residential neighborhood. Industrial samples were collected downwind of the Provident-Williams (PW), Dow Chemical, and Shell-Scotford facilities (n=70) and were often coupled to strong odors. As these samples were collected over a limited time period, they are considered a to be a 'snapshot' of emissions and not a long-term regional assessment. Samples were determined to be representative of local industry and not influenced by urban emissions from the city of Edmonton, which lies 20 km to the SW. A decade of climate data shows that the prevailing wind direction in Fort Saskatchewan is from the NW during the summer [McCallum et al., 2003], and was experienced during the sampling dates (Figure 3.6). Furthermore, significant contributions from in situ photochemistry were considered unlikely, as weather conditions were not favorable for such reactions (cold and rainy).

a. VOC Concentrations and Emissions Signatures

Complete statistics for background and industrial samples collected in Fort Saskatchewan are summarized in Table 3.2. Once again, the influence of point sources is reflected in the large standard deviations associated with industrial plume samples. Total emissions were much greater than those observed in Fort Murray for a similar number of air samples. For instance, the total VOC loading in Fort Saskatchewan was 3.67 ppmv compared to 2.25 ppmv in Fort McMurray. Of the 77 compounds measured, 43 were elevated anywhere

from 1.1 to 64 times over background. This includes each of the alkanes and alkenes measured, as well as some aromatics, oxygenated compounds, and halocarbons.

Figure 3.5. Sampling locations within the Industrial Heartland of Fort Saskatchewan, Alberta (53°4'N, 113°1'W) collected on August 12 and 13, 2010.

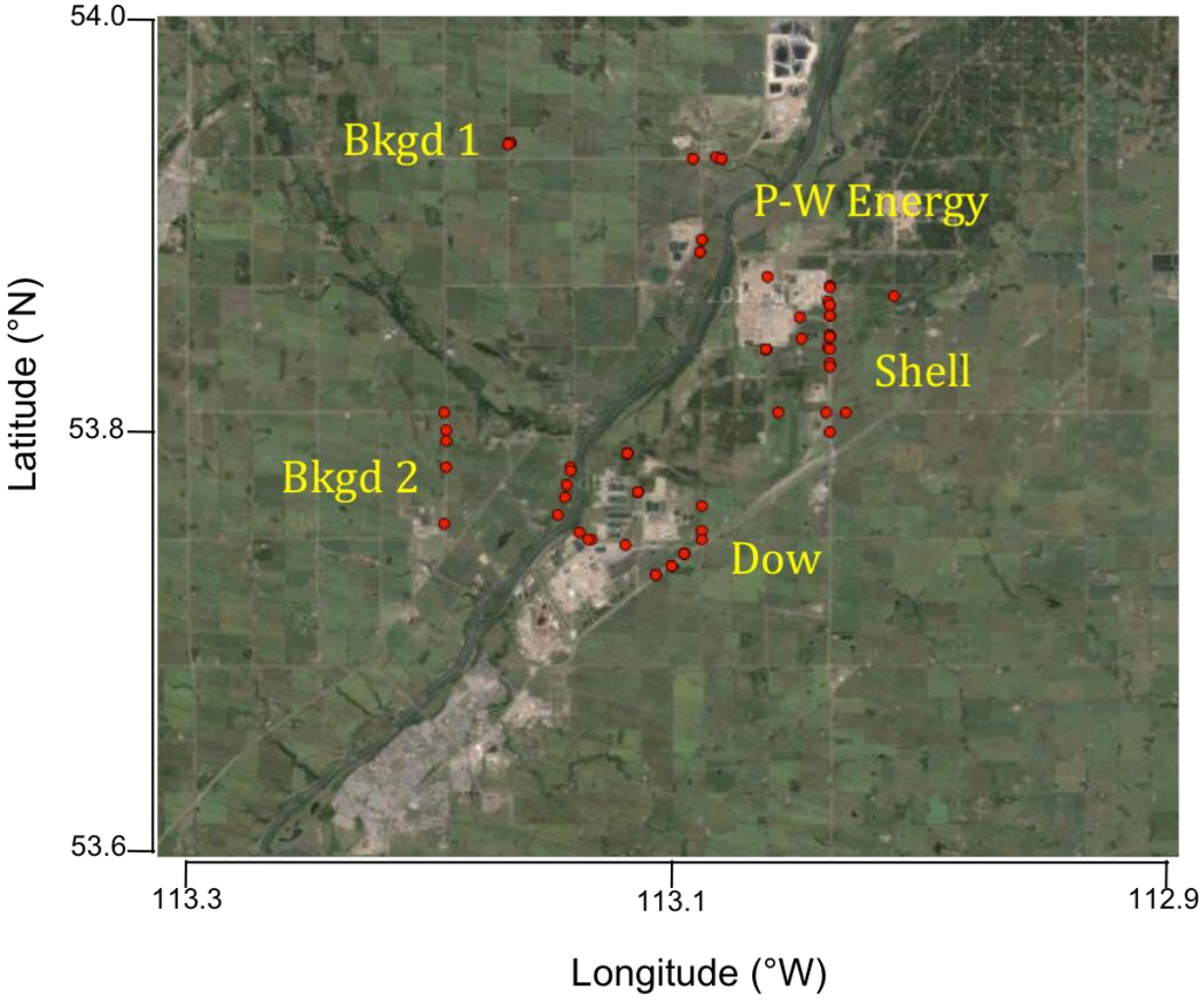

Figure 3.6. Wind rose for Fort Saskatchewan derived from hourly meteorological data and corresponding to air sample collection times during August 12-13, 2010 [Clean Air Strategic Alliance].

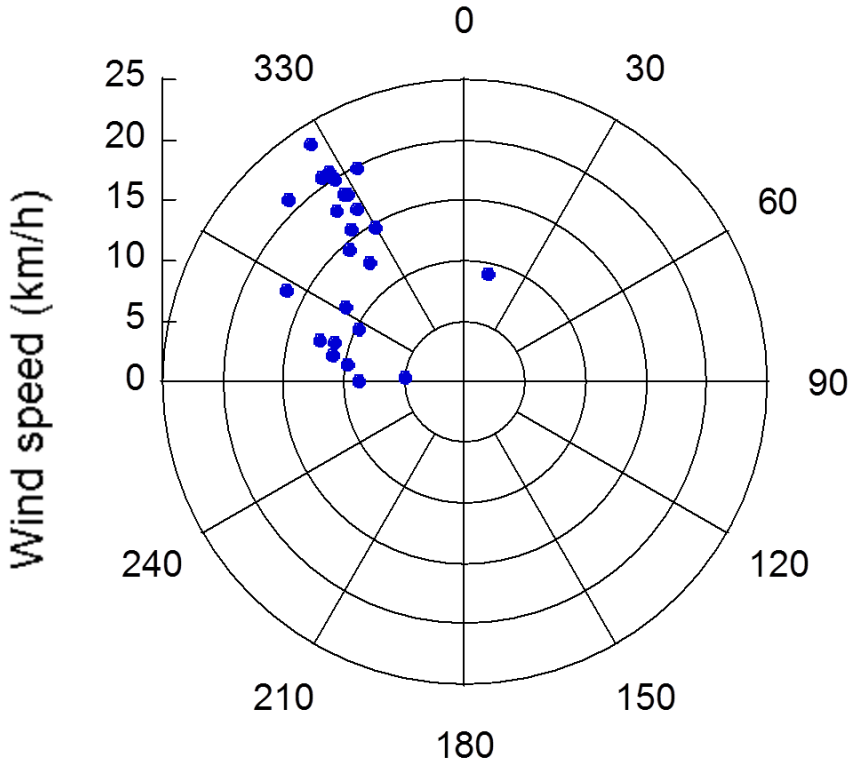

During sample collection, plumes could only be captured from the perimeter of the industrial facilities, sometimes 500 m or more downwind. This means that the extent to which mixing occurred, and plumes were diluted with background air, is unclear. As such, industrial plume averages calculated from the top 10th percentile mixing ratios for each species (n = 8) are also included in Table 3.2. In the top 10% of plume samples, substantial enhancements were observed, ranging from 1.7 to 740 times over background, on average. The compounds with the largest enhancements include ethylbenzene, 3-methylpentane, and 2,3-dimethylbutane.

Table 3.2. Statistics for VOCs measured in samples collected in Fort Saskatchewan, Alberta that showed enhancements in industrial plumes compared to background mixing ratios (August 12-13, 2010). Standard deviation (± 1σ) is shown in parentheses. Samples below the limit of detection (3 pptv for hydrocarbons) are denoted as <LOD.

	Min	**Max**	**Bkgd**	**PW Energy**	**Dow Chemical**	**Shell-Scotford**	**Top 10%**	**Avg. Enh.**
			n = 17	n = 33	n = 12	n = 15	n=8	
CO (ppbv)	115	180	132 (20)	135 (10)	135 (10)	140 (10)	155 (4)	1.1
Methane (ppmv)	1.86	2.15	1.89 (0.04)	1.93 (0.05)	1.90 (0.02)	1.92 (0.02)	1.97 (0.03)	1.1
Alkanes (pptv)								
Ethane	1120	12440	1930 (620)	1290 (3340)	1490 (1940)	12230 (480)	7840 (2250)	1.2
Propane	290	44500	875 (370)	8590 (11360)	2130 (1180)	1890 (1830)	17050 (12200)	4.8
i-Butane	49	26100	170 (100)	3270 (6500)	380 (220)	810 (1340)	10510 (6960)	8.8
n-Butane	85	50170	350 (200)	7650 (13080)	870 (690)	3950 (5850)	21940 (12320)	11.7
i-Pentane	41	103130	250 (440)	5380 (15900)	490 (640)	7860 (19110)	35640 (33460)	18.1
n-Pentane	46	97070	150 (130)	4060 (12070)	330 (500)	6750 (17870)	30570 (31010)	24.7
n-Hexane	11	51950	39 (20)	690 (2070)	70 (60)	3180 (9700)	13260 (16920)	33.7
n-Heptane	4	5350	18 (13)	150 (430)	27 (14)	430 (1020)	1750 (1580)	11.2
n-Octane	<LOD	760	7 (4)	34 (90)	8 (3)	96 (160)	360 (170)	7.0
2,3-Dimethylbutane	<LOD	11640	7 (5)	110 (350)	9 (9)	640 (2150)	2690 (3900)	36.7
2-Methylpentane	13	61800	52 (26)	650 (1890)	85 (54)	3520 (11460)	14600 (20500)	27.1
3-Methylpentane	3	40000	18 (12)	350 (1060)	29 (32)	2270 (7450)	9420 (13400)	49.5
Alkenes (pptv)								
Ethene	7	9420	290 (180)	290 (140)	1590 (2950)	740 (930)	3790 (2920)	3.0
Propene	19	107190	77 (53)	8620 (26600)	130 (180)	810 (1340)	20390 (36480)	41.7
cis-2-Butene	<LOD	3830	4 (4)	320 (970)	4 (3)	29 (42)	740 (1330)	33.3
trans-2-Butene	<LOD	5410	5 (5)	520 (1450)	5 (4)	38 (55)	1040 (1890)	39.7
1,3-Butadiene	<LOD	27350	76 (200)	32 (57)	64 (180)	960 (4990)	3700 (9550)	4.6
Ethyne	140	830	180 (40)	210 (60)	310 (190)	210 (50)	450 (170)	1.4

Table 3.2. (continued) Statistics for VOCs measured in samples collected in Fort Saskatchewan, Alberta that showed enhancements in industrial plumes compared to background mixing ratios (August 12-13, 2010). Standard deviation (± 1σ) is shown in parentheses. Samples below the limit of detection (3 pptv for hydrocarbons) are denoted as <LOD.

Aromatics (pptv)	**Min**	**Max**	**Bkgd**	**PW Energy**	**Dow Chemical**	**Shell-Scotford**	**Top 10%**	**Avg. Enh.**
Benzene	57	6590	90 (34)	280 (400)	120 (70)	1230 (1940)	4340 (1600)	6.0
Toluene	LOD	2690	85 (140)	160 (280)	74 (22)	420 (580)	1340 (600)	2.6
Ethylbenzene	LOD	23290	8 (8)	20 (30)	13 (5)	1440 (4570)	5660 (8290)	64.2
m-Xylene	3	3380	22 (20)	80 (160)	33 (12)	400 (760)	1490 (950)	7.7
p-Xylene	LOD	1220	9 (9)	29 (50)	13 (5)	160 (290)	560 (380)	7.2
o-Xylene	LOD	650	4 (4)	8 (16)	4 (2)	82 (160)	310 (190)	8.5
4-Ethyltoluene	LOD	570	3 (2)	4 (3)	3(2)	59 (110)	92 (50)	8.4
1,2,4-TMB	LOD	240	3 (2)	6 (4)	3 (2)	24 (40)	310 (220)	4.1
1,3,5-TMB	LOD	830	4 (2)	6 (4)	4 (2)	81 (49)	93 (62)	7.8
Oxygenates (pptv)								
MAC	6	20220	61 (26)	250 (180)	90 (300)	1020 (310)	4450 (6380)	7.4
Acetaldehyde	120	74250	1700 (840)	11960 (19070)	2590 (2250)	6070 (8320)	32140 (18310)	4.0
Sulfurous (pptv)								
DMS	8	55	26 (11)	25 (6)	27 (6)	28 (11)	43 (7)	1.1
DMDS	14	290	56 (20)	61 (3)	60 (3)	59 (3)	64 (2)	1.1

In general, the alkanes were the most abundant VOCs emitted in this study region. Downwind of the industrial facilities, their mixing ratios were varied and unlike background samples, followed no trend with carbon chain length. In particular, *i*- and *n*-pentane had maximum mixing ratios of 103 and 97 ppbv, respectively. While these were less than maximum values observed in the HGB region (183 ppbv for each), average pentane mixing ratios were larger in Fort Saskatchewan than in Houston. More specifically *i*- and *n*-pentane averaged 7860 ± 19110 and 6750 ± 17870 pptv downwind of the Shell-Scotford site (high standard deviations driven by concentrated plumes), respectively, compared to 3610 and 2230 pptv in Houston [Gilman et al., 2009].

Correlations between the different types of VOCs were also examined to determine the influence of industrial emissions on local air. Ethane and propane were well correlated in industrial samples (R^2=0.6), and had the highest concentrations downwind of PW and Dow Chemical. In the most concentrated industrial plumes, they were elevated over background by factors of 5.9 and 33, respectively. The isomers of butane also exhibited high correlation, as seen in Figure 3.7a. The largest mixing ratios were downwind of the PW complex, which produces C_2-C_4 alkanes, and Shell-Scotford, which lists a mixture of C_3-C_4 alkanes as some of its products [AIHA, 2012]. The slope of *i*-butane plotted against *n*-butane was 0.47 ± 0.02 for industrial sites. This signature is typical of LPG (liquefied petroleum gas) emissions, and not vehicular exhaust (0.2 – 0.3) or natural gas, which has a 1:1 ratio [Russo et al., 2010]. A similar ratio (0.42 ± 0.03) was observed from measurements over the oil sands region in 2008 [Simpson et al., 2010]. Maximum values in this study were similar to those observed in Mexico City in the 1990s when LPG was a source for butanes [Blake and Rowland, 1995].

The C_5-C_7 alkanes where also elevated downwind of the Shell-Scotford and PW complexes (specifically Access Pipeline), which both produce diluent and process and separate

bitumen [AIHA, 2012]. Shown in Figure 3.7b is a plot of *i*-pentane versus *n*-pentane. For the three industrial plumes, the ratio ranged from 1.1 to 1.3 pptv/pptv. A smaller slope for the pentanes is characteristic of oil or natural gas emissions, illustrating the influence of oil sands processing in the region. This is compared to background samples, which had a slope of 3.2± 0.17, and is more typical of urban emissions [Gilman et al., 2013].

The C_2-C_4 alkenes also showed large enhancements in the Industrial Heartland, ranging from 1.4- to 42 times above average background concentrations. Ethene had the smallest average enhancement over background, with mixing ratios ranging from 290 ± 140 to 1590 ± 2950 pptv in the Fort Saskatchewan plumes. This is within the range for summertime concentrations observed across 28 US cities (260-2450 pptv), but smaller than average HGB values (2692 pptv) [Baker et al., 2008, Gilman et al., 2009]. Propene actually showed the highest maximum mixing ratio (107 ppbv) of all NMHCs analyzed during the Alberta ground study. This value was observed downwind of PW, which has active natural gas liquids and propene fractionation projects [AIHA, 2012]. This propene value is still nearly double the maximum propene value seen in the 2006 Houston study [Gilman et al., 2009].

Sources of atmospheric alkenes and alkynes include incomplete combustion and industrial emissions. A ratio of ethene to ethyne with a low value (1-3) is characteristic of combustion, while a higher value (10-30) is representative of petrochemical emission sources [Ryerson et al., 2003]. When plotted, these two gases had poor to moderate correlation, with a bimodal trend observed in the Shell-Scotford samples (not shown). Examining just the top 10% of industrial plume samples results in a ratio of 10.7 ± 1.0, suggesting the influence of industrial rather than vehicular sources on alkene emissions.

Like many of the other hydrocarbons, all of the C_6-C_9 aromatics analyzed in Fort Saskatchewan had moderate to strong enhancements when compared to background levels

Figure 3.7. Correlation plot of a) i-butane/n-butane and b) i-pentane/n-pentane for samples collected downwind of industrial facilities in Fort Saskatchewan.

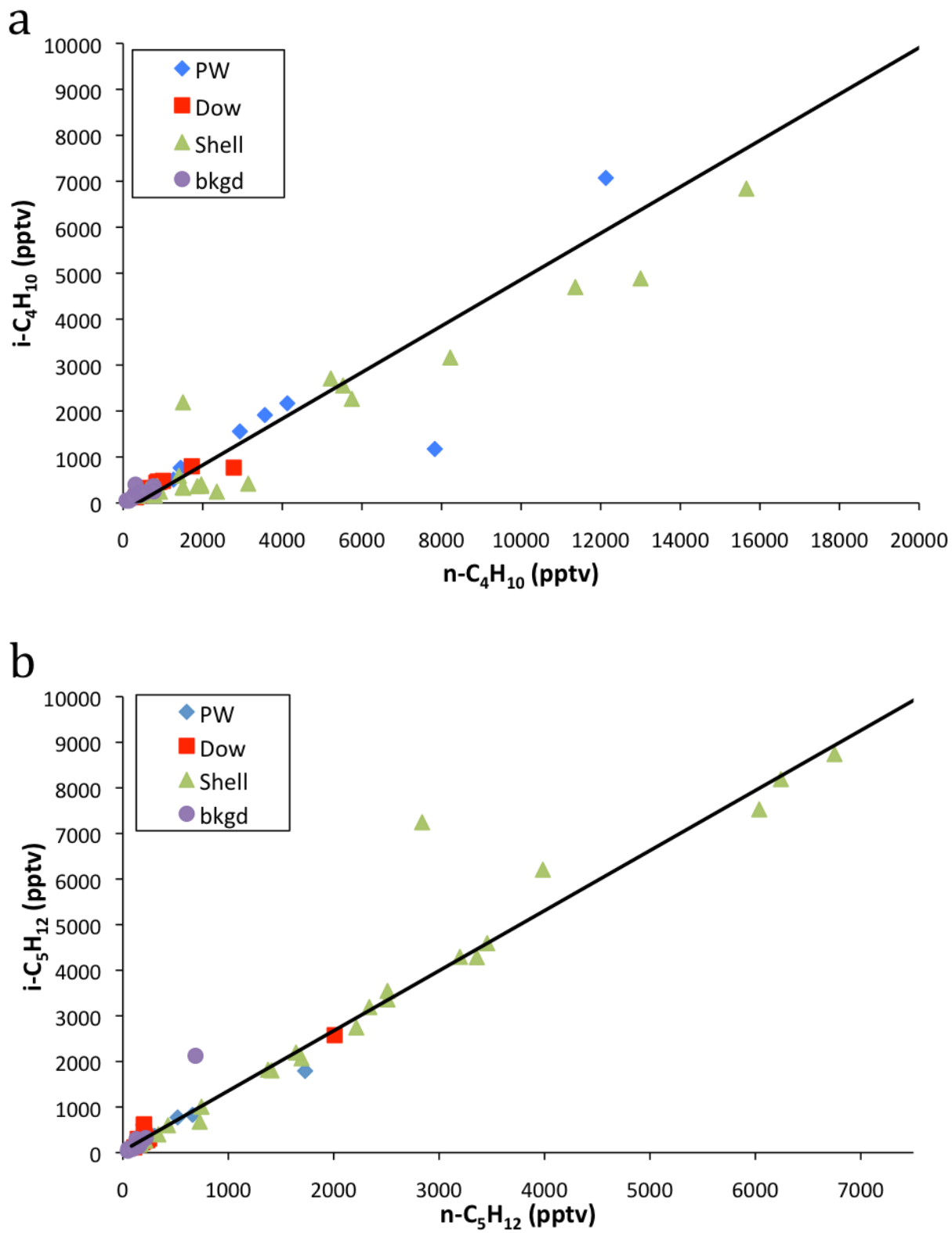

(3.1 – 90 times larger). As with many of the other NMHCs, elevated amounts of aromatics occurred downwind of the Shell-Scotford site. Ethylbenzene was the most elevated aromatic compound. Its maximum concentration, 23,290 pptv, was 3000 times larger than local background. This was the largest maximum enhancement for any of the VOCs in this study, and is nearly 8 times larger than the highest ethylbenzene mixing ratio observed in Houston (3070 pptv). In fact, average values of all of the aromatic compounds in our study were comparable to those in the TexAQS study, with only maximum observed concentrations being lower in Fort Saskatchewan [Gilman et al., 2009].

Toluene and the xylenes correlated strongly with one another ($0.79 \leq R^2 \leq 0.98$) as well as with the C_5-C_7 alkanes ($0.60 \leq R^2 \leq 0.99$). The highest levels of toluene and the xylenes (2.7 ppbv and 0.65 – 3.4 ppbv, respectively) were measured downwind of the Shell Scotford complex, which lists heavy aromatics among its products. It is also houses a bitumen upgrader, which processes diluted oil sands from Fort McMurray. The maximum toluene level was 70 times higher than background, but lower than values in megacities like Mexico City, Tokyo and Beijing (nearly 10 ppbv), or near major petrochemical centers in Texas or Spain (16 – 77 ppbv) [Gilman et al., 2009; Ras et al., 2009]. Similarly, the C_9 aromatics, which include ethylbenzene, trimethylbenzenes, and n-propylbenzene, correlated strongly with n-octane ($R^2 > 0.75$), in the same plume. The Shell-Scotford refinery manufactures a range of products including gasoline, diesel and jet fuel, and reportedly released 0.562 tonnes of ethylbenzene in 2010 [NPRI, 2012]. The petrochemical source of aromatics is also evident when comparing benzene to ethyne or CO. The lack of correlation between these gases suggests little influence from vehicular combustion. Surprisingly, the C_9 aromatics had smaller concentrations than Fort McMurray, implying raw bitumen as a larger source for these compounds than industrial processing.

Enhancements were also observed in oxygen-containing species, particularly methacrolein (MAC) and acetaldehyde, which were 7.4 and 4.0 times greater than background levels. Methacrolein was correlated with C_5-C_7 alkanes, and like these compounds, was elevated downwind of the Scotford complex. Methacrolein and MVK are both major isoprene oxidation products [Montzka et al., 1993], but were uncorrelated during this study ($R^2 < 0.1$). This is likely because the 20 ppbv maximum MAC level exceeds what isoprene oxidation chemistry would predict, and therefore its high concentrations can be attributed almost exclusively to industrial emissions. Similarly, and as in the Fort McMurray samples, acetaldehyde mixing ratios were much larger than if photochemical secondary production were its only source. Its maximum value, of 74 ppbv, or an enhancement 55 times greater than background, was downwind of Shell-Scotford. In 2010, this facility reported a release of 3.9 tonnes of acetaldehyde [NPRI, 2012].

Although samples of industrial plumes were typically associated with some strong odors, DMDS and MVK values were not elevated, as they were in Fort McMurray. This could be due to less bitumen upgrading at the Fort Saskatchewan industrial sites, or could suggest that crude bitumen is itself a natural source of these compounds, as they were also elevated in samples taken near exposed oil sands.

Isoprene, α-pinene and β-pinene are biogenic VOCs, emitted naturally from plant species [Guenther et al., 1995]. Accordingly, average background concentrations of these compounds were higher than in any of the industrial sites (620±190, 24±11, and 37±18 pptv compared to 500±210, 29±19, and 36±21 pptv). The same holds true for biogenics in Fort McMurray, although mixing ratios there were larger than in Fort Saskatchewan. This is because northern Alberta is dominated by the tree coverage of the boreal forest, while Fort Saskatchewan is part of the Edmonton Metropolitan Area. Further, low correlations ($R^2 < 0.1$)

between isoprene and CO suggest that emissions of isoprene are dominated by biogenic, rather than anthropogenic sources.

b. VOC Emissions Reporting

While 40 VOCs were significantly enhanced in industrial plumes as compared to local background concentrations, less than 20 are quantified in the National Pollutant Release Inventory (ethene, propene, 1,3-butadiene, 1,2- dichloroethane, n-hexane, benzene, toluene, ethylbenzene, total xylenes, 1,2,4-trimethylbenzene, acetaldehyde, carbonyl sulfide, chloroform, trichloroethene, HCFC-22) [NPRI, 2012]. Furthermore, most individual companies report emissions for less than half of these VOCs. As Table 3.2 shows, more than 10 different C_2-C_8 alkanes were enhanced in industrial plume samples, but only n-hexane is included in the NPRI. While light alkenes and some aromatic compounds are reported in the NPRI the absence of alkanes is significant, as they can have a large impact on local air quality (will be addressed in the following section). A compound like 1,3-butadiene for instance, can not only undergo photochemical reactions, but is a known carcinogen. However, only one company in the region reports its emissions. In some instances, emissions rates are reported but are not necessarily accurate. For instance, NPRI listings for VOC emissions from an individual Canadian refinery were found to be underestimated by a factor of nearly 20 [Chambers et al., 2008]. Verification of emissions, in the form of independent air quality monitoring will go a long way to improve public inventories in the Heartland.

3.3 Ozone Formation Potential

As described in Section 1.1.2, VOCs and nitrogen oxides (NO_x) are important precursors to the photochemical formation of tropospheric ozone. While the actual amount of O_3 produced is dependent on the oxidation mechanism and NO_x concentrations, the contribution of

individual VOCs to O_3 formation is a function of their concentration and reactivity towards OH [Carter, 1994]. VOCs react with OH on timescales that extend from minutes to days. Essentially, the faster the reaction is with OH, the faster intermediates like HO_2 and RO_2 are produced, which ultimately leads to greater NO oxidation and O_3 formation [Finlayson-Pitts and Pitts, 2000]. Here, contributions of VOCs to OH reactivity are quantified for both Fort Saskatchewan and Fort McMurray in order to assess the potential towards ozone formation.

Reactions of OH radicals with CH_4, CO, VOCs and NO_2 can propagate or terminate the chain reaction of ozone formation. Propagation or termination is influenced by the contribution of each species to the total OH reactivity, or R_{OH} total, which is defined by equation 3.1:

$$R_{OH} = \sum k_{OH+CO}[CO] + k_{OH+CH_4}[CH_4] + k_{OH+VOC}[VOC] + k_{OH+NO_2}[NO_2] \quad (3.1)$$

where k_{OH} is the temperature-dependent OH reaction rate coefficient (cm^3 $molecules^{-1}$ s^{-1}), as reported in Atkinson and Arey [2003]. Brackets denote average concentrations, in molecules cm^{-3} for all compounds, excluding the long-lived halocarbons and photochemically generated alkyl nitrates. The reaction of OH and NO_2 is a termination step that generates nitric acid (HNO_3), removing reactive oxidants that would otherwise lead to O_3 formation. It should be noted however, that NO_2 mixing ratios were not measured in canister samples during this ground study. Previous work in places like Houston, New York, and Mexico City have shown that nitrogen oxides can contribute as much as 50% to R_{OH} [Mao et al., 2010]. For Fort McMurray reactivities, hourly data from the Wood Buffalo Environmental Association monitoring stations for the sampling dates and approximate locations were incorporated into calculations [Clean Air Strategic Alliance]. The calculated reactivity in each location reflects only compounds measured and is likely an underestimation of R_{OH} and not the actual total value.

The overall OH reactivities due to VOCs vary significantly for each of the locations sampled in Fort Saskatchewan, as shown in Figure 3.8. R_{OH} was greater than upwind values at each of the industrial sites, with the greatest potential O_3 formation downwind of the PW Energy complex. In background air, the R_{OH} was 4.08 s^{-1}, which falls within the range of the lowest (local clean air) values in locations like the Gulf of Mexico or Pearl River Delta, which spanned from 1 to 10 s^{-1} [Gilman et al., 2009; Kim et al., 2011; Lou et al., 2010]. Unsurprisingly, biogenic compounds contributed the most to the total background R_{OH} (1.65 s^{-1}) in Fort Saskatchewan, with isoprene accounting for 94% of this biogenic contribution. Oxygenated compounds, had the next highest influence on R_{OH}, followed by CO and CH_4. The later two compounds exhibited small changes in concentrations at each location, leading to a constant contribution to R_{OH} of 0.29 and 0.68 s^{-1}, respectively, and are therefore not included in Figure 3.8.

In comparison, the OH reactivities were 4.89 s^{-1} in the Dow Chemical plume, 12.1 s^{-1} downwind of the Shell-Scotford facility, and 16.6 s^{-1} in the PW plume. In other words, these facilities are 1.2, 3.0, and 4.0 times more likely to generate O_3 under similar NO_x conditions. The composition of R_{OH} downwind of each of the industrial sites is summarized in Table 3.3. In the PW plume, alkenes had the largest impact, responsible for 43% of the total R_{OH}. This value (7.08 s^{-1}) is driven by the large propene concentrations observed. Similar results were seen in airborne studies over Houston, where alkenes were identified as the compounds most responsible for rapid O_3 formation (due to their faster reaction with OH) [Ryerson et al., 2003; de Gouw et al., 2009]. In each of the plumes however, oxygenated species were an important class of compounds, accounting for nearly 30% of the reactivity. Aromatic compounds, on the other hand, had a minimal effect on calculated reactivities, contributing only to R_{OH+VOC} downwind of the Shell-Scotford complex.

Figure 3.8. Total R_{OH+VOC} (in s^{-1}) for the four areas sampled in Fort Saskatchewan during August 2010. Values are colored by VOC type: alkanes, alkenes, aromatics, biogenics, and oxygenates.

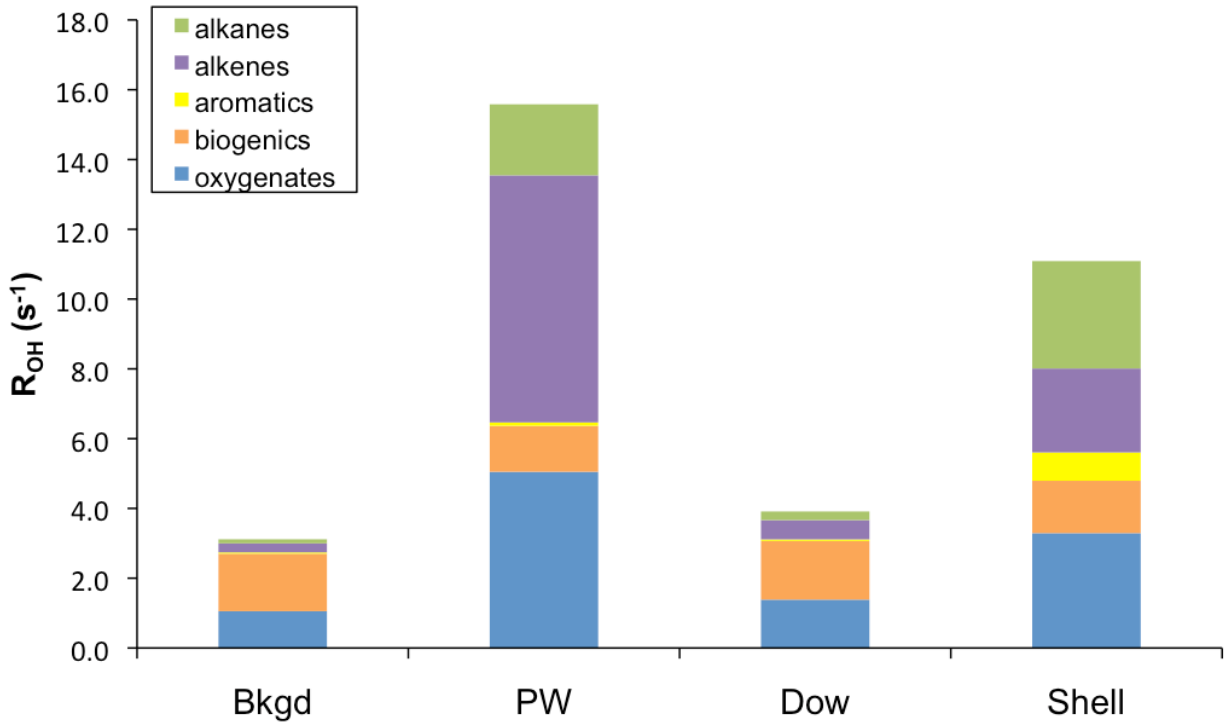

Table 3.3. Hydroxyl reactivity calculated for CO, CH_4, and VOCs at each location as well as the most concentrated industrial plumes sampled in Fort Saskatchewan. Units are s^{-1} for all values.

	Background	**PW Energy**	**Dow Chemical**	**Shell-Scotford**	**10th percentile**
R_{OH} (CH_4)	0.29	0.29	0.29	0.29	0.31
R_{OH} (CO)	0.67	0.68	0.68	0.70	0.78
R_{OH} (VOC)	3.12	15.6	3.91	11.1	58.9
Alkanes	0.12	2.04	0.25	3.08	14.3
Alkenes	0.26	7.08	0.55	2.41	23.1
Aromatics	0.04	0.10	0.05	0.81	2.38
Oxygenates	1.05	5.05	1.39	3.29	16.1
Biogenics	1.65	1.31	1.68	1.50	3.02
R_{OH} (total)	**4.08**	**16.6**	**4.89**	**12.1**	**60.0**

Examining just the most concentrated industrial plumes (top 10th percentile) gives a R_{OH} value of 60 s^{-1}, or nearly 15 times larger than that of background air. This value is comparable to levels in polluted megacities such as Mexico City, Tokyo, and Hong Kong, which ranged from 10 to 100 s^{-1} [Lou et al., 2010].

For Fort McMurray, R_{OH} in background air was similar, both in magnitude (4.79 s^{-1}) and composition (largest contribution from biogenics), to Fort Saskatchewan. The O_3 formation potentials in industrial plumes were also varied, ranging from 4.96 s^{-1} to 10.9 s^{-1}. The VOC profiles are illustrated in Figure 3.9 and summarized in Table 3.4. Unlike what was seen in Fort Saskatchewan, biogenic compounds accounted for more than 15% of R_{OH+VOC} downwind of each industrial plume. This is due to the dense boreal forest that surrounds the oil sands operations region. The largest R_{OH} value was in samples from the Suncor Energy plume. The primary influence on this reactivity came from oxygenated compounds (47% contribution) and was dominated by acetaldehyde. Downwind of the Syncrude facility, the overall R_{OH} was slightly smaller, at 9.02 s^{-1}. In this plume however, aromatics contributed 29% to the OH reactivity. In other words, the high asphaltene content associated with bitumen could have a relatively large effect on regional air quality. In general, alkenes had less of an influence on total R_{OH} in Fort McMurray, despite considerable enhancements of their mixing ratios over background levels.

The values for OH reactivity just described were determined from only the species measured in this study. Mixing ratios for NO_2 were obtained from monitoring stations in the area, and led to an R_{OH+NO2} value of 1.43 s^{-1} [WBEA, 2011]. This reactivity was added to the total R_{OH} and is listed in the bottom row of Table 3.4. However, because NO_2 does not lead to O_3, it is more useful to compare its contribution to the total reactivity (termination) to that of the other species, which propagate O_3 formation. In general, the effect of NO_2 is quite substantial in Fort

Figure 3.9. Total R_{OH+VOC} (in s^{-1}) for four areas sampled in Fort McMurray during August 2010. Values are colored by type of VOC: alkanes, alkenes, aromatics, biogenics, and oxygenates.

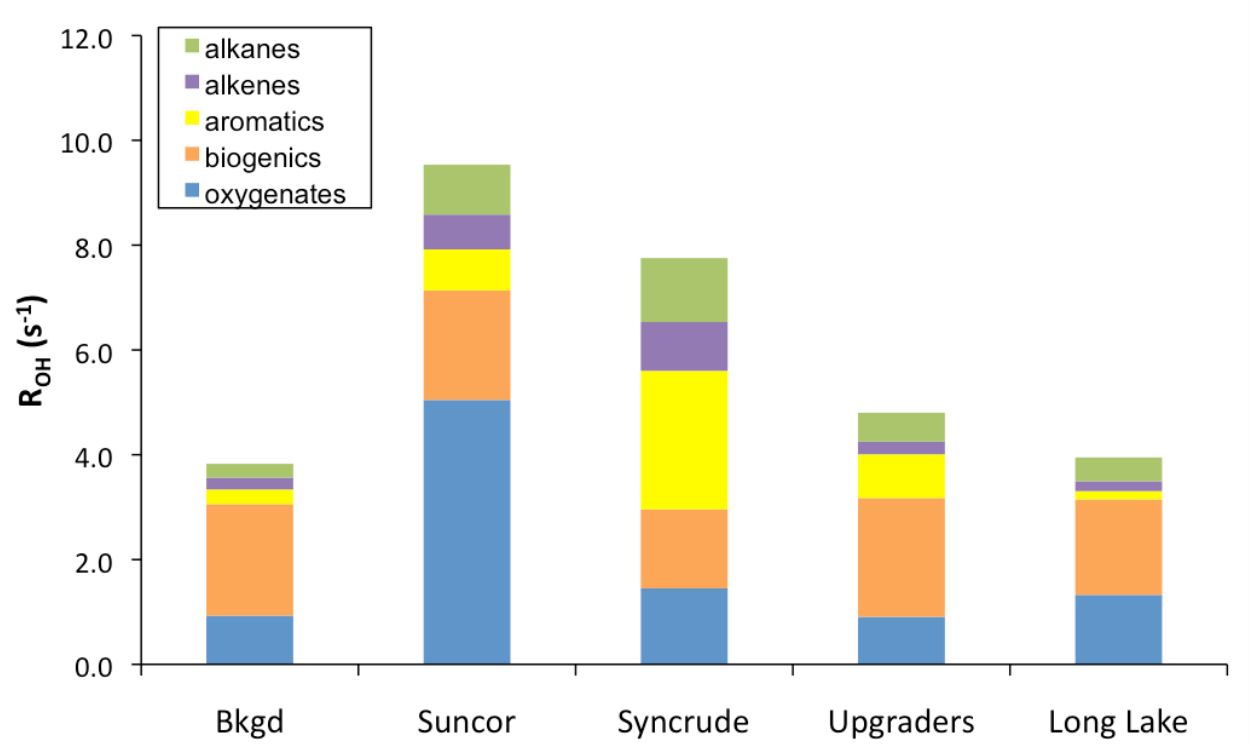

Table 3.4. Hydroxyl reactivity calculated for CO, CH_4, and VOCs at each location sampled in Fort McMurray. Total R_{OH} with the contribution from NO_2 is also included. Units are s^{-1} for all values [WBEA, 2011].

	Background	**Suncor Energy**	**Syncrude**	**Upgraders**	**Long Lake**
R_{OH} (CH_4)	0.31	0.33	0.34	0.32	0.31
R_{OH} (CO)	0.66	0.98	0.92	0.70	0.70
R_{OH} (VOC)	3.83	9.53	7.75	4.80	3.95
Alkanes	0.26	0.95	1.22	0.55	0.45
Alkenes	0.23	0.67	0.93	0.24	0.19
Aromatics	0.28	0.78	2.65	0.83	0.16
Oxygenates	0.93	5.05	1.45	0.91	1.33
Biogenics	2.13	2.09	1.51	2.27	1.82
R_{OH} (total)	**4.79**	**10.9**	**9.02**	**5.83**	**4.96**
R_{OH} with NO_2	**6.22**	**12.3**	**10.5**	**7.26**	**6.39**

McMurray, particularly in the locations with lower total VOC loadings. For instance, in background air NO_2 accounted for 23% of the overall reactivity, while downwind of the industrial facilities, the NO_2 contribution ranged from 11 to 22%.

Hydroxyl reactivity values for both Alberta sampling sites were generally comparable to the HGB region. There, the overall R_{OH} was 10.1 s^{-1}, with VOCs contributing 72% to this value, on average [Gilman et al., 2009]. In industrial plumes in Fort Saskatchewan, the average VOC contribution to the total reactivity was 84%, while in Fort McMurray 68% of the total reactivity can be attributed to VOCs (or 83% if NO_2 reactivity is excluded). Further, the contribution from NO_2 was similar in the two regions, responsible for 18% of R_{OH} in both Houston and Fort McMurray.

Despite the abundance of VOC precursors and large OH reactivities in the industrial plumes, O_3 exceedances were not observed in either region in 2010 [FAP, 2010]. The highest monthly O_3 averages typically occur during spring, while the highest 1-h O_3 averages occur during hot summer afternoons when wind speeds are low [FAP, 2010]. Ozone levels are lower within the center of the Heartland air basin, likely due to the presence of NO_2, which lowers O_3 concentrations through titration and formation of HNO_3. Industrial VOC emissions in Alberta most likely travel into a relatively clean and NO_x-limited background, making local O_3 exceedances uncommon.

3.4 Industrial Heartland Revisited

a. Observed mixing ratios

In July 2012, an additional 90 samples were collected in Fort Saskatchewan, targeting the same industrial facilities. This included 20 background samples, 16 samples downwind of the PW complex, 22 downwind of Dow Chemical, and 32 downwind of the Shell-Scotford

facility. Statistics for these samples are summarized in Table 3.5. As seen in the table, there were enhancements in 25 compounds, ranging from 1.1 to 87 times greater than background levels. The largest enhancements were observed for trans-2-butene and ethylbenzene. It should be noted that oxygenated compounds were not quantified in this second Fort Saskatchewan study due to analytical limitations.

In general, samples in this collection period were not nearly as elevated as in those collected in 2010. However, this appears to be a result of larger background mixing ratios of nearly all measured VOCs compared to two years prior (Figure 3.10a). The only exception is ethane, which was 100 pptv lower in 2012. The C_3-C_5 alkanes were significantly increased in the follow-up study. For instance, average propane and n-butane mixing ratios were 1710 ± 970 and 910 ± 1060 pptv, respectively, compared to 880 ± 370 and 350 ± 200 pptv in 2010. In addition, benzene mixing ratios were nearly double previously observed background values.

Meteorological conditions are likely the cause of these increased mixing ratios. During sampling, winds were weaker and came from a more southerly direction than in the previous study, causing the background air to be more influenced by industrial emissions. However, these higher concentrations also coincide with increased production of heavy crude oil throughout the same two-year period. For example, in 2010 monthly oil production from both upgraded and non-upgraded bitumen averaged 2.33 x 10^5 cubic meters per day, or about 1.4 million barrels per day. In 2012, the average heavy crude production was 2.86 x 10^5 m3/day, or 1.8 million bbl/day [NEB; 2015]. Although not directly linked, it is possible that VOC emissions could have increased in the region due to increased petrochemical processing of oil sands bitumen.

As observed in the previous data set, VOC mixing ratios in industrial plumes were highly variable, spanning several orders of magnitude. Comparisons of average mixing ratios

Table 3.5. Summary of 25 VOCs measured in Fort Saskatchewan, Alberta that showed enhancements in industrial plumes compared to background mixing ratios (July 5-10, 2012). Standard deviation (± 1σ) is shown in parentheses.

	Min	Max	Bkgd	PW Energy	Dow Chemical	Shell-Scotford	Top 10%	Avg. Enh.
			n = 20	n = 16	n = 22	n = 32	n=8	
Alkanes (pptv)								
Methane (ppmv)	1.85	2.23	1.90 (0.07)	1.92 (0.07)	1.95 (0.07)	1.96 (0.09)	2.12 (0.05)	1.0
Ethane	1020	27730	2710 (1070)	3760 (2570)	4240 (5500)	3500 (1810)	10010 (7430)	1.4
Propane	300	74790	1710 (970)	4950 (6530)	5640 (15850)	2180 (1680)	19810 (23300)	2.5
i-Butane	130	52190	550 (470)	6090 (13650)	820 (1310)	100 (90)	14240 (16660)	4.3
n-Butane	90	25970	910 (1060)	2490 (2420)	1200 (1680)	2500 (5330)	10640 (7360)	2.3
i-Pentane	49	27180	490 (810)	2790 (6570)	550 (500)	1810 (4110)	9760 (9490)	3.5
n-Pentane	31	18380	360 (550)	1860 (4440)	360 (300)	1360 (3050)	7030 (6550)	3.3
n-Hexane	9	2980	79 (110)	300 (430)	110 (100)	330 (640)	1290 (960)	3.1
n-Heptane	5	530	32 (40)	58 (45)	42 (40)	73 (110)	240 (160)	1.8
n-Octane	<LOD	120	12 (10)	26 (19)	18 (12)	25 (20)	68 (33)	2.0
2,3-Dimethylbutane	<LOD	370	14 (20)	40 (78)	12 (10)	45 (80)	190 (140)	2.3
2-Methylpentane	7	5490	77 (120)	390 (880)	93 (90)	510 (1250)	2270 (2110)	4.3
3-Methylpentane	<LOD	1660	44 (80)	170 (260)	56 (60)	190 (370)	770 (560)	3.2
Alkenes (pptv)								
Ethene	54	14520	360 (660)	420 (610)	2120 (3550)	970 (1000)	5980 (3810)	3.2
Propene	13	60250	78 (80)	4350 (14940)	140 (190)	100 (90)	8780 (20820)	19.7
cis-2-Butene	14	21090	56 (33)	2220 (5575)	56 (32)	69 (47)	4420 (7460)	14.0
trans-2-Butene	<LOD	18900	7 (10)	1900 (4990)	7 (7)	12 (10)	3800 (6710)	87.2
1,3-Butadiene	<LOD	620	6 (9)	5 (7)	42 (130)	5 (5)	120 (210)	3.1
Ethyne	77	1470	220 (290)	220 (100)	290 (300)	290 (230)	820 (380)	1.2
Aromatics (pptv)								
Benzene	21	184320	170 (110)	145 (100)	130 (150)	7820 (32000)	30110 (62680)	16.1
Toluene	21	1150	130 (260)	118 (90)	130 (140)	200 (200)	560 (190)	1.1
Ethylbenzene	<LOD	21620	21 (39)	30 (20)	35 (32)	4050 (6590)	14320 (5760)	65.8
m/p-Xylene	4	600	61 (130)	47 (50)	56 (70)	121 (140)	340 (150)	1.2
o-Xylene	<LOD	190	21 (40)	18 (20)	20 (25)	32 (40)	110 (40)	1.1

Figure 3.10. Two year comparisons of average VOC mixing ratios in a) local background sampled and downwind of the b) Provident Williams Energy, c) Dow Chemical, and d) Shell-Scotford facilities in Fort Saskatchewan.

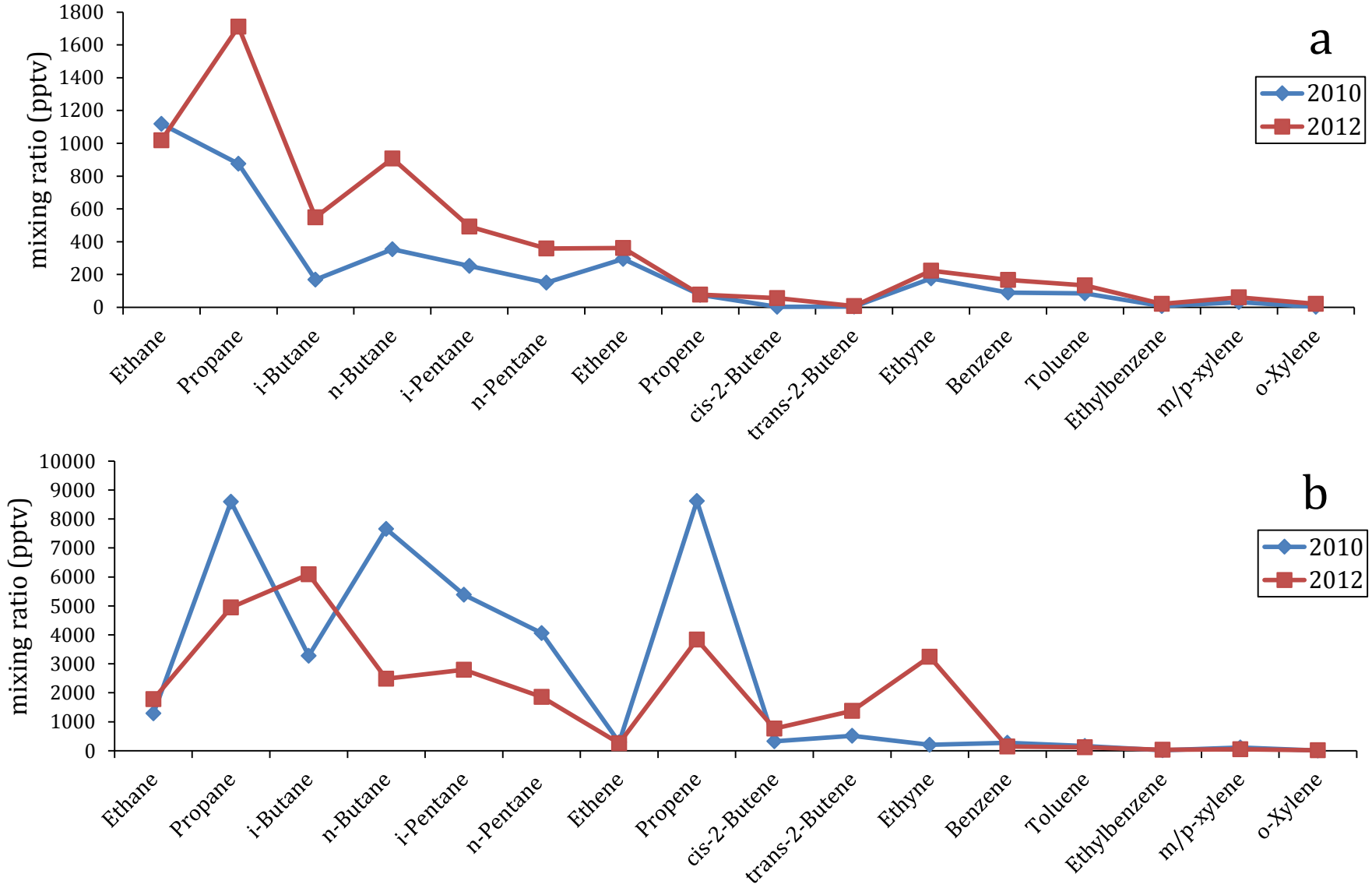

Figure 3.10. Two year comparisons of average VOC mixing ratios in a) local background sampled and downwind of the b) Provident Williams Energy, c) Dow Chemical, and d) Shell-Scotford facilities in Fort Saskatchewan.

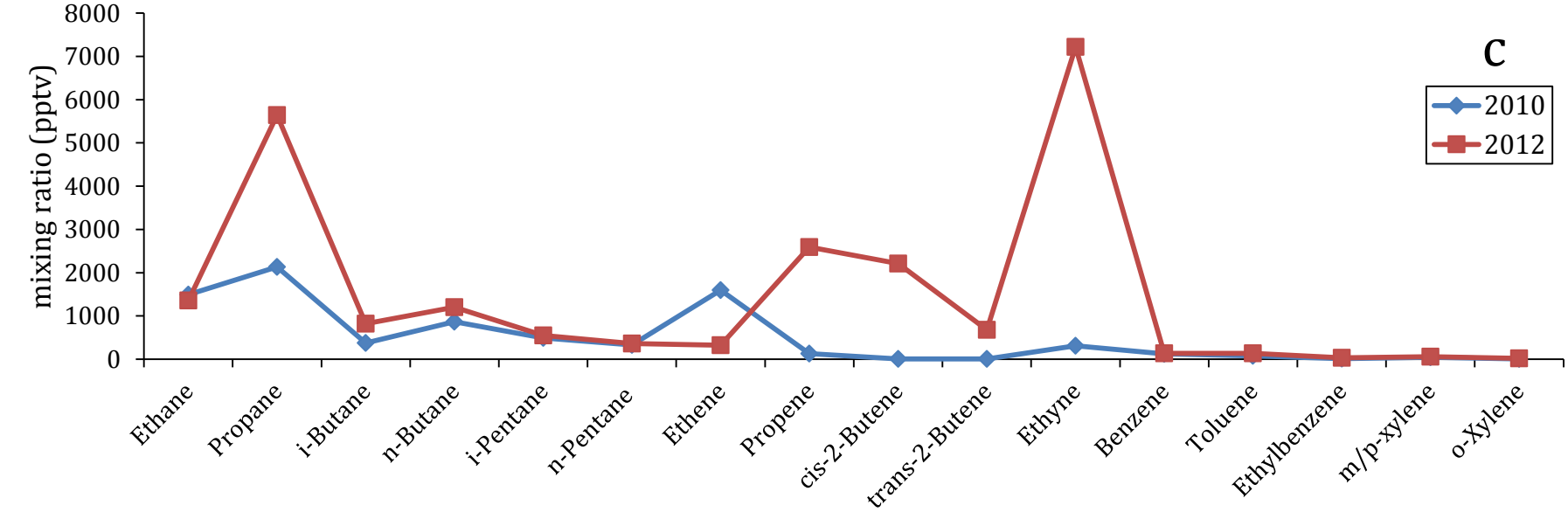

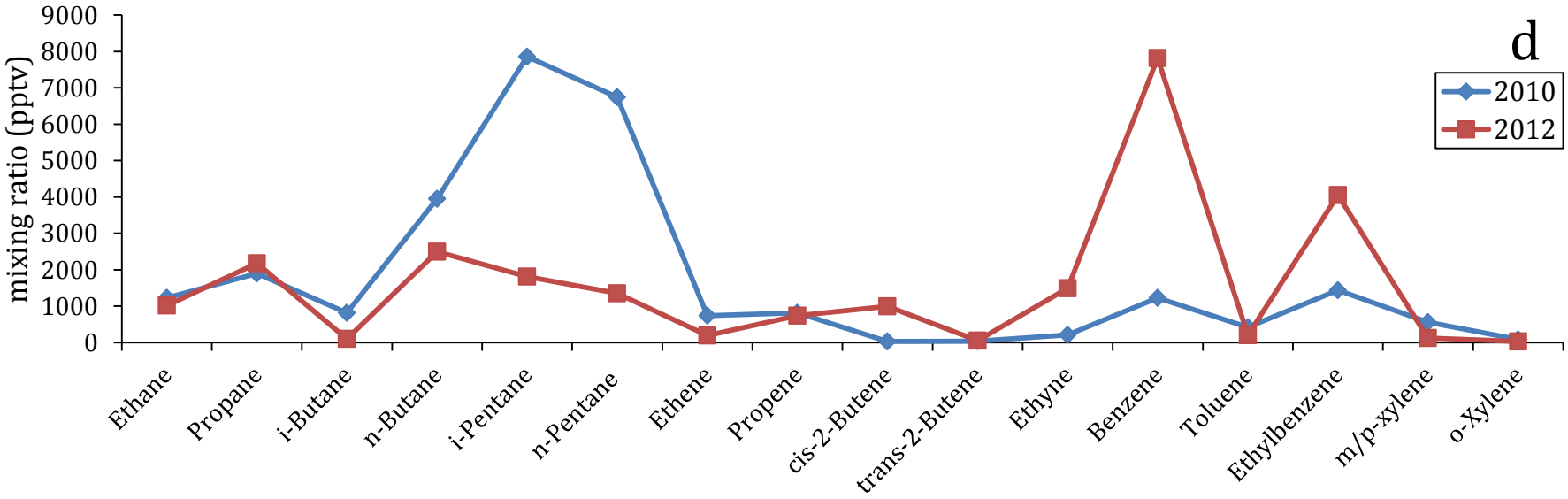

downwind of each facility for the two sample periods are illustrated in Figure 3.10b-d. Once again, alkanes were the most abundantly emitted compounds in the Industrial Heartland, which the highest values observed downwind of the PW facilities. In particular, *iso*-butane had the highest average industrial enhancement and was 4.3 times greater than local background. Propane exhibited the highest observed alkane mixing ratio, at 75 ppbv, or about 44 times over background.

Average ethene mixing ratios were high downwind of each industrial site and were about 3 times larger than background levels, similarly to two years earlier. Propene was also quite elevated near the PW site, although to a lesser extent than in the previous study. Trans-2-butene had the largest enhancement over background of all the alkenes (87x higher), and was heavily emitted downwind of the PW complex.

Once again, high concentrations of aromatic compounds were observed downwind of the Shell-Scotford facility. Benzene had the maximum value of all VOCs measured in the 2012 study, at 180 ppbv. This maximum concentration was 28 times higher than the largest value measured in the previous study. Ethylbenzene was also greater than in 2010 on average, but with the higher background mixing ratios, was once again enhanced by a factor of 65.

Unlike two years earlier, more samples were collected downwind of industrial flares in the 2012 follow-up study. During a flare, any excess/unwanted gas or over-pressurized gas is intentionally burned. Examination of the top 10^{th} percentile of industrial plumes reveals that many of the maximum mixing ratios were seen in these flare samples. This was particularly true for propene and the butenes, which were most elevated in plumes emitted from flares burned at the PW facility. Likewise, alkanes including propane and the butanes were emitted in these plumes. However, some of the highest propane values, as well as ethane, were measured in samples collected near pipelines. These pipelines not only contain bitumen, but some carry

the natural gas used by the energy plants in the region. For example, Atco Pipelines operates an ethane extraction plant in Fort Saskatchewan and has a power station in the Shell-Scotford complex [atcopipelines.com]. In addition, natural gas is often used for bitumen processing and upgrading [NEB, 2006]. As a result, enhancements of heavier alkanes and aromatics were not observed downwind of these plumes.

Table 3.6. VOC mixing ratios for background and industrial plume samples collected in Fort Saskatchewan during February and March 2011.

	Bkgd	**Dow**	**Avg. Enh.**
	n = 4	n = 4	
CO (ppbv)	290 (10)	710 (430)	2.5
Methane (ppmv)	1.93 (0.04)	2.39 (0.28)	1.2
Alkanes (pptv)			
Ethane	3240 (700)	19990 (11920)	6.2
Propane	1500 (280)	21600 (17340)	14.4
i-Butane	350 (280)	4920 (4370)	14.1
n-Butane	620 (380)	12330 (11400)	20.0
i-Pentane	230 (110)	4250 (3960)	18.2
n-Pentane	220 (80)	2010 (1560)	9.2
n-Hexane	57 (17)	840 (670)	14.8
n-Heptane	35 (14)	240 (160)	7.0
n-Octane	17 (9)	70 (30)	4.1
2,3-Dimethylbutane	16 (10)	140 (120)	8.8
2-Methylpentane	59 (44)	760 (600)	12.7
3-Methylpentane	51 (33)	480 (390)	9.4
Alkenes (pptv)			
Ethene	150 (50)	5760 (5750)	38.0
Propene	37 (21)	360 (290)	9.7
cis-2-Butene	370 (350)	7820 (7420)	21.4
trans-2-Butene	12 (6)	130 (120)	11.5
Ethyne	440 (220)	2790 (2010)	6.3
Aromatics (pptv)			
Benzene	150 (30)	480 (240)	3.3
Toluene	200 (130)	680 (580)	3.4
Ethylbenzene	21 (20)	120 (110)	5.8
m/p-Xylene	81 (100)	330 (300)	4.1
o-Xylene	18 (17)	110 (100)	5.9

For a seasonal comparison, samples (n=8) were collected in February and March 2011, between the typical background site and the Dow Chemical plant. Depending on the wind conditions, samples were either representative of background conditions, or were downwind of the industrial site. Table 3.6 contains the average observed background and industrial mixing ratios. Background values are generally comparable to those observed in the summertime, with the exception of methane, ethane, and propane. These gases are the primary components of natural gas, and could correspond to increased use of natural gas for heating in the winter. Industrial samples on the other hand, were significantly enhanced when compared to summertime plumes for many of the VOCs measured. Industrial emissions are not likely increased in the wintertime, but rather the larger mixing ratios are probably a result of seasonal changes in the planetary boundary layer. During the winter months, the mixed layer height is lower, allowing for an accumulation of VOCs closer to the surface [Schnell, 2009].

b. Photochemical reactivity

The multiple sample collection periods in Fort Saskatchewan also allow for a comparison of the air quality impacts between the two years, as well as seasonal comparison. Hydroxyl reactivity was calculated for the 2012 samples and is summarized in Tables 3.7 and 3.8. Total R_{OH} for the background was smaller in the 2012 summertime samples compared to the previous study (3.1 s^{-1} versus 4.1 s^{-1}). This difference is most likely due to the missing oxygenate photochemistry. If the same 2010 mixing ratios for oxygenates are used, R_{OH} increases to 4.2 s^{-1}. In industrial plumes, the absence of oxygenated compounds also affects the R_{OH+VOC} values, where previously these compounds were responsible for roughly 30% of the reactivity. However, even with the inclusion of oxygenated compounds it appears that the Shell plume would still have a lower R_{OH} value. The total VOC reactivity in 2010 was 11.1 s^{-1} and only

3.62 s^{-1} in 2012. Whereas alkanes accounted for 28% of the reactivity in this plume previously (3.1 s^{-1}), their contribution was reduced to 19% in the second set of samples (0.68 s^{-1}). Alkenes on the other hand, still had a significant impact on the anthropogenic R_{OH}, particularly downwind of PW (Table 3.3). Reactivity due to alkenes was 7.1 s^{-1} (45%) in 2010, and increased to 9.1 s^{-1} (78%) in this plume 2012. The role of aromatics to overall reactivity in the industrial samples was similar in both years. In the most concentrated industrial plumes, there was a 33% decrease in total reactivity between the two years, with a total R_{OH} of 40.1 s^{-1}.

Table 3.7. R_{OH} calculated for CO, CH_4, and VOCs at each location, and in the most concentrated industrial plumes, sampled in Fort Saskatchewan during the summer of 2012. Units are s^{-1} for all values.

	Background	**PW Energy**	**Dow Chemical**	**Shell-Scotford**	**10th percentile**
R_{OH} (CH_4)	0.30	0.30	0.30	0.30	0.33
R_{OH} (CO)	0.63	0.70	0.72	0.68	1.05
R_{OH} (VOC)	2.21	11.7	2.84	3.62	38.8
Alkanes	0.25	1.19	0.41	0.68	4.22
Alkenes	0.23	9.15	0.71	0.40	19.6
Aromatics	0.11	0.10	0.11	1.09	3.89
Biogenics	1.61	1.25	1.62	1.44	11.0
R_{OH} (total)	**3.13**	**12.7**	**3.87**	**4.60**	**40.1**

Table 3.8. R_{OH} calculated for CO, CH_4, and VOCs for samples collected in Fort Saskatchewan during the winter in 2011. Units are s^{-1} for all values.

	Background	**Dow Chemical**
R_{OH} (CH_4)	0.30	0.37
R_{OH} (CO)	1.43	3.5
R_{OH} (VOC)	2.55	17.5
Alkanes	0.19	2.65
Alkenes	0.60	12.8
Aromatics	0.14	0.47
Biogenics	1.61	1.62
R_{OH} (total)	**4.28**	**21.5**

Hydroxyl reactivities for the winter samples are listed in Table 3.8, and show a distinct seasonal difference when compared to summertime values. For instance, background R_{OH} total was 4.28 s^{-1}, even with the missing contribution from oxygenated compounds. Furthermore, reactivity due to CO was much greater, with a value of 1.4 s^{-1} (34% contribution) in the winter study, compared to 0.66 s^{-1} (17%) calculated during the previous summer. For the industrial samples, CO is again responsible for 17% of the overall R_{OH}, although the absolute value is larger, at 3.6 s^{-1}. The increased VOC concentrations resulted in the largest R_{OH+VOC} observed during any of the sample periods (17.5 s^{-1}). Alkenes accounted for 73% of this reactivity, while alkanes contributed another 15%.

In spite of these large R_{OH} values, average O_3 concentrations in Fort Saskatchewan were lower in the winter of 2011 than the summers of 2010 or 2012 [FAP, 2010; FAP, 2011; FAP, 2012]. This is due to the reduced photochemistry that occurs in the winter, when daily sunlight hours are at a minimum. Because the reaction of VOCs and OH does not directly lead to ozone formation, R_{OH} is really more of an indicator of overall chemical loading. It also provides information as to which classes of compounds could have the largest effect on local air quality if conditions (sunlight and NO_x levels) supported photochemical O_3 formation.

3.5 References

Alberta's Industrial Heartland Association (AIHA). Industry and Organization Profiles. July 2012. Available from: www.industrialheartland.com/images/stories/industry/aiha_industry_information_july_2012.pdf.

Alboudwarej, H.; Felix, J.; Taylor, S.; Bardy, R.; Bremmer, C.; Brough, B.; Skeates, C.; Baker, A.; Palmer, D.; Pattison, K.; Beshry, M.; Krawchuk, P.; Brown, G.; Calvo, R.; Triana, J.A.C.; Hathcock, R.; Koerner, K.; Hughes, T.; Kundu, D.; de Cardenas, J.L.; West, C. Highlighting Heavy Oil. *Oilfield Rev*. **2006**, 34–53.

Baker, A. K.; Beyersdorf, A. J.; Doezema, L. A.; Katzenstein, A.; Meinardi, S.; Simpson, I. J.; Blake, D. R.; Rowland, F. S. Measurements of nonmethane hydrocarbons in 28 United States cities. *Atmos. Environ*. **2008**, 42 (1), 170–182.

Blake, D.R. and Rowland, F.S. Urban leakage of liquefied petroleum gas and its impact on Mexico City air quality. *Science*. **1995**, 269, 953-956.

Carter, W. P. L. Development of ozone reactivity scales for volatile organic compounds, *J. Air Waste Manage. Assoc*. **1994**, 44, 881–899.

Chambers, A.K.; Strosher, M.; Wootton, T.; et al. Direct measurement of fugitive emissions of hydrocarbons from a refinery. *J. Air Waste Manag. Assoc*. **2008**, 58, 1047-1056.

Clean Air Strategic Alliance. Available from: http://www.casadata.org/Reports/SelectCategory.asp

deGouw, J.A.; Te Lintel Hekkert, S.; Mellqvist, J.; et al. Airborne measurements of ethene from industrial sources using laser photo-acoustic spectroscopy. *Environ. Sci. Technol.* **2009**, 43, 2437-2442.

Fort Air Partnership (FAP). Fort Air Partnership Ambient Air Monitoring Network 2010 Annual Technical Report Network and Data Summary. 2010. Available from: http://www.fortair.org/resources/reports/

Fort Air Partnership (FAP). Fort Air Partnership Ambient Air Monitoring Network 2011 Annual Technical Report Network and Data Summary. 2011. Available from: http://www.fortair.org/resources/reports/

Fort Air Partnership (FAP). Fort Air Partnership Ambient Air Monitoring Network 2012 Annual Technical Report Network and Data Summary. 2012. Available from: http://www.fortair.org/resources/reports/

Filley, C.M.; Halliday, W.; Kleinschmidt-DeMasters, B.K. The Effects of Toluene on the Central Nervous System. *J. Neuropathol. Exp. Neurol*. **2004**, 63(1), 1-12.

Finlayson-Pitts, B.J.; Pitts, J.N. *Chemistry of the Upper and Lower Atmosphere*; Academic Press: San Diego, 2000.

Fortin, T. J., B. J. Howard, D. D. Parrish, P. D. Goldan, W. C. Kuster, E. L. Atlas, and R. A. Harley. Temporal changes in US benzene emissions inferred from atmospheric measurements. *Environ. Sci. Technol*. **2005**, 39, 1403–1408, doi:10.1021/es049316n.

Fraser, M. P., G. R. Cass, and B. R. T. Simoneit (1998), Gas-phase and particle-phase organic compounds emitted from motor vehicle traffic in a Los Angeles roadway tunnel, Environ. Sci. Technol., 32, 2051–2060.

Gilman, J.B.; et al. Measurements of volatile organic compounds during the 2006 TexAQS/GoMACCS campaign: Industrial influences, regional characteristics, and diurnal dependencies of the OH reactivity. *J. Geophys. Res*. **2009**, 114, D00F06, doi:10.1029/2008JD011525.

Gilman, J.B.; Lerner, B.M.; Kuster, W.C.; de Gouw, J.A. Source Signature of Volatile Organic Compounds from Oil and Natural Gas Operations in Northeastern Colorado. *Environ. Sci. Technol*. **2013**, 47, 1297-1305.

Gray, M.R. Tutorial on Upgrading of Oilsands Bitumen (presentation). University of Alberta, 2008.

Guenther, A.; Hewitt, N.; Erickson, D.; Fall, R.; Geron, C.; Graedel, T.; Harley, P.; Klinger, L.; Lerdau, M.; McKay, W.A.; Pierce, T.; Scholes, B.; Steinbrecher, R.; Tallamraju, R.; Taylor, J.; Zimmerman, P. A global model of natural volatile organic compound emissions. *J. Geophys. Res*. **1995**, *100*, 8873-8892.

Hartt, G.M. Oil and natural has emissions in the Gulf of Mexico and the San Joaquin Valley of California. PhD. Thesis, University of California, Irvine, 2013.

Hyne, N.J., Nontechnical Guide to Petroleum Geology, Exploration, Drilling and Production, 2nd ed.; PennWell: Tulsa, 2001; pp 1-5.

Infante, P.F.; White, M.C. Benzene: Epidemiologic Observations of Leukemia by Cell Type and Adverse Health Effects Associated with Low-Level Exposure. *Environ. Health. Perspect*. **1983**, 52, 75-82.

Kim, S.; Guenther, A.; Karl, T.; Greenberg, J. Contributions of primary and secondary biogenic VOC to total OH reactivity during the CABINEX (Community Atmosphere-Biosphere Interactions Experiments)-09 field campaign. *Atmos. Chem. Phys*. **2011**, 11, 8613-8623.

Lou, S.; Holland, F.; Rohrer, F.; et al. Atmospheric OH reactivities in the Pearl River Delta, China in summer 2006: measurement and model results. *Atmos. Chem. Phys*. **2010**, 10, 11243-11260.

Lough, G. C., Schauer, J.J.; Lonneman, W.A.; Allen, M.K. Summer and winter nonmethane hydrocarbon emissions from on-road motor vehicles in the midwestern United States, *J. Air Waste Manage. Assoc.*, **2005**, 55, 629–646.

Mao, J.; Ren, X.; Chen, S.; et al. Atmospheric oxidation capacity in the summer of Houston 2006: comparison with summer measurements in other metropolitan studies. *Atmos. Environ.* **2010**, 44, 4107-4115.

McCallum, K., Scotten, R., Hasham, F. Historical Prevailing Winds: Strathcona County, 2003. Available from: http://www.strathcona.ab.ca/files/Attachment-EEPS-prevailingwinds.pdf.

Millet, D.B., Guenther, A., Siegel, D.A., et al. Global atmospheric budget of acetaldehyde: 3-D model analysis and constraints from in-situ and satellite observations. *Atmos. Chem. Phys*. **2010**, 10, 3405-3425.

Montzka, S.; Trainer, M.; Goldan, P.D.; et al. Isoprene and its oxidation products, methyl vinyl ketone and methacrolein, in the rural troposphere. *J. Geophys. Res*. **1993**, 98 (D1), 1101-1111.

National Energy Board (NEB). Canada's Oil Sands: Opportunities and Challenges to 2015: An Update. An Energy Market Assessment June 2006.

National Energy Board (NEB). Archived Estimated Production of Canadian Crude Oil and Equivalent, February 2015. Available from: https://www.neb-one.gc.ca/nrg/sttstc/crdlndptrlmprdct/stt/archive/stmtdprdctnrchv-eng.html.

National Pollutant Release Inventory (NPRI). National Pollutant Release Inventory Online Data Search. 2012. Available from: http://www.ec.gc.ca/pdb/websol/querysite/query_e.cfm.

Ras, M.R.; Marcé, R.M.; Borrull, F. Characterization of ozone precursor volatile organic compounds in urban atmospheres and around the petrochemical industry in the Tarragona region. *Sci. Total Environ*. **2009**, 407, 4312e4319.

Russo, R.S.; Zhou, Y.; White, M.L.; et al. Multi-year (2004-2008) record of nonmethane hydrocarbons and halocarbons in New England: seasonal variations and regional sources. *Atmos. Chem. Phys*. **2010**, 10, 4909-4929.

Ryerson, T.B.; Trainer, M.; Angevine, W.M.; et al. Effect of petrochemical industrial emissions of reactive alkenes and NOx on tropospheric ozone formation in Houston, Texas. *J. Geophys. Res*. **2003,** 108 (D8). http://dx.doi.org/10.1029/2002JD003070.

Schnell, R.C.; Oltmans, S.J.; Neely, R.R.; Endres, M.S.; Molenar, J.V.; White, A.B. Rapid photochemical production of ozone at high concentrations in a rural site during the winter. *Nat. Geosci.* **2009**, 2, 120-122.

Simpson, I.; Blake, N.J.; Barletta, B.; Diskin, G.S.; Fuelberg, H.E.; et al. Characterization of Trace Gases Measured Over Alberta Oil Sands Mining Operations: 76 Speciated C_2-C_{10} Volatile Organic Compounds (VOCs), CO_2, CH_4, CO, NO, NO_2, NOy, O_3 and SO_2. *Atmos. Chem. Phys. Discuss*. **2010**, 10, 18507–18560.

Wang, J.; Reyniers, M-F.; Marin, G.B. Influence of dimethyl disulfide on coke formation during steam cracking of hydrocarbons. *Ind. Eng. Chem. Res.* **2007**, 46(12), 4134-4148. doi: 10.1021/ie061096u.

Ware, J.H.; Spengler, J.D.; Neas, L.M.; Samet, J.M.; Wagner, G.R.; Coutlas, D.; Ozkaynak, H.; Schwab, M. Respiratory and Irritant Health Effects of Ambient Volatile Organic Compounds: The Kanawha County Health Study. *Am. J. Epidemol*. **1993**, 137(12), 1287-1301.

Wood Buffalo Environmental Association (WBEA). Historical Monitoring Data, August 2010. Available from: http://wbea.org/monitoring-stations-and-data/historical-monitoring-data.

Xiao, Y.; Jacob, D.J.; Turquety, S. Atmospheric acetylene and its relationship with CO as an indicator of air mass age. J. Geophys. Res. **2007**, 112, D12305, doi:10.1029/2006JD008268.

Chapter 4.
Methane Sources in the Barnett Shale of Northern Texas

* portions of this chapter are adapted from Townend-Small, A; Marrero, J.E.; et al. Integrating isotopic and alkane ratio tracers into a bottom-up inventory of methane emissions in an urban natural gas producing region: the Barnett Shale of Fort Worth, Texas, 2015. (*in review*)

4.1 Overview

The Barnett Shale of northern Texas is one of the most developed and productive natural gas shale plays in the United States. Gaseous emissions from the many oil and gas system components in the region have not been fully characterized. Presented in this chapter are measurements of an extensive amount of VOCs and stable isotopic ratios ($\delta^{13}C$ and δD) from 120 whole air canisters collected throughout the Barnett shale in October 2013. Samples were collected in conjunction with the University of Cincinnati as part of the Environmental Defense Fund Barnett Coordinated Campaign. Known CH_4 sources were targeted and included oil and natural gas well pads, compressor stations, distribution pipelines and city gates, cattle feedlots and landfills. As expected, C_1-C_5 alkanes were elevated throughout the region and were similar to or greater than major U.S. cities. For each sample, the percentage of C_1 through C_5 was calculated and used to distinguish thermogenic and biogenic sources from one another. For oil and gas sources (ONG), the alkane composition was used to distinguish dry gas from wet gas and compared to other regions in the United States. Further, the alkane and isotopic ratios were incorporated into a bottom-up CH_4 inventory, developed as part of the Barnett Coordinated Campaign, to predict the composition of CH_4 in the regional well-mixed air. Lastly, analyses of local photochemistry and a statistical source apportionment were conducted.

4.2 Results

From October 16-29, 2013, surface level whole air samples (n = 120) were collected near the city of Fort Worth, Texas, in Denton, Ellis, Erath, Jack, Johnson, Montague, Parker,

Somervell, Tarrant, and Wise counties. Samples were collected at various CH_4 sources in the Barnett Shale region (Figure 4.1). Oil and gas activities are responsible for CH_4 emissions from point sources, such as compressor engine exhaust or venting from tanks that hold separated condensate, as well as fugitive sources, or those that stem from leaks. Well pads, along with the network of gathering, processing, and transmission systems for the produced natural gas were sample targets. Potential urban CH_4 sources, including gas distribution systems, landfills, and wastewater treatment plants were also considered, as well as agricultural sources, like cattle ranches and feedlots. Table 4.1 lists the CH_4 sources sampled and the number of samples collected at each location.

Figure 4.1. Map of the sample locations in the Barnett shale, colored by type of CH_4 source (natural gas wells = grey; compressor stations = blue; processing plants = green; conventional oil wells = red; dairies = burgundy; landfills = purple; background/non source = pink).

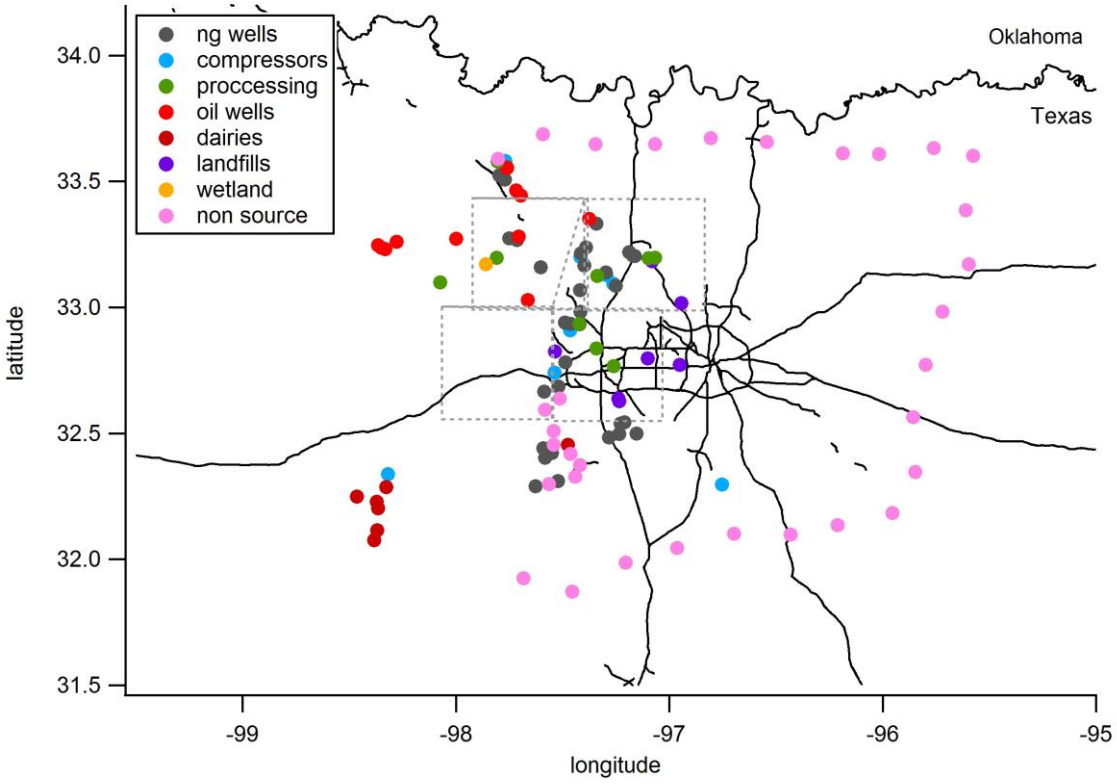

Local background concentrations for the Barnett region were calculated from the perimeter drive around samples (pink points in Figure 4.1), where point sources were avoided (n = 24). Minimum, maximum, and average concentrations for VOCs, including alkanes, alkenes, and aromatics, are summarized in Table 4.2. Background mixing ratios of CH_4 and ethane (C_2H_6) are mapped in Figure 4.2. The average background CH_4 mixing ratio observed in the Barnett region was 1.95 ± 0.07 ppmv (± 1σ). For comparison, the average global baseline CH_4 mixing ratio during the time of the study, measured at the Mauna Loa Observatory in Hawaii, was 1.84 ± 0.01 ppmv. The influence of continuous fugitive hydrocarbon emissions in the region becomes more apparent when looking at the local concentrations of C_2+ alkanes. Ethane was highly enhanced in the region, although more variable, with an average of 8.5 ± 3.7 ppbv. Typical 'clean air' C_2H_6 concentrations, observed in whole air samples collected by the Blake group along the west coast of the United States, ranged from 0.3 to 1.5 ppbv in the fall of 2012. The remaining alkanes (C_3+) listed in Table 4.2 also exhibited high local values.

Table 4.1. Various CH_4 sources targeted throughout the Barnett Shale region and the number of samples collected at each source type.

Thermogenic	number of samples
Natural gas well pads	31
Compressor stations	10
Gathering and processing facilities	3
Distribution systems	4
Transmission and storage	2
Conventional oil wells	12
Biogenic	
Cattle	6
Landfills	8
Freshwater wetland	1
Background	24

Table 4.2. Background mixing ratios of VOCs measured in the Barnett Shale determined from samples collected during a perimeter drive around of the region, away from point sources.

	Min	**Max**	**Median**	**Average**	**SD**
CH_4 (ppmv)	1.83	2.09	1.95	1.95	0.07
CO (ppbv)	106	202	151	146	29
Alkanes (pptv)					
Ethane	4040	16260	8210	8490	3710
Propane	2250	12500	4760	5080	2520
i-Butane	300	3600	1000	1200	850
n-Butane	740	4970	1720	1800	980
i-Pentane	230	1260	560	590	260
n-Pentane	200	1640	520	590	350
n-Hexane	66	580	160	200	140
n-Heptane	21	200	44	64	47
n-Octane	6	140	19	32	33
Aromatics (pptv)					
Benzene	46	240	90	100	44
Toluene	56	470	110	150	110
Ethylbenzene	5	63	15	20	15
m/p-Xylene	11	170	56	66	44
o-Xylene	3	76	17	22	18
Other (pptv)					
Ethene	87	1740	290	420	370
Propene	20	540	62	110	130
Ethyne	180	1220	280	370	230
DMS	3	50	8	10	10

Figure 4.2. Map of CH_4 (top panel) and C_2H_6 (bottom panel) mixing ratios in local background samples collected in the Barnett Shale.

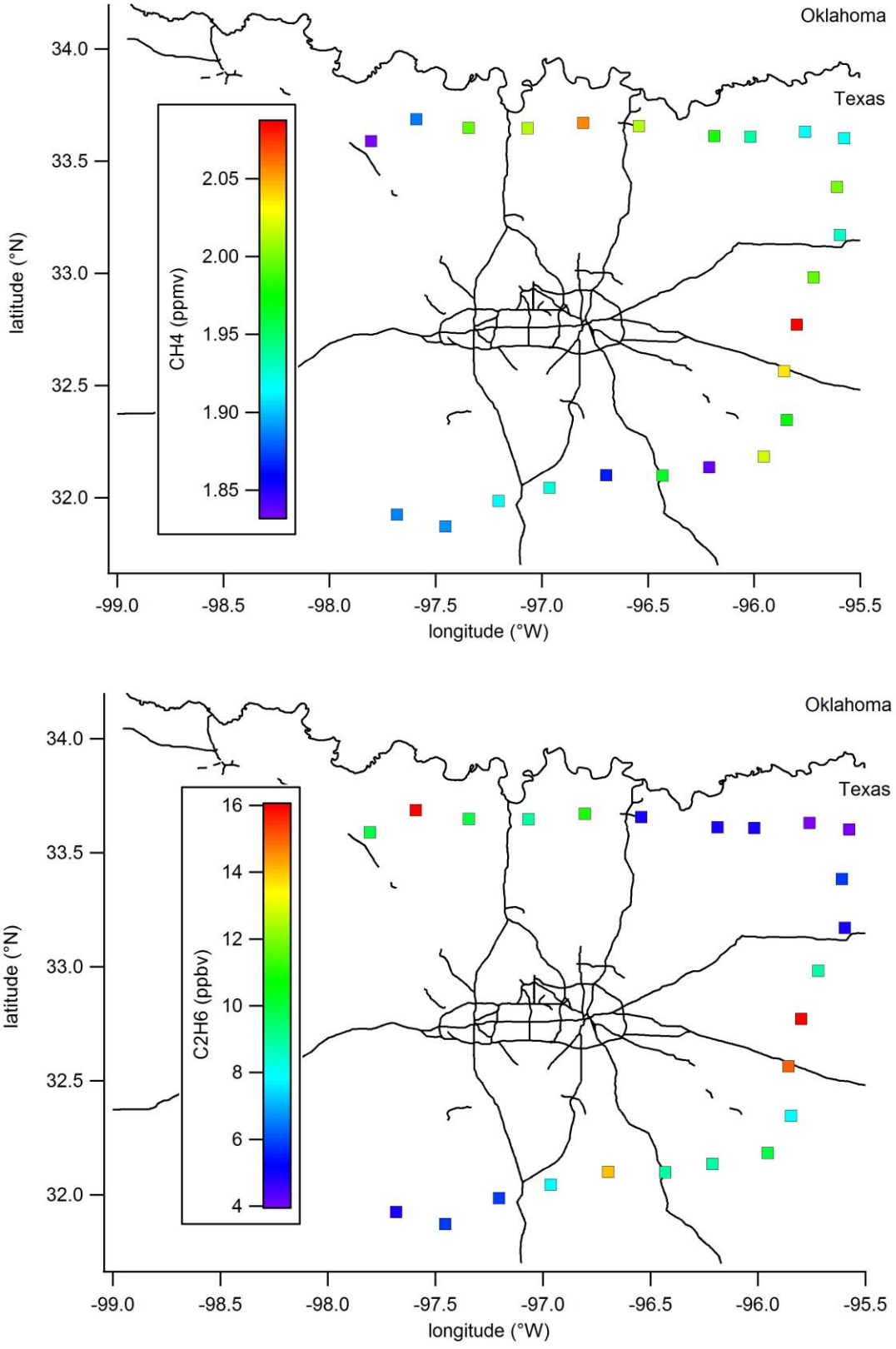

For each of the source types, CH_4 and C_2H_6 are also mapped in Figures 4.3 and 4.4. Natural gas (NG) samples (well pads, compressor stations, and facilities), conventional oil wells, and biogenic methane sources are shown in panels a, b, and c, respectively. Light alkane concentrations were variable and showed no clear spatial trend. Red points in each panel in Figure 4.3 have CH_4 values above the mixing ratio indicated by the color scale. For instance, CH_4 ranged from 2.04 ppmv to 190 ppmv. Six of these NG samples had mixing ratios that exceeded 5.0 ppmv CH_4, indicating the presence of a natural gas leak stemming from some component at the sample site, resulting in a significant CH_4 plume. In fact, a forward looking infrared (FLIR) camera showed that the largest CH_4 plume measured was captured downwind of a well pad that had an opened hatch on one of its storage tanks. Substantital CH_4 plumes were also captured from 2 oil wells and landfills that were sampled. Cattle/dairy feedlots however, did not show spikes in CH_4, but rather exhibited persitant elevated CH_4 concentrations.

Similarly, the C_2H_6 concentrations shown in Figure 4.4 varied and ranged from 10 ppbv to 8.6 ppmv in the natural gas and oil well samples. The 8.6 ppmv sample also had 190 ppmv CH_4. However, the highest C_2H_6 samples did not always correspond to samples with the highest CH_4 concentrations. The ratio of methane to ethane (MER) is therefore one way to characterize oil and gas samples as being either 'wet' (higher MER) or 'dry' (lower MER). This is discussed further in Section 4.3.3. Samples collected at landfills generally had C_2H_6 concentrations similar to or less than the local background. On the other hand, the cattle feedlot samples were slightly elevated above background. This could indicate a mixed influence of sources in the region where samples were collected, possibly amplified by the stronger and more variable winds observed on the day that feedlots were sampled. Average mixing ratios for the remaining alkanes and other VOCs are listed for each source type in Table 4.3 (high standard deviations reflect the large variability in mixing ratios from site to site).

Figure 4.3. Mixing ratios of CH_4 in whole air samples collected in the Barnett Shale at a) natural gas sites b) conventional oil wells and c) landfills and cattle feedlots.

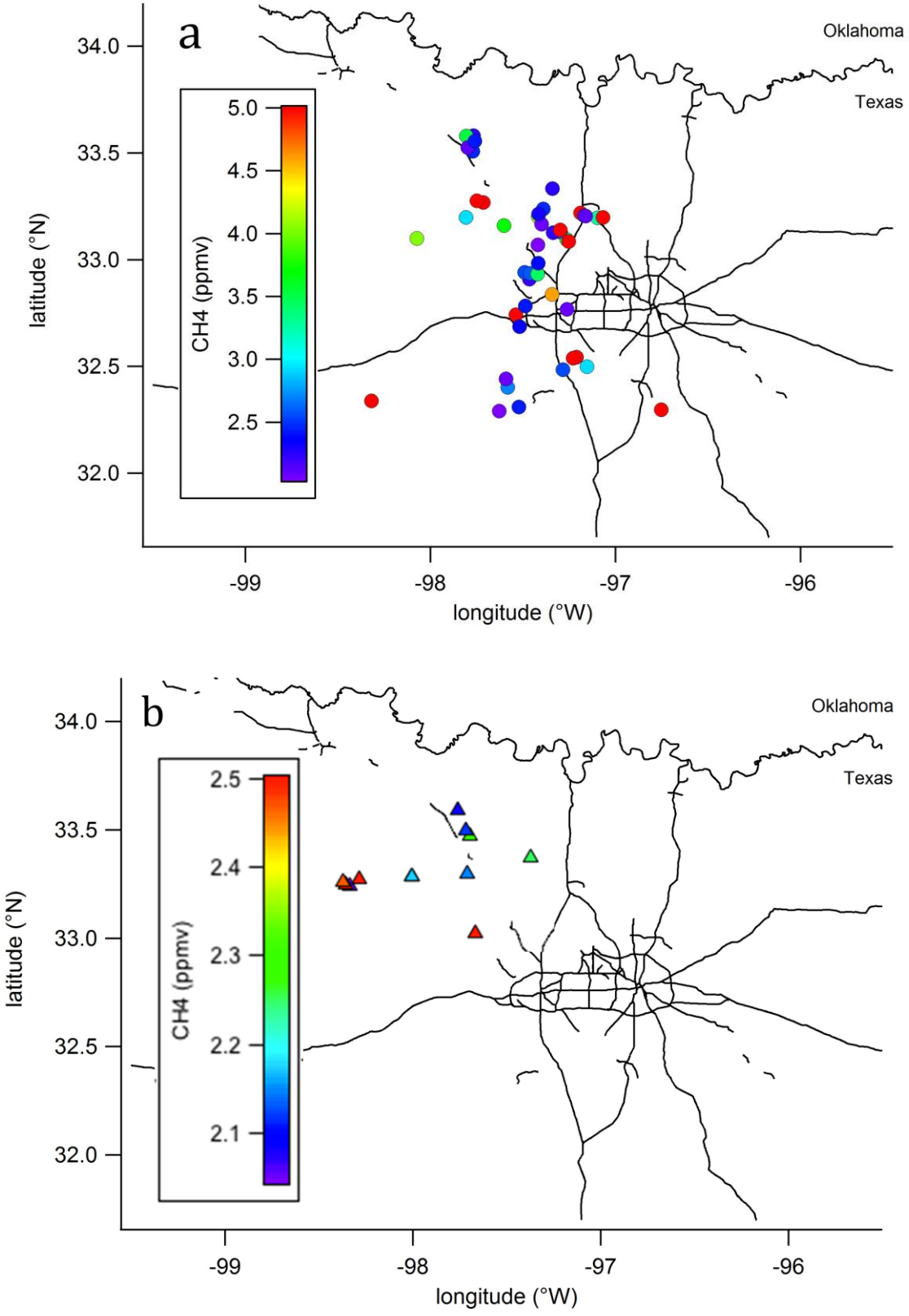

Figure 4.3. Mixing ratios of CH_4 in whole air samples collected in the Barnett Shale at a) natural gas sites b) conventional oil wells and c) landfills and cattle feedlots.

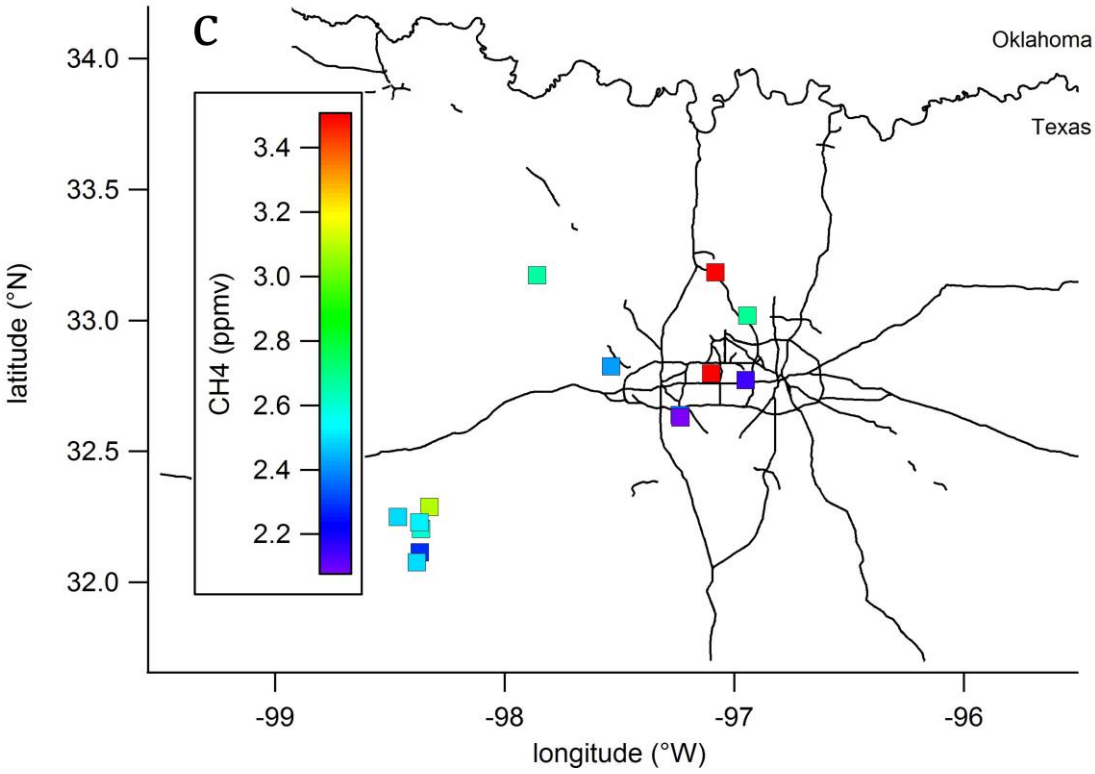

Figure 4.4. Mixing ratios of C_2H_6 in whole air samples collected in the Barnett Shale at a) natural gas sites b) conventional oil wells and c) landfills and cattle feedlots.

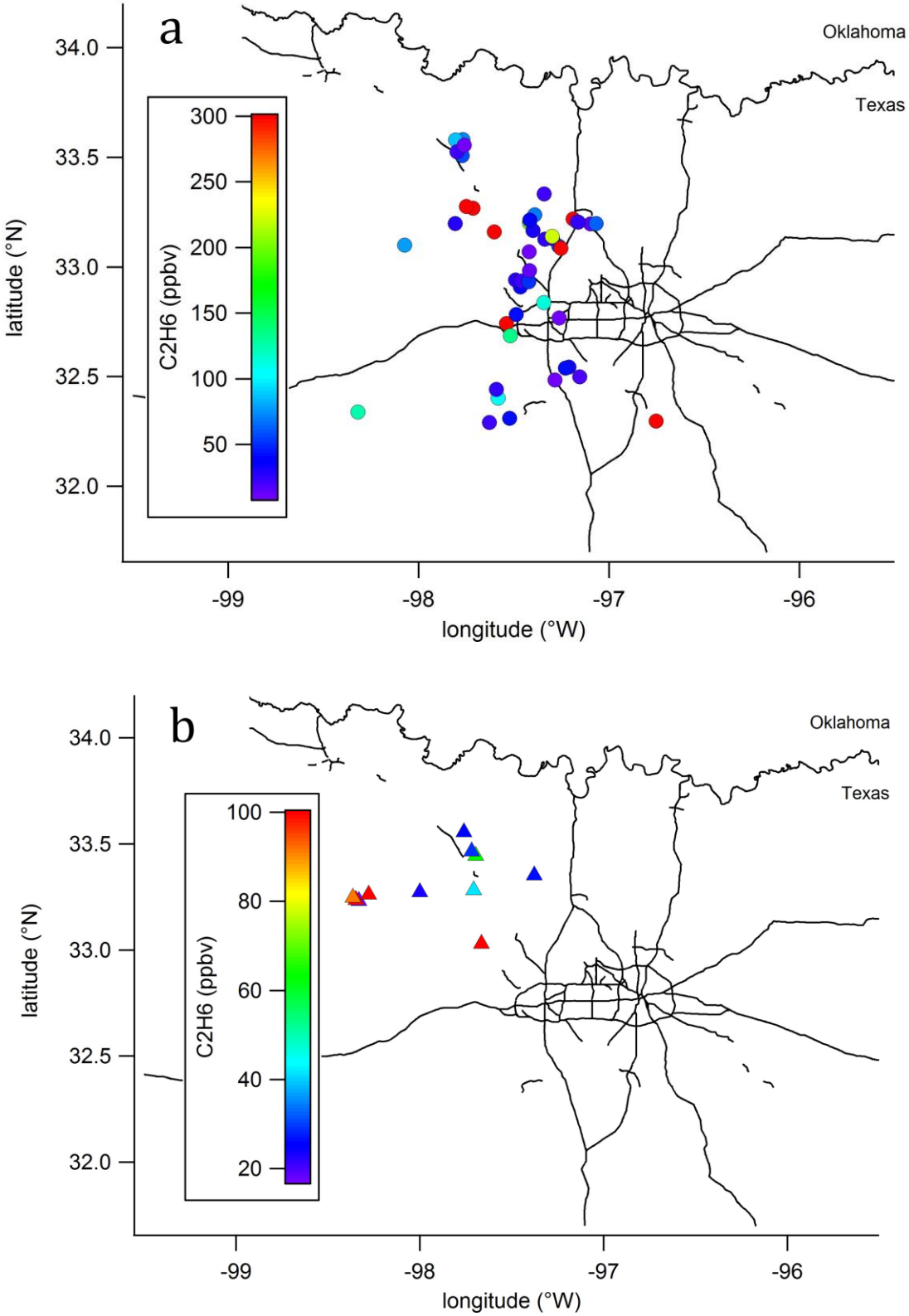

Figure 4.4. Mixing ratios of C_2H_6 in whole air samples collected in the Barnett Shale at a) natural gas sites b) conventional oil wells and c) landfills and cattle feedlots.

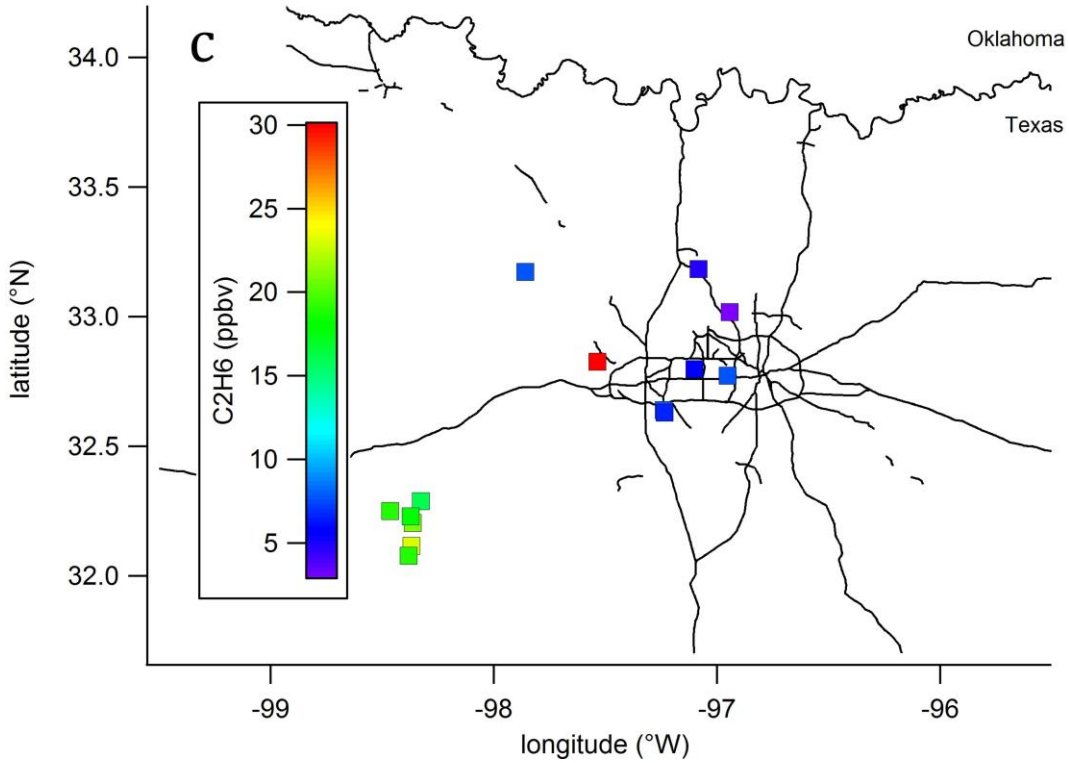

Table 4.3. Average concentrations of VOCs measured at each of the methane sources sampled in the Barnett Shale. Standard error is shown in parentheses (and reflect the large variability in mixing ratios from site to site).

	Oil wells	**NG well pads**	**Compressors**	**Processing**	**Distribution**	**Cattle**	**Landfills**
CH_4 (ppmv)	4.33	4.35	8.12	2.43	3.85	2.50	4.99
CO (ppbv)	181	205	192	150	155	123	130
Alkanes (pptv)							
Ethane	325010 (636750)	179110 (477210)	361920 (695720)	23500 (10070)	77560 (40440)	17780 (4210)	16070 (20170)
Propane	187220 (357140)	69230 (202220)	118625 (258380)	11060 (4800)	19060 (15430)	13400 (4420)	6330 (4630)
i-Butane	25330 (46710)	9630 (23870)	17480 (38490)	2180 (1340)	2200 (1880)	2220 (740)	28840 (11310)
n-Butane	54130 (99090)	20300 (58630)	30090 (52260)	4200 (2160)	5320 (4800)	4650 (1660)	1950 (1070)
i-Pentane	16830 (29120)	6370 (15420)	10100 (17570)	1910 (980)	1670 (1340)	1720 (620)	990 (540)
n-Pentane	17580 (29600)	7690 (22690)	9460 (15400)	1990 (1070)	1670 (1480)	1810 (700)	970 (760)
n-Hexane	9710 (18340)	3210 (9420)	3700 (5840)	590 (240)	520 (470)	500 (230)	270 (150)
n-Heptane	5500 (13070)	1310 (4290)	1260 (2040)	190 (70)	160 (150)	140 (60)	130 (100)
n-Octane	2160 (6380)	440 (1410)	490 (720)	81 (29)	53 (35)	43 (12)	40 (26)

Table 4.3. (continued) Average concentrations of VOCs measured at each of the methane sources sampled in the Barnett Shale. Standard error is shown in parentheses.

	Oil wells	NG well pads	Compressors	Processing	Distribution	Cattle	Landfills
Aromatics (pptv)							
Benzene	820 (1300)	290 (500)	610 (800)	130 (70)	170 (10)	140 (50)	170 (180)
Toluene	2310 (5270)	590 (1190)	910 (1080)	270 (120)	210 (85)	130 (40)	850 (1600)
Ethylbenzene	140 (240)	56 (130)	100 (130)	25 (8)	48 (58)	18 (7)	59 (80)
m/p-Xylene	2600 (7770)	510 (1460)	550 (730)	90 (68)	200 (270)	87 (80)	280 (370)
o-Xylene	310 (760)	86 (220)	120 (120)	34 (28)	56 (77)	17 (10)	87 (120)
Others (pptv)							
Ethene	2130 (2900)	760 (1100)	1540 (3170)	570 (390)	540 (90)	230 (70)	320 (180)
Propene	1040 (2790)	130 (180)	10 (30)	110 (30)	120 (60)	47 (17)	120 (70)
Ethyne	990 (1390)	490 (510)	4160 (10600)	430 (180)	460 (210)	300 (60)	320 (130)
DMS	7 (3)	8 (5)	50 (115)	8 (7)	11 (2)	215 (160)	23 (10)

4.2.1 Characterization of Methane Sources

a. Alkane ratios

Previous studies have used light alkanes to distinguish thermogenic and biogenic methane sources from one another [Wennberg et al., 2012; Peischl et al., 2013]. Alkane ratios relative to methane were determined from plots of C_2H_6, C_3H_8, *n*- and *i*-C_4H_{10}, and *n*- and *i*-C_5H_{12} mixing ratio against CH_4 mixing ratio for each source type sampled in the Barnett Shale. The slope of such a plot provides the alkane ratio by volume, which is the same as the molar ratio.

In Figure 4.5a, C_2H_6 is plotted against CH_4 and colored by source type. The slopes fall into three distinct lobes, associated with oil, natural gas, or biogenic sources of methane. Oil and gas related source types, i.e. compressor stations, distribution lines, oil wells, and natural gas well pads, exhibit greater slopes than cattle and landfill sources. Conventional oil wells have the largest percent ethane relative to methane, at 12.6 ± 1.0% (a molar ratio, calculated by taking the slope and multiplying by 100). Samples related to natural gas have only half as much ethane content. Each of the natural gas sources had a C_2:C_1 ratio of about 6 to 7 percent. There was poor correlation between CH_4 emitted from biological sources and concentration of any other alkanes. At less than 1% ethane, these biological sources of methane are not considered significant sources of ethane.

Similar trends were observed for propane (Figure 4.5b), butanes, and pentanes (not shown). Emissions from conventional oil are enriched in C_2-C_5 alkanes relative to CH_4. Natural gas is about 2% propane relative to methane, and about 1% for the C_4 and C_5 alkanes. Table 4.4 shows the slopes for the various sources in each of these plots. In general, the R^2 values are low, reflecting the high variability across the source types.

Figure 4.5. Correlation plots relative to CH_4 for a) ethane and b) propane. Trendlines are extended to better illustrate slopes, which provide the molar ratio by volume (ppbv/ppbv).

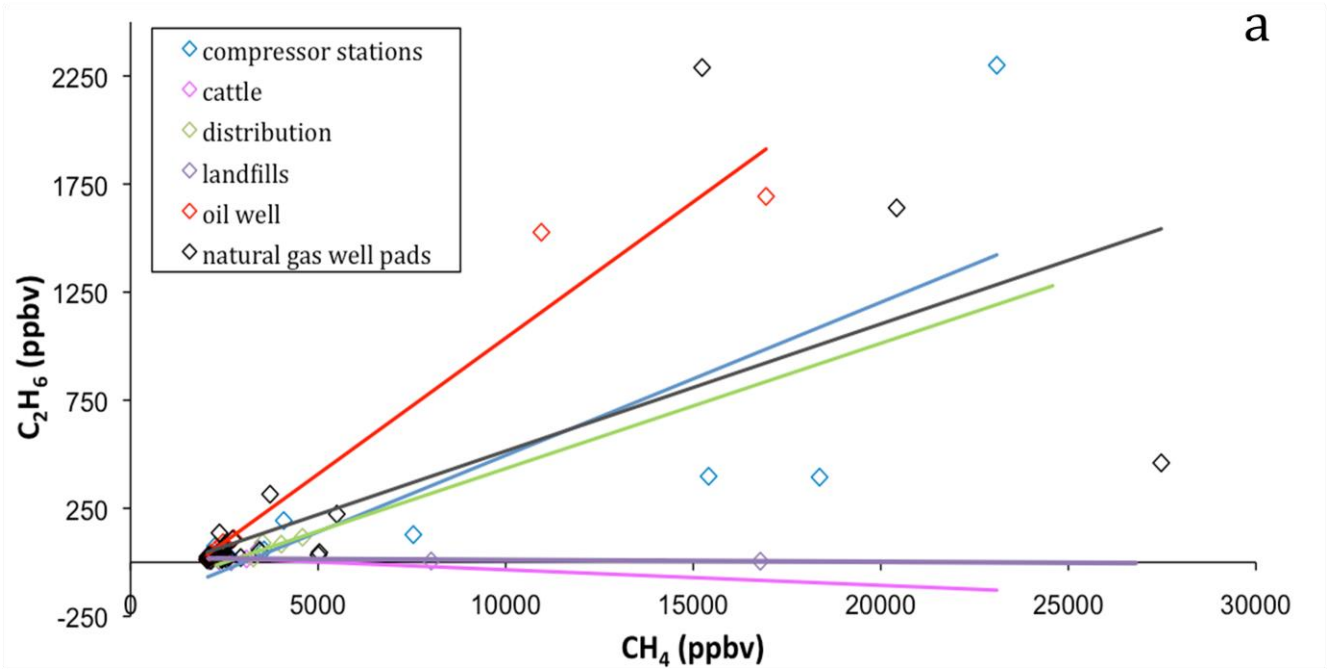

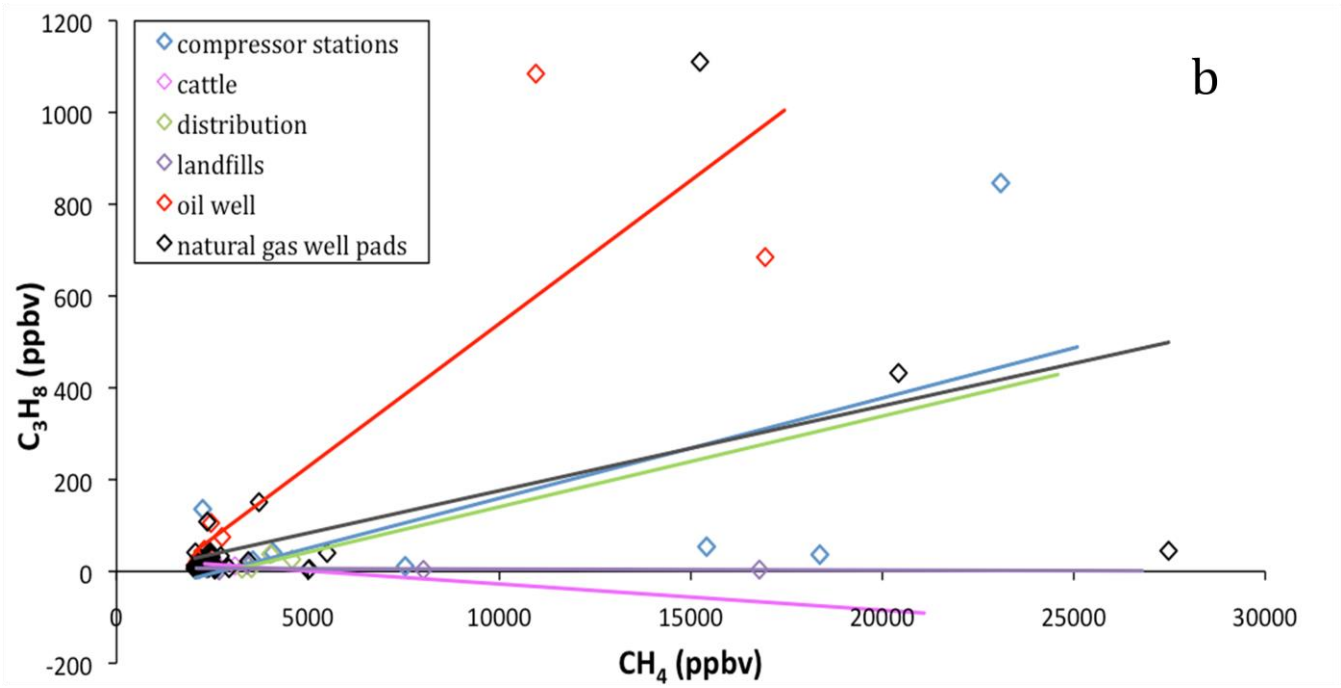

Table 4.4. Ratios of C_2-C_5 hydrocarbons to CH_4 (C_1) in thermogenic CH_4 sources in the Barnett Shale region, as well as R^2 values derived from correlations in Figure 4.5. Biological CH_4 sources are not shown due to lack of correlation.

	Natural gas well	**Compressor**	**Distribution**	**Conventional oil**
$C_2:C_1$	0.06 (0.01)	0.07 (0.02)	0.06 (0.03)	0.13 (0.01)
R^2	0.48	0.65	0.68	0.95
C3:C1	0.02 (0.006)	0.02 (0.009)	0.02 (0.01)	0.06 (0.01)
R^2	0.26	0.44	0.55	0.74
nC4:C1	0.005 (0.001)	0.003 (0.002)	0.005 (0.004)	0.02 (0.003)
R^2	0.21	0.21	0.36	0.68
iC4:C1	0.002 (0.001)	0.003 (0.001)	0.002 (0.001)	0.009 (0.0001)
R^2	0.32	0.42	0.38	0.96
nC5:C1	0.002 (0.001)	0.001 (0.001)	0.001 (0.001)	0.006 (0.001)
R^2	0.20	0.20	0.30	0.85
iC5:C1	0.001 (0.0004)	0.001 (0.001)	0.001 (0.001)	0.006 (0.001)
R^2	0.25	0.25	0.31	0.93

In addition to comparisons with CH_4, correlation analysis was extended to include other hydrocarbon ratios, because regional enhancements were observed in all light alkanes. A correlation plot of propane versus ethane was used to characterize the propane trends, shown in Figure 4.6. Of the oil and natural gas sources sampled, oil wells had the highest propane/ethane ratio, at 0.53 ± 0.05 ppbv/ppbv. This is not unexpected, as oil is richer than natural gas in non-methane hydrocarbons. Local natural gas wells and compressor stations had ratios of 0.41 ± 0.02 and 0.36 ± 0.03 mol propane/mol ethane, respectively. Distribution pipelines and city gates had a ratio of 0.20 ± 0.13 ppbv/ppbv, the lowest of any source sampled. The lowered ratio is due to the processing that occurs to remove higher chained alkanes before the natural gas is distributed [Peischl et al., 2013]. Similar trends were observed in California during airborne campaigns that sampled local ONG wells in Kern County and the Los Angeles Basin. The propane to ethane ratio in the oil fields of Kern County was 0.68 ± 0.02, and even lower for pipeline quality natural gas in the LA Basin [Hartt, 2013; Peischl et al., 2013]. As in

these previous studies, the local oil and gas infrastructure contributes significantly to the atmospheric propane burden.

Figure 4.6. Correlation plot of propane vs ethane for oil and natural gas sources in the Barnett Shale.

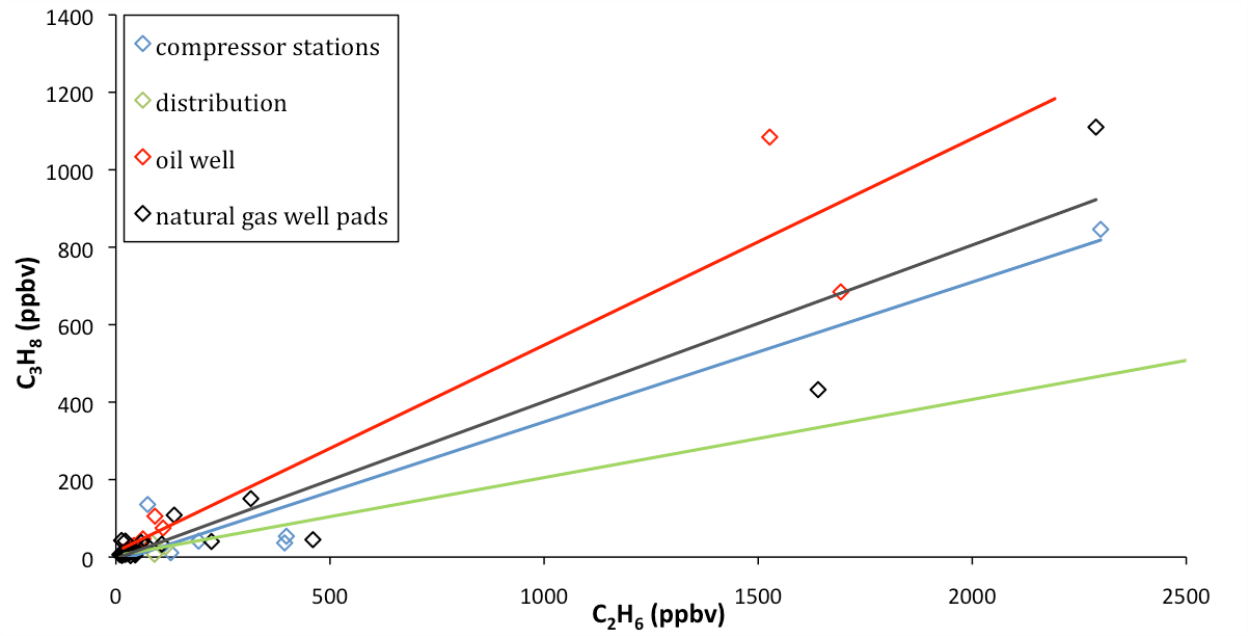

The effect of ONG sources on regional air can also be assessed using the ratio of *i*-pentane to *n*-pentane. For ONG sources in the Barnett Shale, the pentane ratio ranged from 0.7 to 1.1 (ppbv/ppbv). This lowered ratio is similar to surface observations in the Kern County oil fields, where ratios ranged from 0.9-1.4 [Hartt, 2013]. In the Denver-Julesburg basin of northeastern Colorado, the i- to n-pentane ratio ranged from 0.81 to 1.1, measured from tall towers [Gilman et al., 2013]. For comparison, samples in the city of Bakersfield, CA (the largest in Kern County), which also had elevated combustion tracers, the pentane ratios were greater than 2.0. Urban samples were not collected in the cities that lie within the Barnett Shale, which does not allow for a direct comparison to be made. However, local background samples also had a ratio less than 1, indicating the dominating influence of ONG activities in the region.

Although most of the samples collected in this study were collected from public access roads, it does not appear that combustion emissions affected the source samples. Little or no correlation was seen between ethane and tailpipe emissions tracers like ethene and CO. Background samples, on the other hand, did have some correlation with combustion tracers. When ethene was plotted against ethane in these samples, there was a bimodal distribution. In one lobe, the ratio was higher, implying an influence from traffic sources. Some of these samples were collected near roads with more traffic than roads that lead to oil or natural gas wells. The lower lobe, however, had more ethane relative to ethene, illustrating the influence of emissions from ONG sources.

b. Isotopic Ratios

In addition to quantification of VOCs in the Barnett Shale, a subsample from each canister was used for stable isotopic analysis. Laboratory and field studies have previously shown that stable isotopic composition can be used to assess regional CH_4 sources [Fisher et al., 2006; Townsend-Small et al., 2012]. Sub-samples from each canister were analyzed for $\delta^{13}C$ and δD isotopes by the University of Cincinnati using isotope ratio mass spectrometry, as described in Yarnes [2013]. By definition, $\delta^{13}C$ is a measure of the ratio of ^{13}C to ^{12}C, and similarly δD is the ratio of ^{2}H to ^{1}H (reported in parts per thousand, ‰). Because of the wide range of CH_4 concentrations in each of the sources sampled, the isotopic ratio was plotted against the inverse CH_4 concentration. The y-intercept of such a plot is the isotopic composition of the excess CH_4 in the samples. This is known as a Keeling plot [Keeling, 1958, 1961; Pataki et al., 2003]. Figure 4.7 shows Keeling plots of $\delta^{13}C$ and δD for the natural gas and biogenic CH_4 sources. Using the Keeling plot approach, the isotopic signature, or endmember value, was determined for each of the source types targeted in this study. Values for the carbon-13 ($\delta^{13}C$) and deuterium (δD) isotopic endmembers are shown in Table 4.5.

Figure 4.7. Keeling plots for samples collected in the Barnett Shale region of a) $\delta^{13}C\text{-}CH_4$ vs inverse methane concentration ($[CH_4]^{-1}$) from natural gas sources, b) $\delta^{13}C\text{-}CH_4$ vs $[CH_4]^{-1}$ from biological methane sources, c) $\delta D\text{-}CH_4$ vs $[CH_4]^{-1}$ from natural gas, and d) $\delta D\text{-}CH_4$ vs $[CH_4]^{-1}$ from biological sources.

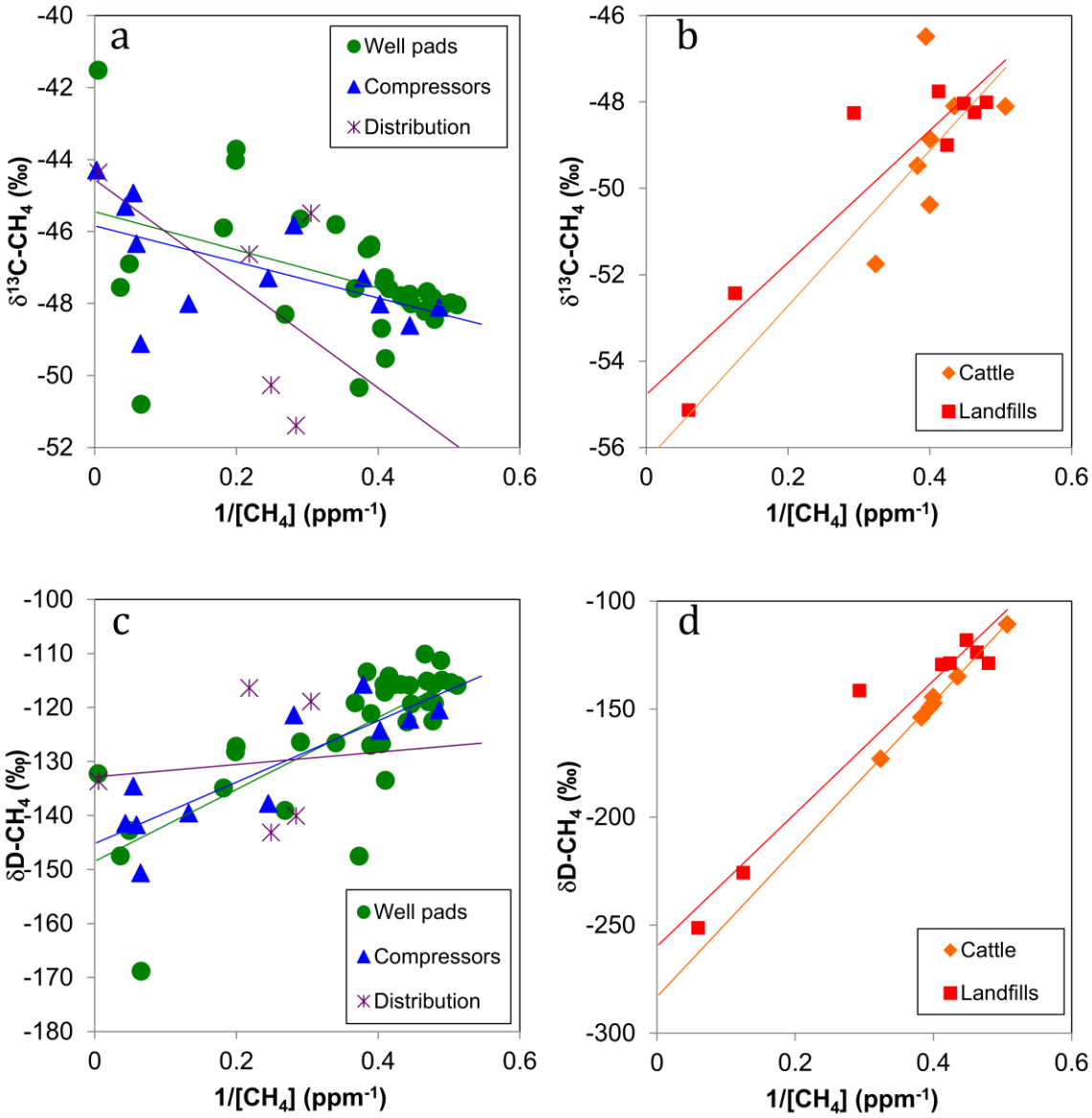

Table 4.5. Stable isotopic endmembers for CH_4 sources in the Barnett Shale region; data are derived from Keeling plots such as those shown in Figure 4.7.

		$\delta^{13}C$		**δD**	
Thermogenic	*n*	*Endmember (‰)*	*SE*	*Endmember (‰)*	*SE*
Natural gas well pads	31	-46.5	0.7	-152	3.9
Compressors and transmission	12	-45.8	0.6	-145	3.2
Distribution systems	4	-44.6	2.9	-133	13.9
Conventional oil wells	12	-49.2	29.5	-170	4.2
Biogenic					
Cattle	6	56.3	4.6	-283	4.4
Landfills	68	-54.8	1.0	-260	12.6
Background	24	-47.9	1.2	-113.7	13.8

Natural gas wells emitted CH_4 with $\delta^{13}C$ and δD signatures of -46.5‰ and -152‰, respectively (Figure 4.7). However, the high variability across the samples showed a weak relationship and resulted in a low correlation coefficient (R^2) value. Other natural gas sources (compressor stations and distribution systems) had similar isotopic signatures to those observed at natural gas wells. Conventional oil wells however, were more depleted in both ^{13}C and D, with endmembers of -170‰ and -49.2‰ for δD and $\delta^{13}C$, respectively. Previous work has shown that biological CH_4 sources are relatively depleted in both D and ^{13}C [Whiticar, 1999; Whiticar and Schaefer, 2007; Townsend-Small et al., 2012]. The same trend was observed in landfills and cattle feedlot samples.

Background samples, which were collected away from any direct source, had an isotopic $\delta^{13}C$ value of -47.9‰, similar to other ONG sources. This suggests that the dominant source of methane in the region is likely thermogenic in nature. A more complete inventory for CH_4 sources and the influence on well-mixed air is addressed in Section 4.4.

c. Background Corrected Ratios

In addition to obtaining plot-derived values, alkane ratios for natural gas production sites were also calculated by correcting for the presence of background air. This was done to account for the fact that samples were collected slightly downwind of each site and not directly at the wellheads or tanks, allowing background air to mix into source samples. For each gas, enhancement over background was calculated as ΔX = [source concentration] – [average background concentration], where X is CH_4, C_2H_6, C_3H_8, C_4H_{10}, or C_5H_{12} [Wennberg et al., 2012]. All samples with concentrations of CH_4 less than 2022 ppb (average background concentration + standard deviation of background measurements) were not included in any analysis. Alkane ratios were determined by dividing the enhancement of C_2 to C_5 alkanes by the enhancement in CH_4 and then multiplying by 100. As in the plot-derived approach, the result is a molar ratio.

Ratios of background corrected C_2:C_1 in individual samples collected downwind of natural gas well pads ranged from 0.3 to 30.7%, with an average of 8.2 ± 7.1% C_2H_6 relative to CH_4. The remaining natural gas sources had an ethane to methane ratio that ranged, on average, from 2.2 ± 1.9 to 7.1 ± 6.3%. In general, the data presented here are in agreement with previous studies conducted in the Barnett Shale that have found mostly low ethane content in natural gas production sites, but with high variability from well to well [ERG, 2012; Zumberge et al., 2012]. Table 4.6 shows data for background-corrected C_2:C_1 (in percent by volume) as compared to the previous studies carried out by the Texas Commission on Environmental Quality and GeoMark Research, LLC. The well pads sampled in our study have a higher average C_2:C_1 than the others, although with only a third as many samples collected. The two previous studies also made measurements at the well pad, either from the wellhead [Zumberge et al., 2012] or from condensate tanks [ERG, 2012]. The UCI samples were collected downwind of

well pads only where CH_4 was elevated, and therefore may represent a higher proportion of tank flashing events than the other two datasets.

In Los Angeles, the C_2:C_1 alkane ratio was measured from ground-based flask samples filled at the Mt. Wilson Observatory in LA county (2007-2008), in airborne samples collected over the LA Basin as part of the ARCTAS (2008) and CalNEX (2010) campaigns, and in pipelines that delivered natural gas to southern California during those sample times [Wennberg et al., 2012; Hsu et al., 2010]. In the Mt. Wilson samples, the ΔC_2H_6: ΔCH_4 (background corrected) ratio was 2.05 ± 0.30%. During the later ARCTAS and CalNex campaigns, samples had C_2:C_1 ratios of 1.70 ± 0.16 and 1.50 ± 0.11%, respectively. Monthly averages of pipeline-quality natural gas during the same seasons were 2.04 ± 0.29, 2.09 ± 0.27, and 1.65 ± 0.25%, respectively [Wennberg et al., 2012; Hsu et al., 2010]. In comparison to the samples collected from distribution systems in the Barnett Shale, the natural gas transported throughout the LA Basin is drier, meaning it contains less ethane relative to methane. In addition to containing wetter gas, the UCI Barnett samples show greater variability (higher standard deviation), although again, this is likely a result of fewer representative source samples. A further analysis of wet and dry natural gas is presented in Section 4.3.3.

Table 4.6. Background corrected C_2:C_1 ratios from natural gas production sites from the current study as compared to two previous studies. [a]ERG, 2012. [b]Zumberge et al., 2012.

	This study	**TCEQ[a]**	**Zumberge et al.[b]**
n	31	102	129
Natural gas well pads			
Average	8.2 (7.1)	5.0 (4.3)	4.5 (1.2)
Minimum	0.3	1.0	0.8
Maximum	30.7	13.4	13.1
Median	7.5	2.1	2.1
Compressor stations			
Average	7.1 (6.3)	-	-
Distribution systems			
Average	3.4 (1.8)	-	-
Oil wells			
Average	12.8 (3.7)	-	-

In general, for samples taken downwind of natural gas production sites, there was a poor correlation between $\delta^{13}C$ and CH_4 concentration (Figure 4.7). A plot of $\delta^{13}C$ versus background corrected C_2:C_1 and C_3:C_1 ratios, shown in Figure 4.8, reveals that carbon isotopic composition of CH_4 decreases with increasing concentrations of C_2H_6 and C_3H_8. In other words, greater isotopic depletion is observed with increasing natural gas wetness. A similar trend was observed for well pads sampled in the Zumberge et al. [2012] study, due to varying degrees of thermal maturation of shale gas in the Barnett.

Figure 4.8. Relationship between $\delta^{13}C$-CH_4 and C_2:C_1 (left panel) and C_3:C_1 (right panel) in samples taken near natural gas well pads in the Barnett Shale.

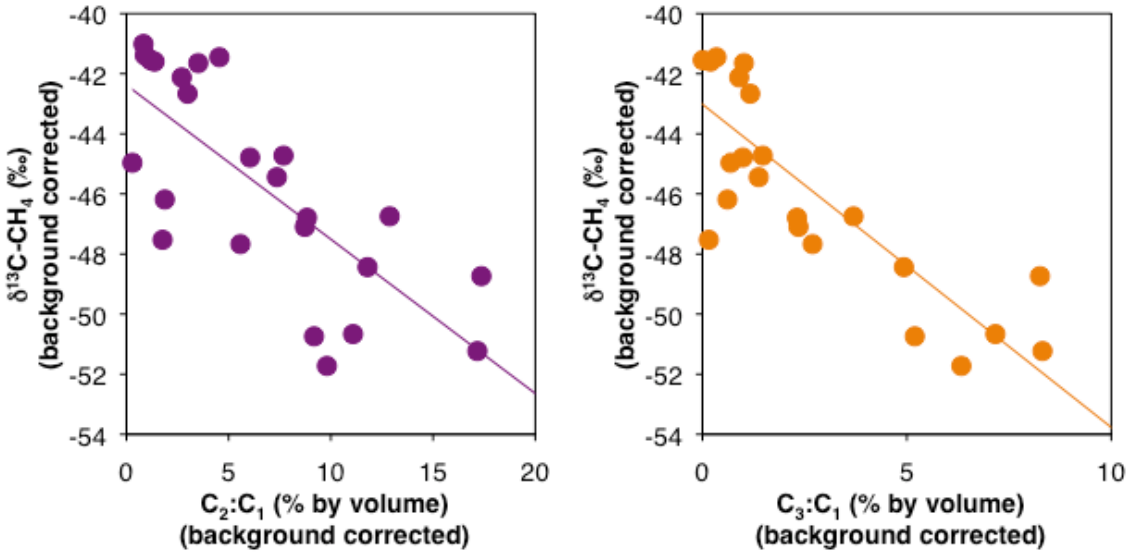

4.2.2 Natural gas composition

Background corrected mixing ratios were also used to calculate the hydrocarbon composition of the various source types sampled. The volume percentage was determined for C_1-C_5 alkanes, benzene, toluene, ethylbenzene and the xylenes (BTEX). Although they were measured, other VOCs were not included in this calculation (CO, C_6+ alkanes, cyclic alkanes, other aromatics, etc.). The average volume percentages are summarized in Table 4.7. Not

surprisingly, biogenic source samples were composed almost entirely of CH_4. Landfills, in particular, were composed of 98.9 ± 3.1% CH_4, on average. Well pads and compressor stations had similar profiles, which is expected, as both are associated with unprocessed natural gas. Their alkane compositions were approximately 88% CH_4 and 6% C_2H_6. The removal of higher order alkanes during processing is reflected in the composition of samples that were taken near processing plans and distribution pipelines, which were 95% CH_4 on average. Oil well samples were only 77.8 ± 6.9% CH_4, with the highest percentages of C_2H_6 and C_3H_8 of all ONG samples. BTEX compounds were also found to be the most abundant in oil samples, making up on average about 0.2% of the natural gas.

The alkane composition of natural gas in this study was also compared to typical US raw gas profiles reported by the Gas Processors Association (GPA), to natural gas composition for each of the counties in the Barnett Shale, as reported by the TCEQ, and to California oil fields (Table 4.7). Because the primary components of natural gas vary depending on the reservoir source from where it is produced, the GPA provides 3 different hydrocarbon profiles for natural gas [Gas Processors Association, 1991]. The calculated CH_4 content in ONG sources in this study falls well within the range of the GPA values for wet (71.3%) and dry (92.4%) gas. Further, the wide range of values observed at natural gas well pads (87.7± 10.9% CH_4), reflects the variability in gas 'wetness' in the study region. GPA wet gas values closely resemble the sampled conventional oil wells, while their values typical of processed gas (separated from liquid condensate) match samples collected in this study.

Natural gas composition was calculated by the TCEQ for the 66 gas producing counties throughout the state of Texas [ERG, 2012]. Whole air samples were collected at ONG sites in 6 of those gas-producing counties within the Barnett Shale. The county averaged TCEQ percentages are also shown in Table 4.7. While a complete comparison cannot be made,

Table 4.7. Hydrocarbon composition as described by average percentage of alkane and aromatic compounds present in all source types sampled in the Barnett Shale. For comparison typical natural gas composition values from the Gas Processors Association are shown, as well as values derived from the TCEQ and values for oil fields in Kern County, Califorina.

	CH_4 (%)	**C_2H_6 (%)**	**C_3H_8 (%)**	***i*-C_4H_{10} (%)**	***n*-C_4H_{10} (%)**	***i*-C_5H_{12} (%)**	***n*-C_5H_{12} (%)**	**BTEX (%)**
Natural Gas Wells	87.7 (10.9)	6.6 (4.7)	3.4 (4.5)	0.4 (0.7)	1.0 (1.6)	0.4 (0.7)	0.4 (0.7)	0.1 (0.1)
Compressor stations	87.9 (16.6)	5.2 (3.2)	3.3 (5.8)	0.5 (1.0)	1.8 (4.5)	0.6 (1.3)	0.6 (1.6)	0.1 (0.3)
Distribution systems	95.8 (2.2)	3.3 (1.7)	0.6 (0.7)	0.1 (0.1)	0.2 (0.2)	-	-	-
Processing	95.4 (4.1)	2.9 (2.1)	0.8 (1.1)	0.1 (0.1)	0.3 (0.4)	0.2 (0.3)	0.2 (0.3)	0.1 (0.1)
Conventional Oil	77.8 (6.9)	9.7 (2.3)	7.3 (2.8)	0.8 (0.4)	2.5 (1.3)	0.8 (0.4)	0.9 (0.5)	0.2 (0.2)
Dairies	95.1 (2.6)	1.9 (1.0)	1.7 (0.9)	0.2 (0.1)	0.6 (0.3)	0.2 (0.2)	0.2 (0.2)	-
Landfills	98.9 (3.1)	1.0 (1.0)	0.3 (0.5)	0.1 (0.1)	0.1 (0.1)	0.1 (0.1)	0.1 (0.1)	0.1 (0.1)
GPA wet gas [a]	71.3	13.3	9.7	1.0	3.2	0.6	0.9	-
GPA dry gas [a]	92.4	5.0	1.7	0.1	0.5	0.1	0.2	-
GPA processed gas [a]	95.5	2.9	0.9	0.3	0.2	0.1	0.1	-
TCEQ Counties [b]								
Denton	94.8	1.5	0.1	0.02	0.02	-	-	-
Jack	89.2	4.2	4.2	0.1	0.7	0.2	0.2	0.1
Johnson	92.7	3.3	0.6	0.1	0.1	0.05	0.03	-
Montague	79.8	9.7	5.9	0.4	1.5	0.3	0.3	-
Tarrant	94.6	1.8	0.1	0.01	0.01	-	-	-
Wise	81.9	8.0	4.2	0.6	1.4	0.4	0.4	0.1
Kern County, CA[c]	79.9	7.2	7.4	1.0	2.2	1.1	0.7	0.5

[a] Gas Processors Association, 1991, [b] ERG, 2012, [c] Hartt, 2013.

because too few air samples were collected in each county, alkane percentages appear to be comparable between the studies. In Montague County, for instance, which sits in the more oil producing area of the Barnett, the TCEQ reports that natural gas is 79.8% CH_4 and 9.7% C_2H_6, as compared to 77.8 ± 6.9% and 9.7 ± 2.2% in this study.

Lastly, the composition of natural gas was calculated from 42 air samples collected in October 2012 in Kern County, California. Unlike the Barnett Shale, Kern County has declining natural gas production and is a primarily oil producing area, with over 52,000 active wells. As such, the alkane composition is similar to conventional oil wells in the Barnett. While still a fraction of the overall composition, BTEX compounds were slightly higher in Kern County (0.5%), though this could be due to the increased number of motors in operation at oil well sites [Hartt, 2013].

4.2.3 Wet Gas vs. Dry Gas

The high standard errors associated with natural gas composition values reported are indicative of the variability in gas wetness throughout the Barnett Shale. Therefore, these alkane percentages were used to further distinguish between wet and dry natural gas in the region. First, ONG sources were sorted based on their ethane content. Samples with less than 5% C_2H_6 were considered 'dry' and those with more than 5% C_2H_6 were considered 'wet.' Using this classification scheme, methane/ethane enhancement ratios (MERs) were determined. For oil and natural gas emissions in the southwestern United States, MERs typically range from 7:1 up to 50:1 [Jones et al., 2000; Katzenstein et al., 2003], compared to coal bed methane, which can have an MER near 5000 [Xiao et al., 2008]. Figure 4.9 is an MER plot for the Barnett ONG samples. The samples fall into two distinct lobes, with wet gas having a slope of 8.2 ± 0.5, while the dry gas MER is 45 ± 3. It should be noted that all oil samples fell within in the slope of wet

samples, and alone have an MER of 7.6 ± 0.5 (not shown). For comparison, MERs calculated individually for ONG samples in the Kern County oil fields ranged between 5 and 45. Biological sources, due to their high methane content, generally have MERs greater than 50:1. While not shown here, cattle feedlot samples had an MER of 70:1, on average.

Figure 4.9. Enhanced CH_4 plotted against C_2H_6 for samples collected at natural gas well pads, compressor stations, and conventional oil wells. The MER, given by the slope, differs for wet (blue) and dry (red) ONG samples.

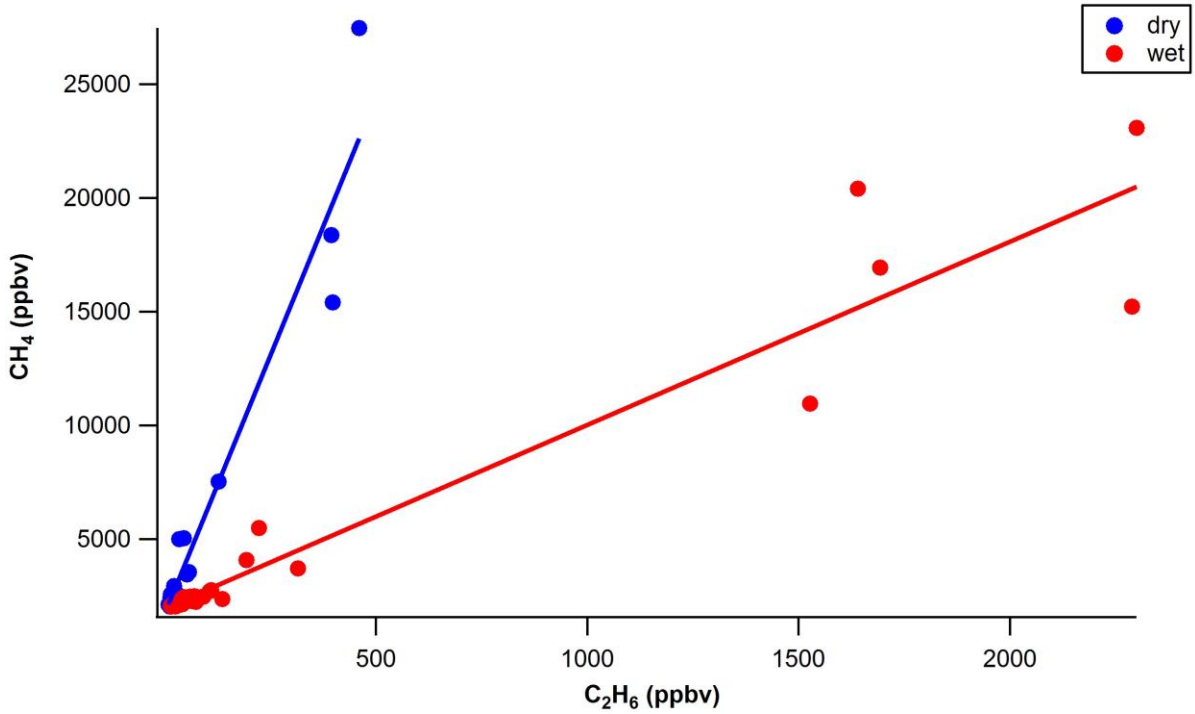

In addition to oil fields in California, natural gas from the Denver-Julesburg and Uintah Basins, as well as the Marcellus, Haynesville, and Fayetteville Shales was examined from ground based and aircraft measurements. Samples were collected between 2012-2014 and analyzed for C_2-C_7 VOCs [Gilman et al., 2014]. Plot-derived enhancement ratios (slopes) relative to propane were determined for each region and are shown in Figure 4.10. Each of these basins has a slightly different hydrocarbon profile. The more western ONG reservoirs, including the Barnett Shale and Denver and Uintah Basins, have the lowest C_2H_6/C_3H_8 enhacement ratios, while the shales that lie east of the Barnett have a greater C_2H_6 to C_3H_8 ratio. Looking at the

heavier alkanes relative to propane suggests that the natural gas signatures from the Barnett and Marcellus Shales appear to be the driest. This figure also reveals that the more western basins have a lower iso- to n-pentane ratio. However, while this ratio is useful for highlighting the influence of ONG emissions on ambient air, it cannot be used to distinguish between wet and dry gas reservoirs.

Natural gas composition not only varies across the United States (Figure 4.10), but also varies greatly within a shale basin (Table 4.7). As mentioned in Section 1.2.5, the geological makeup of the Barnett Shale affects the distribution of oil and gas in the region and its wetness. In general, the dry gas region lies to the east and includes Johnson and Tarrant counties, which are two of the most productive counties. The western portion of the region, on the other hand, is characterized by wetter gas and oil reservoirs [Mukhopadhyay and Dow, 1994]. To assess whether samples reflect this geographic trend, the alkane composition of ONG samples was mapped. In Figure 4.11a, the percent composition of ethane in oil and gas samples is shown. Points are colored by ethane percentage, with the warmer colors representing higher ethane content. Overlaid on the figure are regions where oil, wet gas, and dry gas are typically found and are shown in yellow, orange, and red, respectively [Oil & Shale Gas Discovery News, 2014]. Overall the spatial trend is unclear, with $\%C_2H_6$ appearing quite variable. That is, orange and red points can be found in the dry gas region of the map.

However, the relationship between geographic location and wetness of the oil and gas is better illustrated with C_3H_8 percentage (Figure 4.11b). The lowest propane containing samples (cool colors) were located primarily in the dry gas zone. Moreover, the highest $\%C_3H_8$ values were found exclusively in samples collected in the more oil-prone, northwestern portion of the Barnett Shale (in Montague and Jack counties).

Figure 4.10. Enhancement ratios relative to propane for C_2-C_5 alkanes for 6 natural gas reservioirs: the Barnett Shale (black), Fayetteville Shale (red), Haynesville Shale (green), Marcellus Shale (purple), Denver-Julesburg Basin (blue), and Uintah Basin (orange).

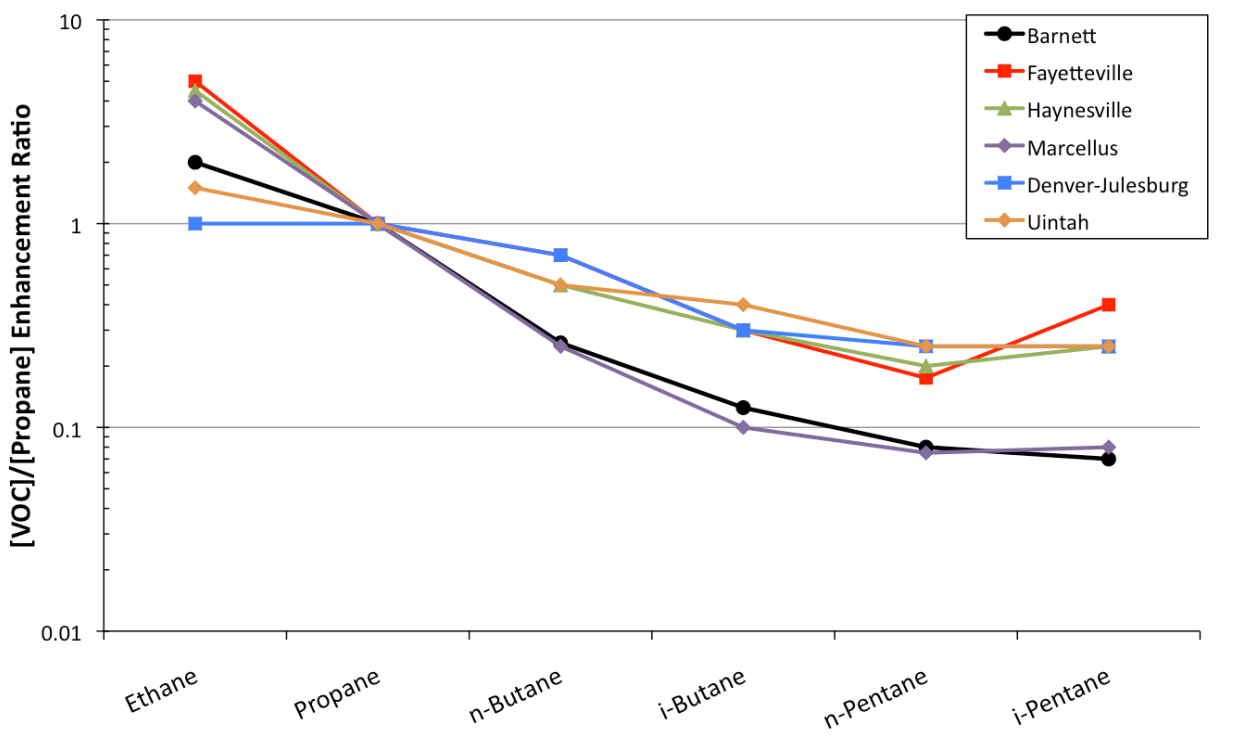

Figure 4.11. Map of a) ethane and b) propane percentage in oil and natural gas samples collected in the Barnett Shale, showing that the driest gas is found to the east in the region.

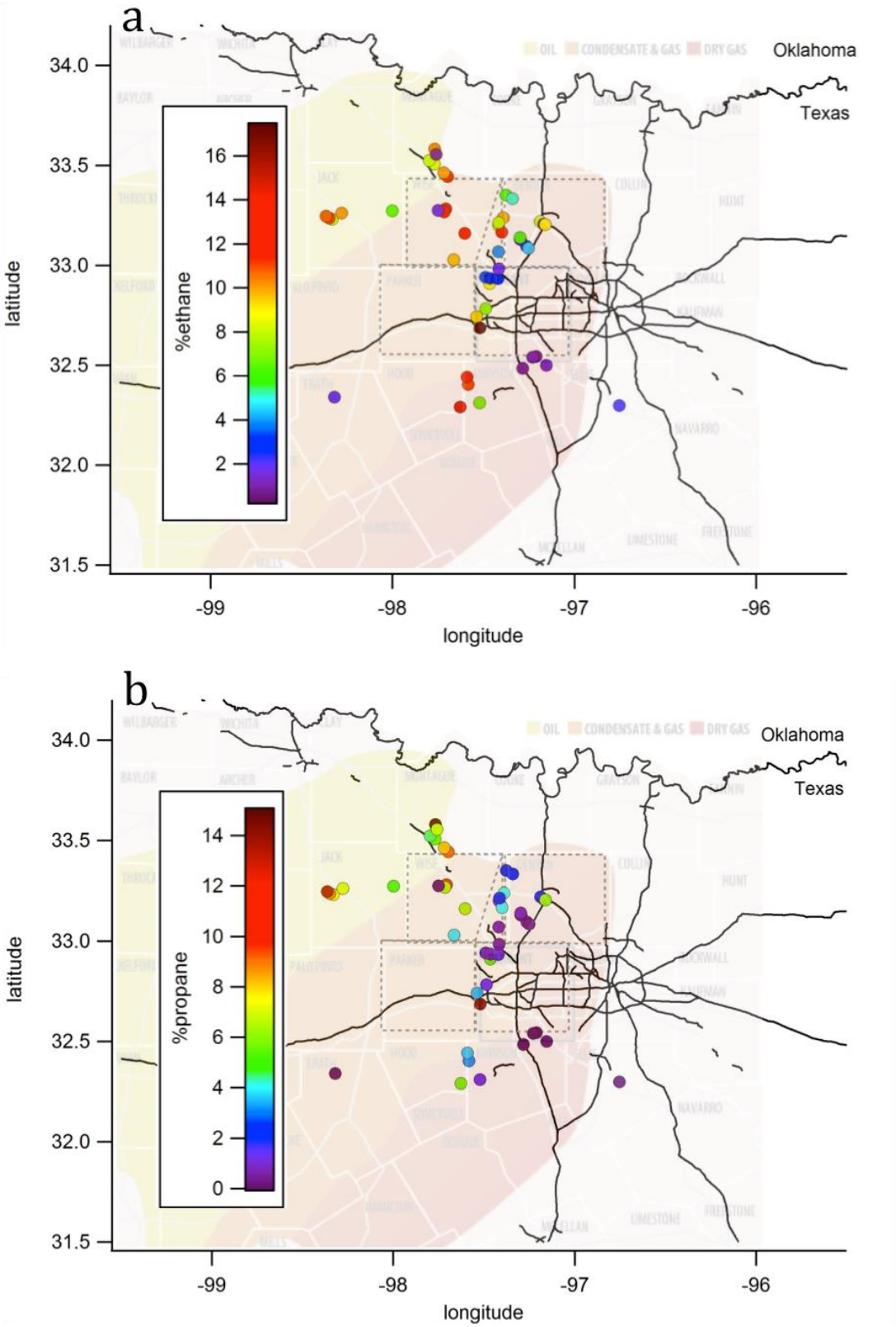

4.3 Statistical Source Apportionment

During this campaign, samples were generally collected downwind of sources, that is, in close proximity to (<100m) but not directly at a holding tank or wellhead. The result is some degree of atmospheric mixing. While a background correction can help remove some of this interference, it cannot account for the co-location of VOC sources. For instance, some of the gas well pads sampled also housed on-site compressor engines, while conventional oil wells have motor-operated jump jacks. This potentially introduces VOCs typically associated with combustion emissions. Furthermore, cattle were often seen roaming on or near wells, mixing emissions from ONG and biological sources. The effect of these various sources is evident in background samples, which had high concentrations of multiple compounds. Figures like 4.10 and 4.11 highlight the advantage of incorporating a more extensive number of VOCs when trying to characterize the various CH_4 sources in the region. To better understand and expand upon the source characterization provided by alkane ratios and isotopic composition, source apportionment through PMF was utilized.

Positive matrix factorization (PMF) is a mathematical source/receptor model often used in atmospheric studies to identify a set of factors that can represent major emission sources. This multivariate analysis uses a mass balance approach that accounts for all *j* (=1,2,…m) chemical species (and their uncertainties) in *i* (=1,2,…n) number of samples as contributions from *k* (=1,2,…p) independent sources [Paatero, 1997]. The dataset matrix (X_{ij}) is separated into matrices that describe factor profiles (f_{kj}) and their respective contributions (g_{ik}). A residual matrix (e_{ij}), which accounts for the difference between the predicted outcome and (X_{ij}), is then added to matrix pair as described by equation 4.1 [Paatero, 1997]:

$$x_{ij} = \sum_{k=1}^{p} g_{ik} f_{kj} + e_{ij} \qquad (4.1)$$

Solutions generated by PMF are constrained such that only non-negative solutions can be obtained, making it an improvement over previously used factor analysis, like principal component analysis [Paatero and Tapper, 1994; Paatero, 1997]. The PMF solution also works to minimize the object function (Q) by incorporating the measurement uncertainties (u_{ij}) [Paatero, 1997]:

$$Q = \sum_{i=1}^{n} \sum_{j=1}^{m} \left[\frac{e_{ij}}{u_{ij}} \right]^2 \tag{4.2}$$

The US Environmental Protection Agency's PMF [EPA PMF 3.0, Washington, DC] software was used to identify and determine the contribution of ONG, non-fossil fuel, and combustion emissions sources. The enhancement for each compound over local background (in pptv) was used as the model input data. For compounds where there was no enhancement over background, or where missing value indicators had been used (denoted as -888 or -999), the detection limit was used. For most VOCs this was 3 pptv. Input data also included uncertainties based on instrumental (GC) accuracies. One of the strengths of PMF is that uncertainty is adjusted so data points at or below the detection limit are weighted less than measurements at higher concentrations [Paatero, 1997]. This weighting is based on the signal-to-noise ratios derived from concentration/uncertainty scatter plots. Compounds with high signal-to-noise ratios are classified as "strong," while those with lower signal-to-noise ratios are marked as "weak" or "bad." Compounds classified as "bad," such as trimethylbenzenes or pinenes, were excluded from model runs due to high uncertainty or low mixing ratios. In addition, four samples with exceptionally high CH_4 or CO concentrations were removed from analysis. After several iterations, more compounds were classified as "weak" or "bad" if they were not well modeled.

Table 4.8 summarizes the compound strength designations ultimately used in analysis. The number of model base runs was set to 30 and the number of factors set to 5. An additional 5% modeling uncertainty was used to adjust for non-Gaussian distribution in residuals. The VOCs modeled by the PMF software made up approximately 70% of VOC mass measured. A comparison of observed data (O) to predicted values (P) was used to determine how well the model fit each species. Slopes for the O/P plots showed that the model generally provided an accurate prediction for most compounds. For CH_4 and the remaining alkanes, both straight-chained and branched, slopes were close to 1.0 and R^2 values were high (Table 4.8).

Table 4.8. Uncertainty input weightings used to classify compounds modeled by the EPA PMF software, and the slopes of observed versus predicted plots. Values for compounds with slopes less than 0.4 and low correlations are not shown.

	Model Weighting	O/P slope	O/P R^2
Alkanes			
Methane	Strong	1.0	1.0
Ethane	Strong	0.71	0.87
Propane	Strong	1.0	0.96
i-Butane	Strong	0.65	0.87
n-Butane	Strong	0.98	0.99
i-Pentane	Strong	0.92	0.99
n-Pentane	Strong	0.99	0.99
n-Hexane	Strong	0.98	0.97
n-Heptane	Weak	1.1	0.95
n-Octane	Weak	1.0	0.94
Aromatics			
Benzene	Weak	0.40	0.50
Toluene	Weak	-	-
Ethylbenzene	Weak	-	-
m/p-Xylene	Weak	-	-
Other			
CO	Strong	0.60	0.57
Ethene	Weak	-	-
DMS	Weak	-	-

Figure 4.12. Emissions factors determined from PMF model analysis for samples collected in the Barnett Shale. Profiles of these factors are representative of emissions from a) oil wells b) natural gas wells, and c) combustion sources.

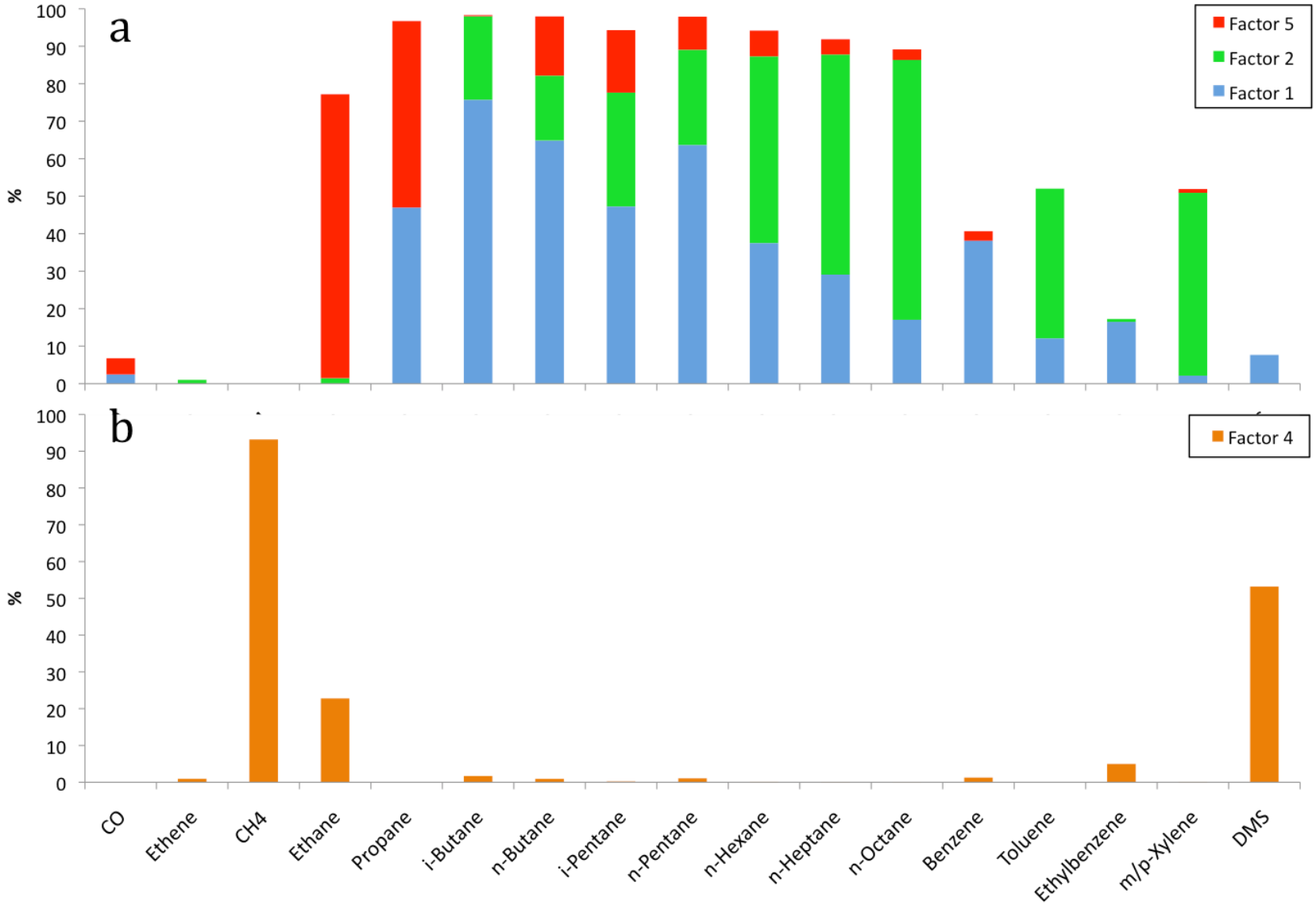

Figure 4.12. Emissions factors determined from PMF model analysis for samples collected in the Barnett Shale. Profiles of these factors are representative of emissions from a) oil wells b) natural gas wells, and c) combustion sources.

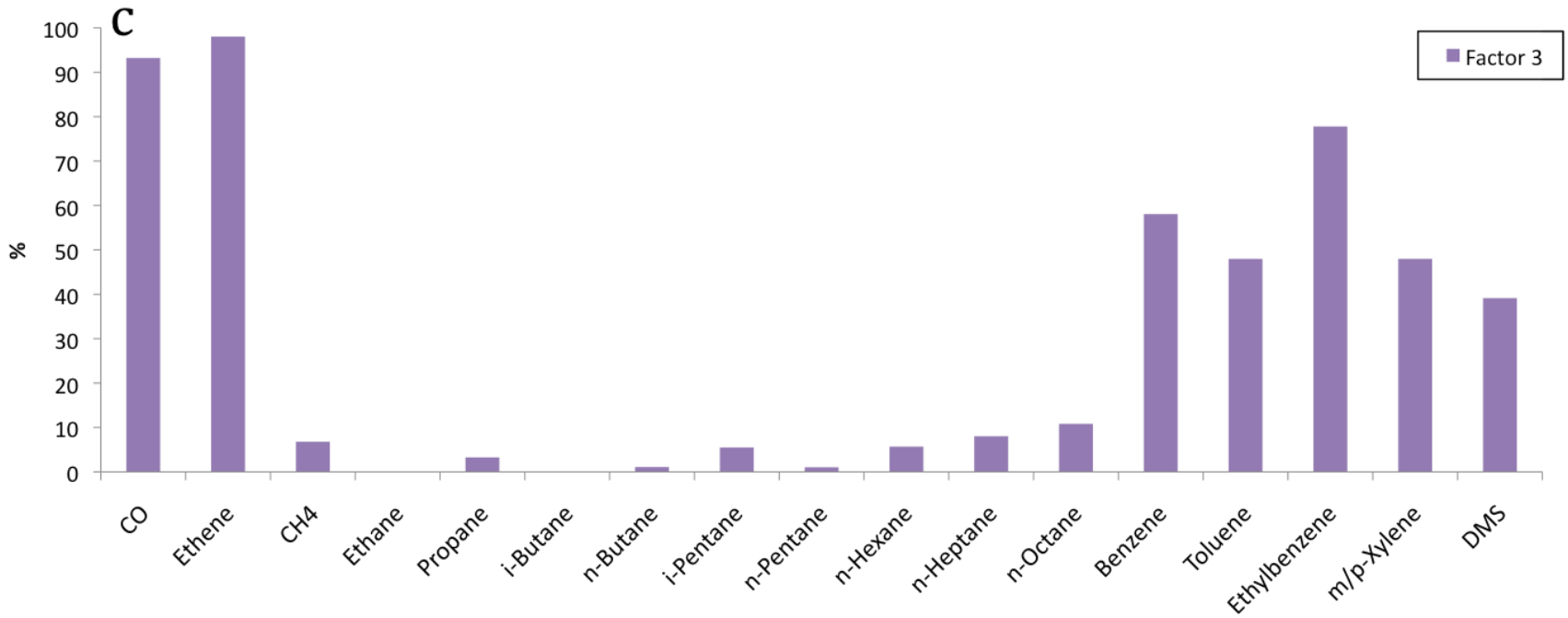

Interpretation of the resultant factor profiles revealed an emission source characteristic of combustion. This profile, seen in Factor 3 in Figure 4.12c, was comprised of 93% CO, 98% ethene and significant proportions of the aromatic compounds. A large number of vehicles were not present while source samples were collected, meaning this profile is not representative of incomplete combustion from tailpipes. Rather, this factor likely arises from compressor engines, at stations and on well pads, as well as pump jacks at conventional oil well sites. This also explains the 7% CH_4 associated with Factor 3. Alkane ratios (Section 4.2.1.a) did not show a strong correlation between ONG and combustion tracers, however PMF reveals some overlap between the two.

Factors 1, 2, and 5 (Figure 4.12a) combine to show an emissions profile consistent primarily with oil emissions and a slight natural gas signal. These factors contain over 90% of the each of the C_3+ alkanes, as well as 50% each of benzene, toluene, and xylenes. There is also a contribution of about 7% CO to these factors, again due to co-location of engines and ONG wells. Factor 5 exhibits a strong C_2H_6 and C_3H_8 signal, at 76% and 50%, respectively, but minimal contribution from the remaining alkanes. It is possible, therefore, that the model mixed oil and some natural gas emissions in this factor.

However, in spite of how closely linked O&NG emissions are, a CH_4 signal is missing from Factors 1, 2, & 5. Instead, 93% of CH_4 is contained within Factor 4 and is more representative of emissions from natural gas. This profile, shown in Figure 4.12b, also contains 23% C_2H_6, reflecting the wetness associated with natural gas emissions in the Barnett Shale. Factor 4 also contains 53% of dimethyl sulfide (DMS), which is consistent with emissions from biological CH_4 sources. Increased DMS has been observed from dairies located in the California Central Valley [Yang, 2009]. Indeed, samples collected downwind of cattle feedlots in the Barnett also had increased DMS.

Overall, the Barnett Shale is a challenging study region, with many VOC emissions sources simultaneously in play. While a statistical source apportionment through PMF did help in distinguishing combustion emission from oil and natural gas, the model could not successfully separate emissions from biogenic CH_4 and natural gas. In the future, a regional grid study, in conjunction with source sampling, could be more useful in assessing the local ambient air.

4.4 Integration into a Bottom-up CH_4 Inventory

One of the primary goals of the Barnett Coordinated Campaign was to develop a bottom-up CH_4 inventory, including median, low-end, and high-end flux estimates (in kg/hr) for various biogenic and thermogenic sources in the region. The inventory is shown in Table 4.9 [Lyon et al., *in review*]. The isotopic and plot derived alkane ratios presented in this chapter were integrated into the inventory in order to infer the composition of CH_4 in well-mixed air. To do so, the percent contribution of each CH_4 source to total emissions was multiplied by the representative endmember and summed over all sources. For example, the median emission estimate for active natural gas well pads is 16,400 kg hr^{-1} out of a total 73,915 kg hr^{-1}, or 22%. This value was then multiplied by the C_2:C_1 alkane ratio of 6.0% for natural gas well pads, and repeated for the remaining sources. A sum of these values gives an estimate of the C_2:C_1 ratio for well-mixed air of 4.1%. The alkane ratios for biogenic CH_4 sources were left blank, as their plots revealed little correlation. Wastewater treatment plants and gasoline-powered vehicles were not sampled in this study, so literature values for isotopic composition were used [Townsend-Small et al., 2012]. As samples were not collected from geological seeps and inactive or abandoned wells, their composition was assumed to be the same as active natural

Table 4.9. Bottom-up inventory of CH_4 sources in the Barnett Shale region [Lyon et al., *in review*] as well as alkane and isotopic signatures of each source. Three estimates of the composition of total CH_4 emitted from the region are shown in the bottom row.

	CH_4 flux (kg CH_4/hr)	low end flux (kg CH_4/hr)	high end flux (kg CH_4/hr)	$\delta^{13}C$-CH_4 (‰)	δD-CH_4 (‰)	C_2H_6:CH_4 (%)	C_3H_8:CH_4 (%)
Active Gas Well Pads	16,400	15,400	17,300	-45.4	-148	6.0	2.0
Active Oil Well Pads	1,800	1,700	1,900	-49.2	-170	13.0	6.0
Inactive Wells	630	320	1,270	-45.4	-148	6.0	2.0
Well Completions	150	30	290	-45.4	-148	6.0	2.0
Gathering Compressors	18,700	12,900	26,000	-45.4	-148	6.0	2.0
Gathering Pipelines	900	800	1,200	-45.4	-148	6.0	2.0
Processing Plants	5,500	3,700	8,100	-45.4	-148	6.0	2.0
Transmission Compressors	1,200	800	1,700	-45.8	-145	7.0	3.0
Transmission Pipelines	230	190	300	-45.8	-145	7.0	3.0
Storage Facilities	360	250	500				
Local Distribution	2,600	2,100	3,400	-44.6	-133	6.0	2.0
Natural Gas Vehicles	135	10	675	-44.6	-133	6.0	2.0
ONG sources total	**48,605**	**38,200**	**62,635**				
Other industrial sources	60	20	130	-45.4	-148	6.0	2.0
Vehicles (gas & diesel)[1]	150	150	150	-30.3	-122	-	-
Landfills	11,300	5,000	16,900	-54.8	-260	-	-
Livestock	11,900	10,800	13,500	-56.3	-283	-	-
Wastewater Treatment[1]	800	600	900	-46.7	-298	-	-
Geological Seepage	1,100	530	800	-45.4	-148	6.0	0.3
Other sources total	**25,310**	**17,100**	**32,380**				
Total Emissions	**73,915**			**-48.6**	**-188**	**4.2**	**1.4**
Low End		**55,300**		**-48.5**	**-186**	**4.5**	**1.5**
High End			**95,015**	**-48.6**	**-188**	**4.2**	**1.4**

[1] Townsend-Small et al., 2012.

gas wells [Etiope et al., 2013; Kang et al., 2014]. Lastly, natural gas vehicles, which comprise a small portion of this inventory, were assumed to have a composition similar to distribution gas. Ratios of butanes and pentanes to methane were not included due to generally low statistical significance for these ratios in most sources.

The bottom-up inventory predicts a contribution of ONG sources to the overall CH_4 flux that ranges between 65-70% for the 3 possible scenarios. Calculated alkane and isotopic ratios are well aligned with this greater ONG signature. For instance, the estimated C_2:C_1 ratios were 4.2%, 4.5%, and 4.2% for the median, low and high-end emissions scenarios. For C_3:C_1, the ratios were 1.4%, 1.5%, and 1.4%, respectively. These ratios are more similar to oil and gas endmember values, but do not eliminate the influence of biological sources of CH_4. The calculated isotopic compositions also more closely resemble that of oil and gas sources, falling between -48 and -49‰ for $\delta^{13}C$ and ranging between -186 and -188‰ for δD.

The CH_4 inventory and estimated C_2:C_1 ratios were also used to calculate flux estimates of C_2H_6 in the Barnett Shale region, for median, low-end, and high-end scenarios. The predicted ratios were simply multiplied by the CH_4 emission estimate for each scenario and adjusted for the mass difference between CH_4 and C_2H_6. The median flux was 5900 kg C_2H_6 hr^{-1}, with low and high-end estimates of 4600 and 7500 kg C_2H_6 hr^{-1}. This range of values is in good agreement with a top-down estimate of 6600 ± 200 kg C_2H_6 hr^{-1}, developed from aircraft measurements as part of the same campaign [Smith et al., *in review*]. If the background corrected C_2:C_1 ratios are used instead of the plot-derived values, the C_2H_6 estimate increases to 7700 kg hr^{-1}, with low and high-end fluxes of 6100 and 9800 kg C_2H_6 hr^{-1}.

For further comparison, the alkane ratios from previous studies (Table 4.6) were used to calculate a C_2H_6 emission estimate. Natural gas production data from the Zumberge et al. (2012) study yielded a C_2H_6 flux of 4600 kg C_2H_6 hr^{-1} (3600 – 5800 kg C_2H_6 hr^{-1}), while the

TCEQ study lead to a flux of 5000 kg hr^{-1} (4000 – 6300 kg C_2H_6 hr^{-1}) [ERG, 2012]. The various C_2H_6 estimates are summarized in Table 4.10. In general, there is a wide range in C_2H_6 fluxes, stemming from high variability in C_2:C_1 of CH_4 from production sites in the Barnett Shale. In addition, there is a larger contribution of ONG sources to total emissions predicted by the top-down C_2H_6 estimate when compared to the bottom-up prediction (71-85% ONG vs 65-70%). One possible explanation for this difference is that emissions from oil wells are contributing to an ONG over prediction if only the ethane to methane ratio is used to distinguish between CH_4 sources. This highlights the challenges associated with using a single source apportionment indicator for constraining emissions from oil and gas production. As seen in Figure 4.11, the inclusion of propane as a source indicator is helpful in distinguishing between oil and natural gas sources of CH_4. So overall, while UCI canister samples may be limited in their ability to provide full and spatially resolved coverage, compared to high resolution airborne C_2H_6 measurements [Smith et al., in review], one of their strengths is addition of propane to the data set.

Table 4.10. Summary of C_2H_6 flux estimates derived from alkane ratios in the current study, compared to estimates from previous ground based studies and airborne measurements also collected as part of the Barnett Coordinated Campaign.

	UCI (plot based)	UCI (bkgd corrected)	Zumberge	TCEQ	Aerodyne (top-down)
Median (kg hr^{-1})	5900	7700	4600	5000	6600
Low-end (kg hr^{-1})	4600	6100	3600	4000	-
High-end (kg hr^{-1})	7500	9800	5800	6300	-

When compared to other locations, the Barnett Shale region has a larger contribution from biological sources to the overall CH_4 emissions, in spite of the high natural gas production. For instance, studies in Los Angeles, from hydrocarbon and isotopic analyses, report that the dominant source of CH_4 is fugitive emissions from natural gas infrastructure, while up to 30% of CH_4 emissions in the Barnett Shale can be attributed to biological sources [Wennberg et al.,

2012; Peischl et al., 2013; Townsend-Small et al., 2012]. The Barnett results are more similar to the Denver-Julesburg Basin, where non-ONG sources like cattle and waste treatment make up nearly 25% of CH_4 emissions, despite also being home to a large oil and gas industry [Petron et al., 2014].

4.5. Regional Photochemistry

As mentioned in Section 1.1.2b, the Dallas-Fort Worth region is designated as a non-attainment region, with frequent exceedances over the allowable 8-hour ozone standard. The first step in the formation of ozone is the reaction with OH radicals, which generate the alkyl radicals that through subsequent reaction with O_2 and NO_x lead to ozone generation (Section 1.1.2a). The reaction rate of VOCs with OH radical varies depending on the species, meaning that each compound can be assessed for its relative contribution and importance in ozone formation [Gilman et al., 2009]. While the actual amount of ozone produced is a function of NO_x conditions, the OH reaction rate is still be a useful, predictive quantity.

Hydroxyl reactivity, $R_{OH}= \Sigma k_{OH-X}*[X]$, was calculated for X = CO, CH_4, and measured NMHCs, and used as a proxy for potential ozone production in the Barnett Shale. Average mixing ratios of VOCs from background samples were used in calculations of R_{OH} since a regional assessment of well-mixed air was desired. As seen in Figure 4.13a, the overall R_{OH} for the region was 3.04 s^{-1}. This is comparable to R_{OH} for background samples collected in Fort Saskatchewan, Alberta (Section 3.3). In the Barnett Shale, CH_4 and CO accounted for 10 and 24% of the reactivity, respectively. NMHCs were the dominant species, responsible for 2.00 s^{-1}, or about 66% of the OH reactivity. Biogenic species (isoprene, alpha- and beta-pinene) accounted for 56% of the $R_{OH\text{-}NMHC}$, due to background samples being collected in the more

rural parts of the region and away from point sources. Removing input from biogenics and CO allows for an evaluation of the importance of anthropogenic hydrocarbons.

The reactivity drops to 1.16 s^{-1} when considering only the anthropogenic hydrocarbons (Figure 4.13b). Alkanes had the most significant contribution to this R_{OH}, responsible for 47% of the reactivity, while CH_4 accounted for 26%. Despite their decreased abundance relative to CH_4 and the other alkanes, alkenes still were responsible for 16% of the background R_{OH} value. This is due to faster reaction rates with hydroxyl radical, making them more efficient in the potential formation of ozone. The collection of background samples from the perimeter of the Barnett Shale was done from roads, suggesting that the presence of alkenes and aromatics is most likely from vehicular exhaust.

Using results from the PMF source apportionment analysis, the ozone forming potential due to oil and natural gas infrastructure was evaluated. To do so, the R_{OH} of each VOC was multiplied by the percentage of that VOC included in the 4 oil or natural gas factors determined from PMF. However for CH_4, the PMF model could not resolve the amount of CH_4 from ONG versus biological sources. To account for this difference, an additional correction was made. The Barnett campaign-derived CH_4 inventory predicts that up to 70% of the regional CH_4 arises from ONG sources, so this number was applied to the $R_{OH\text{-}CH4}$ value. Using the source apportionment and inventory results, $R_{OH\text{-}ONG}$ is 0.81 s^{-1} (Figure 4.13c). That is, ONG sources account for 70% of the reactivity from anthropogenic hydrocarbons in the Barnett Shale. When considering only ONG emissions, alkanes contribute to 63% of the $R_{OH\text{-}ONG}$, which is 97% of the contribution towards the total anthropogenic R_{OH}. CH_4 accounts for another 34% of $R_{OH\text{-}ONG}$, or 94% of the anthropogenic R_{OH}, while ONG only explains 25% of the reactivity of aromatic (BTEX) compounds. Alkenes, which previously contributed 16% of the R_{OH}, are almost negligible in $R_{OH\text{-}ONG}$, illustrating that their emissions are likely primarily from vehicle exhaust.

Figure 4.13. Hydroxyl reactivity rates (R_{OH}) for a) all VOCs measured in the Barnett Shale and b) anthropogenic hydrocarbons. This includes CH_4, alkanes, alkenes, and aromatics. The contribution of ONG sources to the hydrocarbon reactivity ($R_{OH\text{-}ONG}$) is shown in panel c. Note that the scale of the y-axis changes in each panel.

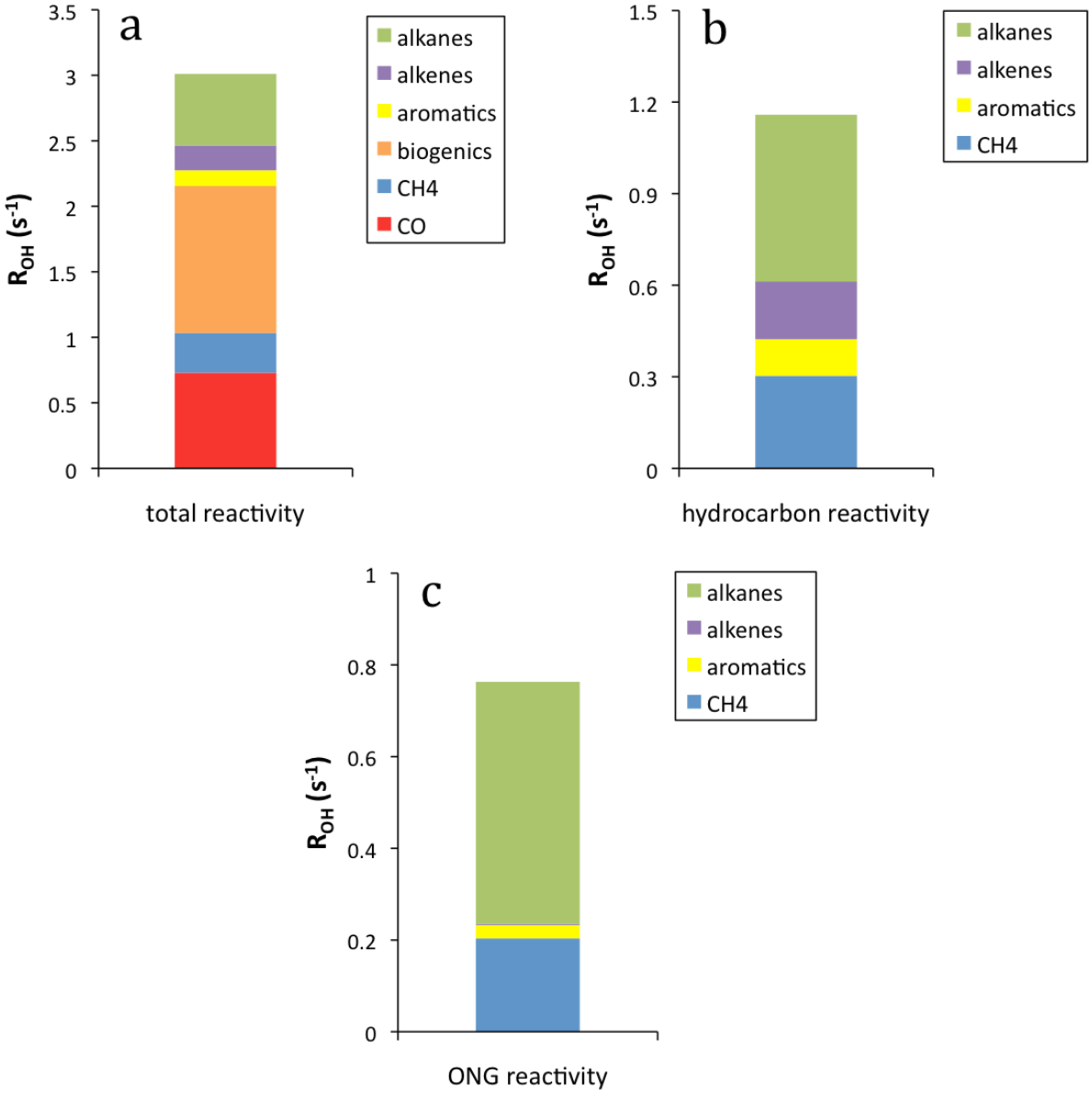

Values for R_{OH} reveal that hydrocarbon emissions in the region can have a direct effect on local air quality, with fugitive emissions from oil and natural gas contributing significantly. For comparison, assessment of air masses in Kern County, CA had similar hydroxyl reactivities ranging from 0.6 to 1.48 s^{-1}. However, values in both California and the Barnett Shale were only about half as big as in the Denver-Julesburg basin, where R_{OH} from NMHCs was up to 3 s^{-1} [Gilman et al., 2013].

4.6 References

Eastern Research Group (ERG). Condensate tank oil and gas activities: Final Report. Prepared for the Texas Commission on Environmental Quality, Air Quality Division. 2012. Available at https://www.tceq.texas.gov/assets/public/implementation/air/am/contracts/reports/ei/5821199776FY1211-20121031-ergi-condensate_tank.pdf

Etiope, G.; Drobniak, A.; Schimmelmann, A. Natural seepage of shale gas and the origin of "eternal flames" in the Northern Appalachian Basin, USA. *Mar. Petrol. Geol*. **2013**, 43, 178-186, doi:10.1016/j.marpetgeo.2013.02.009.

Fisher, R.; Lowry, D.; Wilkin, O.; Sriskantharajah, S.; Nisbet, E.G. High-precision, automated stable isotope analysis of atmospheric methane and carbon dioxide using continuous-flow isotope-ratio mass spectrometry. *Rapid Comm. Mass Spectrom*. **2006**, 20, 200-208, doi:10.1002/rcm.2300.

Gas Processors Association: The Gas Processing Industry: Its Function and Role in Energy Supplies, available at http://www.ihs.com/products/industry-standards/org/gpa/list/index.aspx, 1991.

Gilman, J.B.; et al. Measurements of volatile organic compounds during the 2006 TexAQS/GoMACCS campaign: Industrial influences, regional characteristics, and diurnal dependencies of the OH reactivity. *J. Geophys. Res*. **2009**, 114, D00F06, doi:10.1029/2008JD011525.

Gilman, J.B.; Lerner, B.M.; Kuster, W.C.; de Gouw, J.A. Source Signature of Volatile Organic Compounds from Oil and Natural Gas Operations in Northeastern Colorado. *Environ. Sci. Technol*. **2013**, 47, 1297-1305.

Gilman, J.B.; Lerner, B.M.; Warneke, C.; Graus, M.; Lui,R.; Koss, A.; Yuan, B.; Murphy, S.; Alvarez, S.; Lefer, B.; Min, K.-E.; Brown, S.S.; Roberts, J.M.; Osthoff, H.S.; Peischl, J.; Ryerson, T.B.; de Gouw. J.A. Primary emissions and secondary formation of volatile organic compounds from natural gas production in several major U.S. shale plays. Oral presentation at the AGU Fall Meeting, San Francisco, CA, December 2014.

Hartt, G.M. Oil and natural has emissions in the Gulf of Mexico and the San Joaquin Valley of California. PhD. Thesis, University of California, Irvine, 2013.

Hsu, Y. K.; VanCuren, T.; Park, S.; Jakober, C.; Herner, J.; FitzGibbon, M.; Blake, D. R.; Parrish, D. D. Methane emissions inventory verification in southern California. *Atmos. Environ*. **2010**, 44 (1), 1−7, DOI: 10.1016/J.Atmosenv.2009.10.002.

Jones, V.T. III; Matthews, M.D.; Richers, D.M. (1999). Handbook of Exploration Geochemistry: Vol. 7. Geochemical remote sensing of the subsurface. Light hydrocarbons for petroleum and gas prospecting. Amsterdam, The Netherlands. Elsivier.

Kang, M.; Kanno, C.M.; Reid, M.C.; Zhang, X.; Mauzerall, D.L.; Celia, M.A.; Chen, Y.; Onstott, T.C. Direct measurements of methane emissions from abandoned oil and gas wells in Pennsylvania. *Proc. Nat. Acad. Sci*. **2014**, doi:10.1073/pnas.1408315111.

Katzenstein, A.S.; Doezema, L.A.; Simpson, I.J.; Blake, D.R.; Rowland, F.S. Extensive regional atmospheric hydrocarbon pollution in the southwestern United States. *P. Natl. Acad. Sci*. **2003**, 100, 11975-11979.

Keeling, C.D. The concentration and isotopic abundances of atmospheric carbon dioxide in rural areas. *Geochim. Cosmochim. Acta*. **1958**, 13, 322-334, doi:10.1016/0016-7037(58)90033-4.

Keeling, C.D. The concentration and isotopic abundances of carbon dioxide in rural and marine air, *Geochim. Cosmochim. Acta*. **1961**, 24, 277-298, doi:10.1016/0016-7037(61)90023-0

Lyon, D.; Zavala-Araiza, D.; Alvarez, R.; Harriss, R.; Palacios, V.; Lan, X.; Lavoie, T.; Mitchell, A.; Yacovitch, T.; Hamburg, S. Constructing a spatially-resolved methane emission inventory for the Barnett Shale region. *In review.*

Mukhopadhyay, P.K.; Dow, W.G. Vitrinite reflectance as a maturity parameter: applications and limitations. American Chemical Society Symposium Series, 570, 1994.

Oil & Shale Gas Discovery News. What is the Barnett Shale Formation, 2014. http://oilshalegas.com/barnettshale.html

Paatero, P. Least squares formulation of robust non-negative factor analysis. *Chemometr. Intell. Lab*. **1997**, 37, 23-35.

Paatero P. and Tapper U. Positive matrix factorization: a non-negative factor model with optimal utilization of error estimates of data values. *Environmetrics.* **1994**, 5, 111-126.

Pataki, D.E.; Ehleringer, J.R.; Flanagan, L.B.; Yakir, D.; Bowling, D.R.; Still, C.J.; Buchmann, N.; Kaplan, J.O.; Berry, J.A. The application and interpretation of Keeling plots in terrestrial carbon cycle research. *Global Biogeochem. Cycles*. **2003**, 17, 1022, doi:10.1029/2001GB001850.

Peischl, J.; Ryerson, T.B.; Brioude, J.; Aikin, K.C.; Andrews, A.E.; Atlas, E.; Blake, D.R.; Daube, B.C.; de Gouw, J.A.; Dlugokencky, E.; Frost, G.J.; Genter, D.R.; Gilman, J.B.; Goldstein, A.H.; Harley, R.A.; Holloway, J.S.; Kofler, J.; Kuster, W.C.; Land, P.M.; Novelli, P.C.; Santoni, G.W.; Trainer, M.; Wofsky, S.C.; Parrish, D.D. Quantifying sources of methane using light alkanes in the Los Angeles basin, California*. J. Geophys. Res. Atmos*., **2013**, 118, 4974-4990.

Pétron, G.; Karion, A.; Sweeney, C.; Miller, B.R.; Montzka, S.A.; Frost, G.J.; Trainer, M.; Tans, P.; Andrews, A.; Kofler, J.; Helmig, D.; Guenther, D.; Dlugokencky, E.; Lang, P.; Newberger, T.; Wolter, S.; Hall, B.; Novelli, P.; Brewer, A.; Conley, S.; Hardesty, M.; Banta, R.; White, A.; Noone, D.; Wolfe, D.; Schnell, R. A new look at methane and nonmethane hydrocarbon

emissions from oil and natural gas operations in the Colorado Denver-Julesburg Basin. *J. Geophys. Res*. **2014**, 119, 6386-6852, doi:10.1002/2013JD021272.

Smith, M.L.; Kort, E.A.; Karion, A.; Sweeney, C.; Herdon, S.; Newberger, T.; Wolter, S.; and Yacovitch, T. Airborne ethane observations in the Barnett shale: Quantification of ethane flux and attribution of methane emissions. *In review*.

Townsend-Small, A.; Tyler, S.C., Pataki, D.E., Xu, X., Christensen, L.E. Isotopic measurements of atmospheric methane in Los Angeles, California, USA: Influence of "fugitive" fossil fuel emissions. *J. Geophys. Res*. **2012**, 117 (D7), D07308.

Wennberg, P.O.; Mui, W.; Wunch, D.; Kort, E.A.; Blake, D.R.; Atlas, E.L.; Santoni, G.W.; Wofsy, S.C.; Diskin, G.S.; Jeong, S.; Fischer, M.L. On the sources of methane to the Los Angeles atmosphere. *Env. Sci Technol*. **2012**, 46 (9282-9289), doi:10.1021/es301138y.

Whiticar, M.J. Carbon and hydrogen isotope systematics of bacterial formation and oxidation of methane. *Chem. Geol*. **1999**, 161, 291-314, doi:10.1016/S0009-2541(99)00092-3.

Whiticar, M.J.; Schaefer, H. Constraining past global tropospheric methane budgets with carbon and hydrogen isotope ratios in ice. *Philos. Trans. R. Soc. A.* **2007**, 365, 1793-1828,doi:10.1098/rsta.2007.2048.

Yang, M-Y. Characterization of VOC Emissions from Various Components of Dairy Farming and Their Effect on San Joaquin Valley Air Quality. Ph.D. Thesis, University of California – Irvine, 2009.

Yarnes, C. δ13C and δ2H measurement of methane from ecological and geological sources by gas chromatography/combustion/pyrolysis isotope-ratio mass spectrometry, Rapid *Comm. Mass Spec*. **2013**, 27 (1036-1044), doi:10.1002/rcm.6549.

Zumberge, J.; Ferworn, K.; Brown, S. Isotopic reversal ('rollover') in shale gases produced from the Mississippian, Barnett, and Fayetteville formations. *Mar. Petr. Geol*., **2012**, 31, 43-52.

Xiao, Y.; et al. Global ethane budget and regional constraints on US sources. *J. Geophys Res. Atmos*. **2008**, 113, D21.

Chapter 5.
Health Implications of Oil and Natural Gas Emissions

* portions of this chapter are adapted from Simpson, IJ; Marrero, JE; Batterman, S; Meinardi, S; Barletta, B; Blake, DR. "Air quality in the Industrial Heartland of Alberta, Canada and impacts on human health." *Atmos. Environ.* **2013**, 81, 702-709.

5.1 Harmful VOCs and their Potential Health Effects

The economically viable production of oil and natural gas from unconventional sources has become possible through the utilization of horizontal drilling and hydraulic fracturing. However, the increased application of these technologies is not without controversy and environmental concerns. Among these issues is the use of water. During oil sands surface extraction, the mixture of water and chemicals that remains after the bitumen has been separated is collected into tailings ponds. Over time, these ponds can potentially leech contaminants into fresh water aquifers [CAPP, 2014b]. Similarly during hydraulic fracturing, fracking fluid, which contains undisclosed amounts of inorganic salts and various organics, can seep into and pollute the groundwater [Rahm, 2011; Howarth et al., 2011].

Another potential environmental impact of the development of unconventional fossil fuels is the fugitive emissions from oil and natural gas infrastructure. While it is agreed that natural gas emits less carbon than coal per unit of energy produced, its primary component is CH_4, a greenhouse gas more warming potential than CO_2 [Pacala and Socolow, 2004; IPCC, 2007]. In particular, the CH_4 emissions during the completion of hydraulically fractured wells may reduce its apparent climate benefits [Howarth et al., 2011; Karion et al., 2013]. As the previous two chapters have shown, emissions from equipment leaks and industrial and petrochemical flaring or venting also release significant amounts of VOCs into the atmosphere, some of which can affect human health.

Throughout the past decade, shale gas operations have moved closer to urban centers and densely populated areas. This has contributed to growing public concerns regarding exposure to hazardous air pollutants (HAPs) [Adgate et al., 2014]. The U.S. EPA defines HAPs as toxic components in the air that are either known or suspected to cause serious health effects, such as cancer, neurological disorders, respiratory problems, and reproductive effects or birth defects. The list of HAPs contains 187 pollutants, including hexane, 1,3-butadiene, and benzene, toluene, ethylbenzene, and the xylenes, referred to as BTEX compounds [US EPA, 2011]. Their health effects range from irritation of the skin, eyes and respiratory tract, dizziness, gastric irritation, and vomiting caused by short-term exposure, to the more severe blood disorders, blindness, nervous system impacts, and cancer, which can develop from long-term exposure [Infante and White, 1983; Ware et al., 1993; Filley et al., 2004; US EPA, 2013].

Each of the HAPs mentioned are emitted in abundance from vehicular combustion, as well as industrial activities and oil and natural gas production, as highlighted in the previous chapters. The ground-based measurements made in Fort Saskatchewan and the Barnett Shale were further used to assess the potential health impacts of oil and gas emissions. In the Industrial Heartland, the link between VOC emissions and cancer incidence was investigated. In Texas, two methods were used to estimate the emission rate of a known carcinogen emitted from oil and natural gas activities.

5.2 Public Health Impacts of VOC Emissions in Alberta

Samples collected in Fort Saskatchewan industrial plumes revealed enhancements in each of the 6 HAPs aforementioned. The known carcinogens, 1,3-butadiene and benzene, were elevated nearly 5 and 6 times over background levels, respectively (Table 5.1). Ethylbenzene, which is considered potentially carcinogenic, was the most elevated VOC in this study, with an

industrial enhancement 60 times greater than background air [IARC, 2010]. The potential human health impact of the exposure to these elevated VOC concentrations was investigated using data from the Alberta Cancer Board. Two documents were obtained, containing tables and figures of cancer incidences in Alberta. These memos provided analyses specifically focused on comparing the industrial three-country area of Fort Saskatchewan, Strathcona County, and Sturgeon County to the rest of the Edmonton-area health region, as well as the rest of Alberta [Chen 2006, 208]. Forty-three major industries are operated within this region: 18 in Fort Saskatchewan, 16 in Srathcona County, and 9 in Sturgeon County [AIHA, 2012].

Table 5.1. Average industrial enhancements for the VOCs measured in Fort Saskatchewan considered hazardous to human health.

VOC	Avg. Ind. Enhancement
n-Hexane	35
1,3-Butadiene	5
Benzene	6
Toluene	3
Ethylbenzene	60
Xylenes	8

Surveillance data collected between 1994 and 2006 reveal elevated age-standardized incidence rates for male hematopoietic cancer and male non-Hodgkin lymphoma in the three-county (3C) area compared to other Alberta areas [Chen, 2008]. Incidence rate is defined as the number of new cancer cases divided by population size, normalized to 100,000 people. To reduce the yearly fluctuations in cancer cases caused by small population size, the mean standardized incidence rate was calculated for the region within two five-year periods (1997-2001 and 2002-2006). The results of these analyses are illustrated in Figure 5.1. Although the sample size is small, an increased incidence rate of male hematopoietic (affecting the blood and lymphatic systems) cancers is observed.

Figure 5.1. Mean standardized incidence rates (± 1σ) of hematopoietic cancer among males from 1997-2001 and 2002-2006. "3C" is the three county-area of Fort Saskatchewan and Strathcona and Sturgeon Counties; "CHR" denotes the Capital Health Region of Edmonton; "ALB" is the rest of Alberta. Each area is excluded from the next larger region.

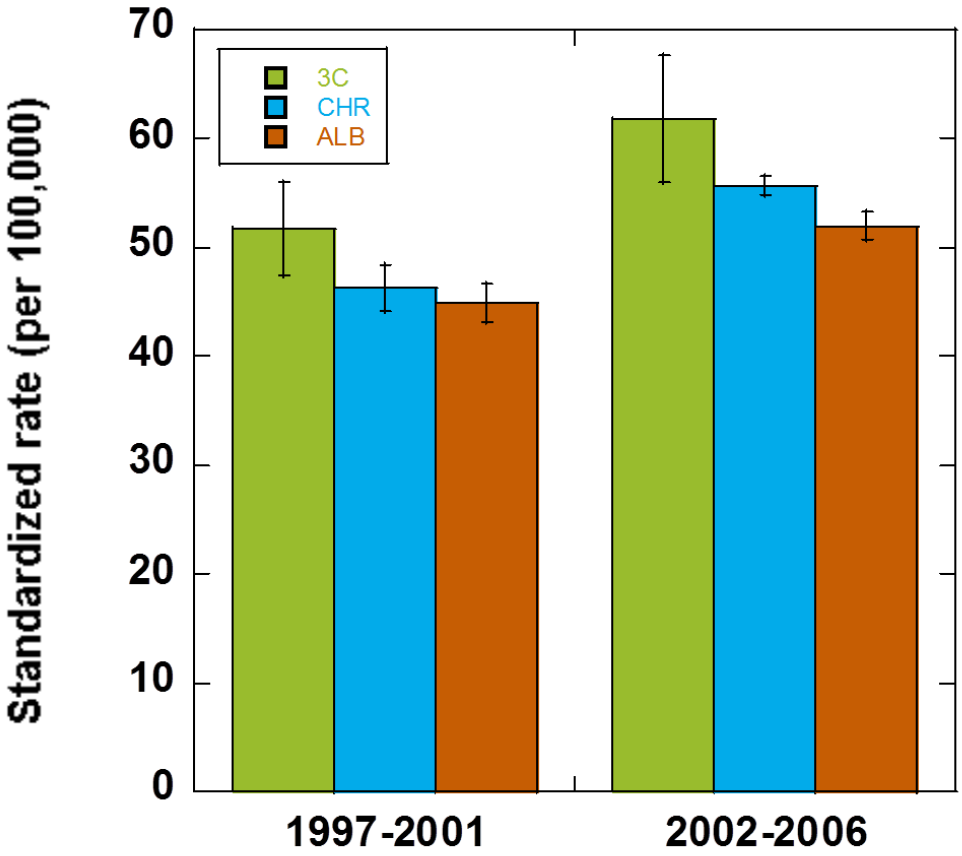

Previous studies have also shown the increased risk of hematopoietic cancers for people living downwind of industrial facilities. For example, exposure to benzene and 1,3-butadiene across nearly 900 census tracts near Houston, Texas was linked to an increase of childhood lymphohematopoietic cancer incidence [Whitworth et al., 2008]. Exposure to these compounds was highest in the Houston Ship Channel, where a large number of petrochemical and other chemical industries are located. Even relatively low VOC exposure rates have been associated with cancer rates. For a population living near an oil refinery in Sweden, the leukemia incidence was elevated despite a relatively low estimated annual industrial contribution to VOC concentrations of 0.63 ppb for benzene and 0.23 ppb for 1,3-butadiene

[Berregard et al., 2009]. For comparison, average mixing ratios downwind of the Shell-Scotford facility were 1.2 ppb and 0.96 ppb for these two compounds, respectively (Table 3.2).

As our understanding of the chemistry and toxicity of compounds continues to improve, recommended exposure limits also evolve. For instance, the exposure limit suggested for benzene in occupational settings has been reduced from a value of 100 ppm in 1947 to a current value of 1 ppm [Wong et al., 1999; McHale et al., 2010; Smith, 2010]. However, adverse health effects have been observed at levels below 1ppm, and some literature suggests that exposure to benzene at any level is unsafe [McHale et al., 2010; Qu et al., 2002; Lan et al., 2004; Xing et al., 2010]. Essentially benzene does not have a functional low-dose threshold, so several small exposures can have the same effect of one larger exposure [Smith, 2010].

In an area like the Industrial Heartland, the population is exposed to a mixture of compounds, making the understanding of potential health effects even more complex. Exposure to a combination of toxic compounds, even at lower concentrations, may exacerbate the effects on bodily systems or specific organs [Basso et al., 2011]. So while VOC levels observed in Fort Saskatchewan were generally below existing guidelines (the average 1-hr ambient air quality standard for benzene in Alberta is 9 ppb), the health effects could still be significant [Chambers et al., 2008].

All in all, a direct causal relationship between the elevated VOC concentrations observed and the increase in cancer incidences cannot be made here. Aspects such as the genetic makeup of the population, lifestyle factors, and statistical variability must also be considered. However, this study stresses the need for improved and continued VOC and health observations in the area, in order to more fully understand human health impacts. Factors that could help establish a stronger link include, but are not limited to, improved VOC emissions and exposure estimates; regular evaluations and better cancer surveillance broken down by cancer

type; inclusion of potential covariates such as employment history and residence; and statistical and epidemiological analysis to determine spatial or temporal patterns.

5.3 Benzene Emission Estimate for the Barnett Shale

In Section 4.3.3, natural gas well pad samples were categorized as dry if they contained less than 5% ethane by volume, and wet if they contained a greater ethane percentage. Oil samples can also be considered as wet based on their ethane content, which was greater than 5% for all samples. When compared to dry natural gas, wet gas samples exhibited higher average mixing ratios (by a factor of 2-15) for nearly every VOC measured in this study. As shown in Table 5.2, this includes the potentially harmful BTEX compounds.

Table 5.2. Comparison of average (±1σ) VOC mixing ratios in wet and dry natural gas samples collected in the Barnett Shale.

	n-Heptane (pptv)	n-Octane (pptv)	Benzene (pptv)	Toluene (pptv)	Ethylbenzene (pptv)	Xylenes (pptv)
Dry gas	290 ± 430	100 ± 130	230 ± 320	360 ± 430	50 ± 75	260 ± 180
Wet gas	3200 ± 8360	1180 ± 3780	590 ± 940	1360 ± 3170	100 ± 180	1540 ± 2500
W:D Ratio	11	12	3	4	2	6

Also calculated in Chapter 4 is the percentage of alkane and aromatic compounds in the composition of each of the sources sampled in the Barnett Shale (Table 4.7). Focusing on just the oil and wet gas samples reveals a higher content of BTEX compounds than in the dry natural gas samples. Values are summarized in Table 5.3. Wet gas emissions from compressor stations had 3 times as much BTEX as compressors that handled dry natural gas. Similarly, in samples collected downwind of well pads producing wet gas, the BTEX content was 1.5 times greater than dry gas wells.

In a report compiled by the Eastern Research Group (ERG), they evaluated measurements of BTEX content in emissions from oil and condensate storage tanks (which contain separated natural gas liquids). Storage tank vent gas was analyzed for VOC content at 19 different well pads. The average BTEX percentage by mass in the ERG report was 1.36% [ERG, 2012]. By comparison, UCI oil and natural gas samples were only 0.46-0.79% BTEX by mass (Table 5.3). The difference can be attributed to distance from sample location. In the ERG study measurements were taken directly at storage tanks and were not effected by atmospheric dilution like the UCI canister samples.

Table 5.3 BTEX composition (in %vol and %mass) for wet and dry gas samples compared to ERG values calculated for condensate tanks.

	BTEX dry gas (%vol)	BTEX wet gas (%vol)	BTEX dry gas (%mass)	BTEX wet gas (%mass)	ERG BTEX (%mass)[1]
Compressors	0.06	0.20	0.31	0.55	-
NG well pads	0.05	0.12	0.27	0.46	1.36
Oil wells	-	0.17	-	0.79	-

[1]Eastern Research Group

During Barnett campaign two air samples were collected at a well pad actively undergoing hydraulic fracturing (it is unclear if it was during the injection or flowback phase). These samples did not have elevated concentrations of BTEX compounds relative to other natural gas well pad samples. However, they were enhanced in BTEX compounds when compared to background concentrations, as shown in Table 5.4. Previous studies conducted in various U.S. shale plays have found enhancements, sometimes beyond federal guidelines, of compounds like benzene near oil and gas operational sites [Macey et al., 2014]. For that reason, whole air samples were used to estimate the emission rate of benzene for the Barnett Shale.

Table 5.4 Average mixing ratios (in pptv) for BTEX compounds at well pads actively being hydraulically fractured compared to other well pads and background values.

	Fracking wells	All NG wells	Background
Benzene	190 ± 90	290 ± 500	100 ± 40
Toluene	680 ± 570	590 ± 1190	150 ± 110
Ethylbenzene	54 ± 26	56 ± 130	20 ± 15
Xylenes	230 ± 50	600 ± 840	90 ± 30

Two approaches were used to calculate a regional benzene flux. In the first method, ground based CH_4 flux measurements at individual well pads estimated from the Picarro Surveyor™ were utilized. The Picarro Surveyor™ was launched in 2012 as a way to directly measure and map methane plumes downwind of a fugitive emission sources. It consists of a 12-foot pole mounted to the front of a vehicle with four sampling inlets that measure CH_4 concentration. The sample ports are linked to simultaneously measured wind speed and location data to generate a 2-dimensional image of the plume, which is then extrapolated to give a CH_4 flux. The resultant flux measurements have a 30% error associated with them [Tsai et al., 2013]. Six of these plume measurements were collected in conjunction with a canister sample.

From the canister samples, the ratio of benzene (C_6H_6) to CH_4 was found and multiplied by the CH_4 flux from the plume scanner (in kg/hr) and the molecular weight ratio [T. Tsai, personal communication, November, 2014]. As seen in Figure 5.2, a scatter plot of C_6H_6 to CH_4 provided a molar ratio of 0.0002. The average benzene flux from the six canister samples was 4.9 g/hr. However, this value is representative of emissions from an individual well pad. To determine a regional benzene flux, this value was multiplied by the number of actively producing gas wells (n=17,000) [TCEQ, 2014]. Using this method, the overall benzene emission estimate for the Barnett Shale is 84 ± 26 kg/hr.

The second approach for estimating a regional C_6H_6 flux is similar to the way ethane fluxes were calculated in Section 4.4. A plot of C_6H_6 against CH_4 in background samples was used to determine the molar ratio in well-mixed air (Figure 5.3). The slope, which was 0.003, was then multiplied by the median, low-end, and high-end CH_4 flux estimates from the bottom-up inventory [Lyon et al., in review]. Only the contribution from oil and natural gas sources was considered (values shown in Table 5.5). However, because background samples were used to determine the C_6H_6 to CH_4 ratio, they exhibit some influence from biogenic CH_4 sources. Therefore, the derived fluxes likely represent the lower bound estimate. The median C_6H_6 flux estimate was 63 ± 22 kg/hr, with low and high end estimates of 48 ± 16 to 84 ± 29 kg/hr.

Figure 5.2. Correlation plot of C_6H_6 vs. CH_4 in air samples collected simultaneously with CH_4 flux measurements from the Picarro Surveyor.

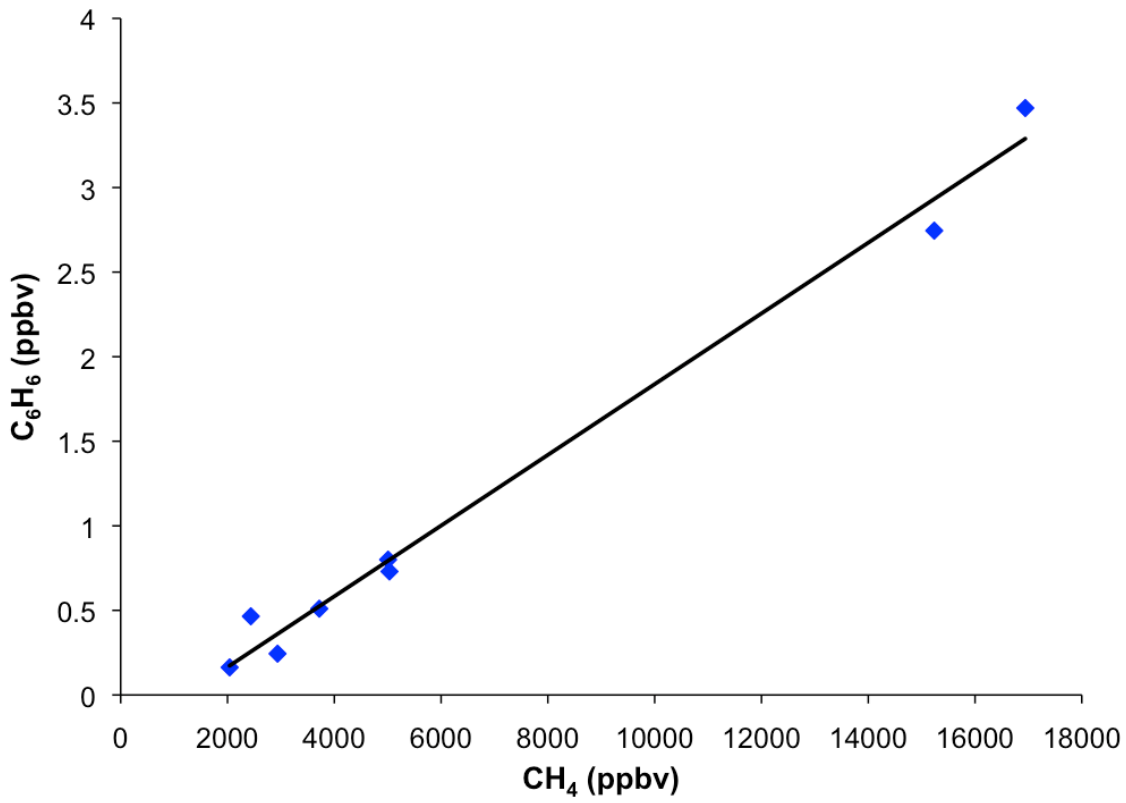

Figure 5.3. Correlation plot of C_6H_6 vs. CH_4 for background air samples collected in the Barnett Shale .

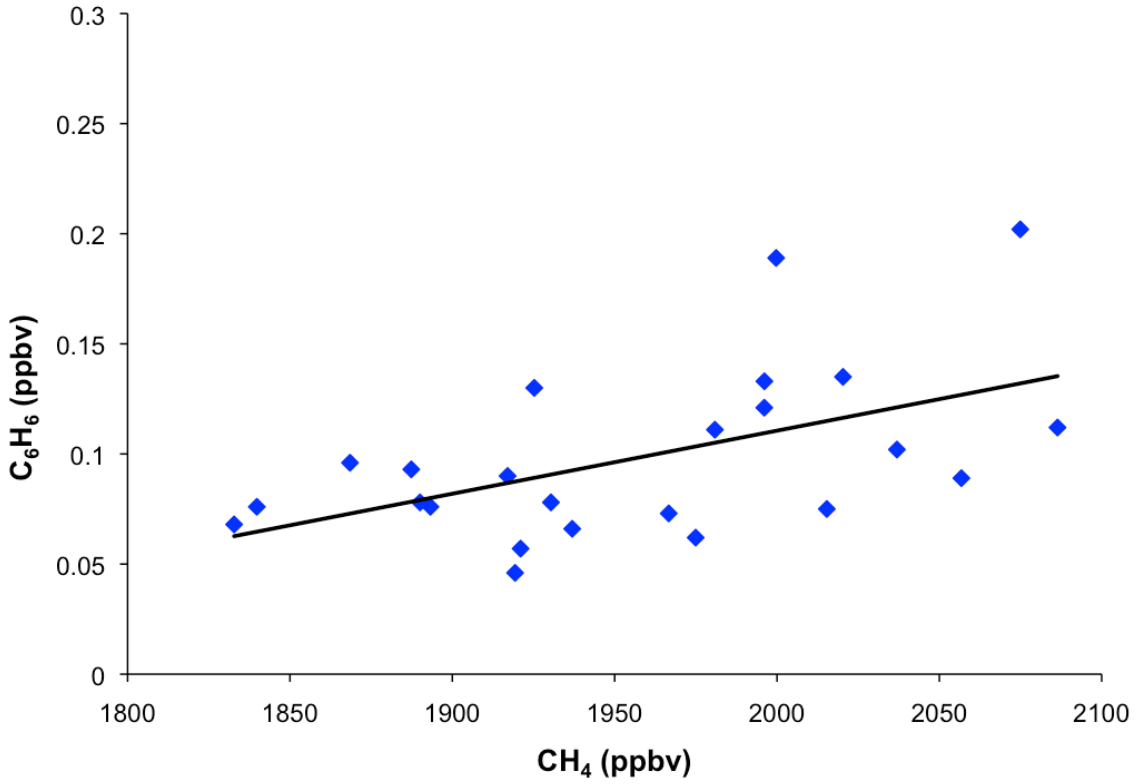

Benzene flux estimates using both methods are summarized in Table 5.5. Each of the calculated values has approximately 30% error, which accurately represents the large variability in VOC emissions measured throughout the region. The estimate derived using the Picarro plume scanner is in good agreement with the high-end value predicted using the CH_4 inventory, but is 1.3 and 1.8 times larger than the median and low-end estimates, respectively. However, this can be expected since the plume scanner was only triggered when a large enough CH_4 concentration, or leak, was detected. Because not all well pads actually have such large fugitive emissions, this value is biased towards higher numbers. It is likely though, that any measurement-derived estimate of emissions for the region is going to exhibit this "fat tail" distribution, where a sample number of sources are responsible for the majority of emissions.

Table 5.5. Comparison of benzene emission estimates determined from the Picarro Surveyor™ measurements and derived from the Barnett Shale bottom-up CH_4 inventory.

	CH_4 (kg/hr)	C_6H_6:CH_4 (%)	C_6H_6 (kg/hr)
Plume scanner[1]	-	0.02	84 ± 26
CH_4 inventory[2]		0.03	
ONG Median	45,450		63 ± 22
ONG Low-end	34,405		48 ± 16
ONG High-end	59,990		84 ± 29

[1] T. Tsai, personal communication
[2] Lyon et al., *in review*

Despite the high degree of uncertainty here, which partially stems from the limited number of samples, there is a significant regional source of atmospheric benzene. But whether the emission of benzene equates to a larger public health risk is unclear. A study using data from TCEQ monitoring sites throughout the Barnett Shale found that VOCs emitted from the region do not exceed many of the state and federal health regulations/standards [Bunch et al., 2013]. Most of data were collected from monitoring stations in the dry gas region of the Barnett, and not in areas wetter and VOC-enriched gas or oil (although this may be suitable because the Barnett is relatively dry when compared to other reservoirs as seen in Section 4.3.3).

However, as previously mentioned, even low exposure rates of carcinogens can potentially be harmful to a population. Moreover, as is the case in the Barnett Shale, oil and natural gas production sites lie within the communities, and are continuing to move closer to homes and places of work [Adgate et al., 2014]. As a result, public concern about the health effects related to VOC exposure has increased. Yet, comprehensive population-based studies that factor in accurate baseline data, quantification of VOC emissions, human exposure to VOCs, disease surveillance, and the extent of future development, still do not exist [Adgate et al., 2014]. More research is needed to address these uncertainties; particularly as gas production from unconventional sources continues to expand across the globe.

5.4 References

Alberta's Industrial Heartland Association (AIHA). Industry and Organization Profiles. July 2012. Available from: www.industrialheartland.com/images/stories/industry/aiha_industry_information_july_2012.pdf.

Adgate, J.L.; Goldstein, B.D.; McKenzie, L.M. Potential public health hazards, exposures and health effects from unconventional natural gas development. *Environ. Sci. Technol*. **2014**, 48(15), 8307-8320. DOI: 10.1021/es404621d

Barregard, L.; Holmberg, E.; Sallsten, G. Leukaemia incidence in people living close to an oil refinery. *Environ. Res*. **2009**, 109(8), 985–990.

Basso E, et al. Cytogenetic biomonitoring on a group of petroleum refinery workers. *Environ. Molec. Mutagen.* **2011**, 52, 440–447.

Bunch, A.G.; Perry, C.S.; Abraham, L.; Wikoff, D.S.; Tachovsky, J.A.; Hixon, J.G.; Urban, J.D.; Harris, M.A.; Haws, L.C. Evaluation of impact of shale gas operations in the Barnett Shale region on volatile organic compounds in air and potential human health risks. *Sci. Total Environ*. **2014**, 468-469, 832-842.

Canadian Association of Petroleum Producers. *The Facts on: Oil Sands*.; 2014b; http://www.capp.ca/getdoc.aspx?DocId=242473&DT=NTV, accessed November 5th, 2014.

Chambers, A.K.; Strosher, M.; Wootton, T.; et al. Direct measurement of fugitive emissions of hydrocarbons from a refinery. *J. Air Waste Manag. Assoc*. **2008**, 58, 1047-1056.

Chen, Y. Ten year (1994-2003) cancer incidence in Fort Saskatchewan, Strathcona and Sturgeon counties. Division of Population Health and Information, Alberta Cancer Board, Edmonton Alberta, Canada, Memo, tables and figures, dated June 26, 2006.

Chen, Y. Ten year (1994-2006) cancer incidence in Fort Saskatchewan, Strathcona and Sturgeon counties. Division of Population Health and Information, Alberta Cancer Board, Edmonton Alberta, Canada, Memo, tables and figures, dated Aug. 22, 2008.

Eastern Research Group (ERG). Condensate tank oil and gas activities: Final Report. Prepared for the Texas Commission on Environmental Quality, Air Quality Division. 2012. Available at https://www.tceq.texas.gov/assets/public/implementation/air/am/contracts/reports/ei/5821199776FY1211-20121031-ergi-condensate_tank.pdf

Filley, C.M.; Halliday, W.; Kleinschmidt-DeMasters, B.K. The Effects of Toluene on the Central Nervous System. *J. Neuropathol. Exp. Neurol*. **2004**, 63(1), 1-12.

Howarth, R.W.; Santoro, R.; Ingraffea, A. Methane and the greenhouse-gas footprint of natural gas from shale formations. *Clim. Change*, **2011**, DOI 10.1007/s10584-011-0061-5.

International Agency for Research on Cancer (IARC). IARC Monographs on the Evaluaiton of Carcinogenic Risks to Humans. 2010. Available from http://monographs.iarc.fr/ENG/Classification/index.php.

Infante, P.F.; White, M.C. Benzene: Epidemiologic Observations of Leukemia by Cell Type and Adverse Health Effects Associated with Low-Level Exposure. *Environ. Health. Perspect*. **1983**, 52, 75-82.

Intergovernmental Panel on Climate Change (IPCC). *Climate Change 2007 The Scientific Basis. Contribution of the Working Group I to the Fourth Assessment Report*. Cambridge Univ. Press: New York, 2007.

Karion, A.; *et al*. Methane emissions estimate from airborne measurements over a western United States natural gas field. *Geophys. Res. Lett.* **2013**, *40*, 1-5, doi:10.1002/grl.50811.

Lan, Q.; et al. Hematotoxicity in workers exposed to low levels of benzene. *Science*. **2004**, 306, 1774–1776.

Lyon, D.; Zavala-Araiza, D.; Alvarez, R.; Harriss, R.; Palacios, V.; Lan, X.; Lavoie, T.; Mitchell, A.; Yacovitch, T.; Hamburg, S. Constructing a spatially-resolved methane emission inventory for the Barnett Shale region. *In review.*

Macey, G.P.; Breech, R.; Chernaik, M.; et al. Air concentrations of volatile compounds near oil and gas production: a community-based exploratory study. *Environ. Health*. **2014**, 13:82, 1-18. http://www.ehjournal.net/content/13/1/82.

Pacala, S.; Socolow, R. Stabilization wedges: Solving the climate problem for the next 50 years with current technologies, *Science,* **2004**, 305, 968-972.

Rahm, D. Regulating hydraulic fracturing in shale gas plays: The case of Texas. *Energy Policy*. **2011**, 39, 2974-2981.

Tsai, T.; Rella, C.; Crosson, E. Plume scanner technology to quantify fugitive methane emission of point sources quickly and easily. Presented at the NOAA Global Monitoring Annual Conference, May 2013, Picarro, Inc. Available from: http://www.esrl.noaa.gov/gmd/publications/annual_meetings/2013/slides/99-130416-A.pdf

McHale, C.M.; et al. Global gene expression profiling of a population exposed to a range of benzene levels. *Environ Health Persp*. **2010**, 119(5), 628–634.

Qu, Q.; et al. Hematological changes among Chinese workers with a broad range of benzene exposures. *Am. J. Ind. Med.* **2002**, 42(4), 275–285.

Smith, M.T. Advances in understanding benzene health effects and susceptibility. *Annu. Rev. Publ, Health*. **2010**, 31(1), 133–148.

U.S. Environmental Protection Agency. *Air and Radiation. Outdoor Air - Industry, Business, and Home: Oil and Natural Gas Production;* Washington, DC, 2011; http://www.epa.gov/oaqps001/community/details/oil-gas_addl_info.html, accessed March 26th, 2015.

U.S. Environmental Protection Agency. *Air and Radiation. Technology Transfer Network - Air Toxics Web Site*; Washington, DC, 2013; http://www.epa.gov/airtoxics/allabout.html, accessed March 26th, 2015.

Ware, J.H.; Spengler, J.D.; Neas, L.M.; Samet, J.M.; Wagner, G.R.; Coutlas, D.; Ozkaynak, H.; Schwab, M. Respiratory and Irritant Health Effects of Ambient Volatile Organic Compounds: The Kanawha County Health Study. *Am. J. Epidemol*. **1993**, 137(12), 1287-1301.

Whitworth, K.W.; Symanski, E.; Coker, A.L. Childhood lymphohematopoietic cancer incidence and hazardous air pollutants in southeast Texas, 1995–2004. *Environ. Health Persp.* **2008**, 116(11), 1576–1580.

Wong, O.; Trent, L.; Harris, F. Nested case-control study of leukaemia, multiple myeloma, and kidney cancer in a cohort of petroleum workers exposed to gasoline. *Occup. Environ. Med*. **1999**, 56, 217–221.

Xing, C.; et al. Benzene exposure near the U.S. permissible limit is associated with sperm aneuploidy. *Environ. Health Persp*. **2010**, 118(6), 833–839.

Chapter 6.
Summary and Conclusions

Volatile organic compounds are emitted from a variety of biogenic and anthropogenic atmospheric sources, including the production, distribution and consumption of fossil fuels. The development of unconventional oil and natural gas has rapidly increased in the last decade, particularly in the United States and Canada, in order to quell rising energy demand and reduce dependency on foreign sources. However, emissions of a variety of VOCs have increased along with the expanded infrastructure, influencing not only the global climate, but also local air quality and public health.

Alberta, Canada is home to vast reserves of oil sands, a heavy crude known as bitumen. Whole air samples collected downwind of industrial sites near the urban service area of Fort McMurray revealed elevated mixing ratios of 40 VOCs. Using tracer analysis, it was determined that emissions from the oil sands mining and upgrading are the dominant source of VOCs in the region.

Also located in Alberta is Canada's Industrial Heartland, which is the largest hydrocarbon processing center in the country. More than 40 chemical, petrochemical, and oil and gas industries operate in the region. Samples collected downwind of these chemical and oil industries, some of which process bitumen, exhibited considerable enhancements in nearly all hydrocarbons measured. A follow-up study conducted two years later also showed the persistent emissions of VOCs. Using hydroxyl reactivity it was shown that the most concentrated industrial plumes have as much potential to affect local photochemistry as the world's largest megacities. However, due to the relatively clean air background, ozone concentrations do not frequently exceed federal standards. While many of the VOCs measured in this study were found to be emitted in large quantities, they are not well represented in

national inventories. Further monitoring in the region and improved inventories are needed and will be beneficial to the public, as these compounds not only have important role in photochemistry but also can have public health impacts.

The Barnett Shale, located in northern Texas, is one of the most developed natural gas reservoirs in the U.S., responsible for nearly 6% of the country's natural gas from its more than 17,000 wells. Fugitive hydrocarbon emissions are deserving of much attention because they can occur during each stage of natural gas production and from any component along the production chain. So while methane is cleaner than coal, the accumulation of emissions from the high concentration of wells in the region can potentially have a significant impact. In addition to methane emissions from oil and natural gas sources, the Barnett region is home to nearly one million cattle, as well as numerous landfills and other urban sources. Ninety whole air samples collected at these various sources were analyzed for hydrocarbons and stable isotopes. Using tracer analysis and statistical source apportionment techniques, unique emissions signatures were determined for biological and thermogenic methane sources. Further, a distinction was made between dry and wet natural gas, and it was found that the Barnett Shale is a relatively dry shale play when compared to others across the country. As was observed in Alberta, emissions from oil and natural gas are the dominant VOC source.

Lastly, the potential public health effects from these oil and gas emissions were investigated. In Alberta, we saw that industrial emissions could be correlated with increased male hematopoietic cancer incidence rates observed in the region over a 10-year period. In order for a direct causal link to be made however, more information is needed, such as exposure history for the local population and a more accurate understanding of the health impacts associated with low exposure to a complex mixture of compounds. But overall, a reduction in emissions, particularly of known carcinogens, is both warranted and prudent.

In Texas, despite the primarily dry nature of natural gas in the region, potentially harmful VOCs are being emitted from the Barnett Shale region. Using two approaches, benzene fluxes were calculated for the region, and ranged from 48 ± 16 to 84 ± 26 kg C_6H_6 hr^{-1}. This may be a substantial amount of benzene, particularly since wells are so close to a large population of people. More comprehensive studies focused on addressing uncertainties in health surveillance and VOC exposure are required, however. A more complete understanding of the Barnett Shale will go a long way in predicting the future environmental and health impacts of the development of other shale gas plays in the U.S. and across the globe.